Interspecies differences in oocyte fine structure and dynamics of oogenesis in pelagic fishes

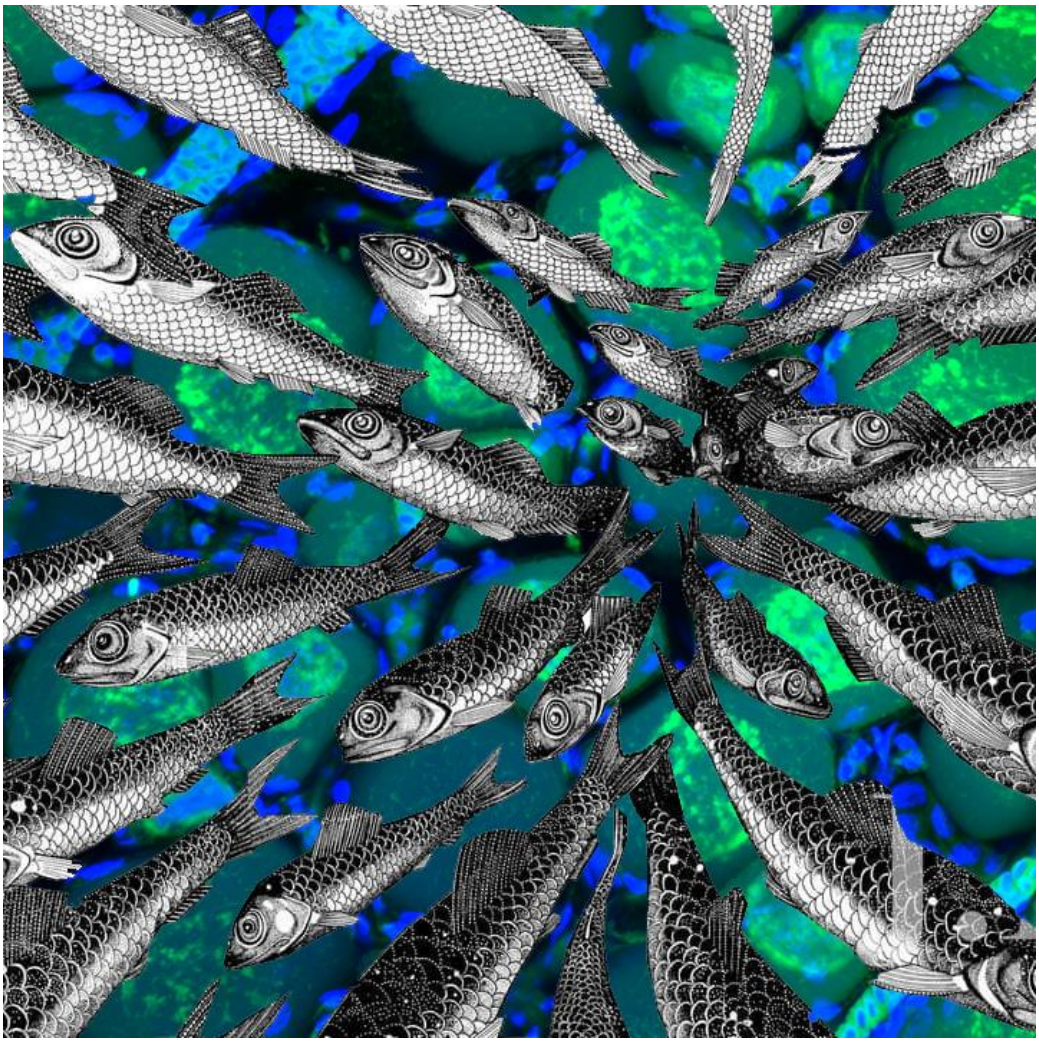

Doctoral dissertation

Katerina Charitonidou

ARISTOTLE UNIVERSITY OF THESSALONIKI
FACULTY OF SCIENCES
SCHOOL OF BIOLOGY
DEPARTMENT OF ZOOLOGY
LABORATORY OF ICHTHYOLOGY

Interspecies differences in oocytes fine structure and dynamics of oogenesis in pelagic fishes

PhD Dissertation

KATERINA CHARITONIDOU

Graduate of the School of Biology,
Aristotle University of Thessaloniki, Greece

This research is co-financed by Greece and the European Union (European Social Fund-ESF) through the Operational Programme «Human Resources Development, Education and Lifelong Learning» in the context of the project "Strengthening Human Resources Research Potential via Doctorate Research – 2nd Cycle" (MIS-5000432), implemented by the State Scholarships Foundation (IKY).

Ευρωπαϊκή Ένωση
European Social Fund

Operational Programme
Human Resources Development, Education and Lifelong Learning
Co-financed by Greece and the European Union

ΕΣΠΑ 2014-2020
ανάπτυξη - εργασία - αλληλεγγύη

THESSALONIKI 2023

ΑΡΙΣΤΟΤΕΛΕΙΟ ΠΑΝΕΠΙΣΤΗΜΙΟ ΘΕΣΣΑΛΟΝΙΚΗΣ
ΣΧΟΛΗ ΘΕΤΙΚΩΝ ΕΠΙΣΤΗΜΩΝ
ΤΜΗΜΑ ΒΙΟΛΟΓΙΑΣ
ΤΟΜΕΑΣ ΖΩΟΛΟΓΙΑΣ
ΕΡΓΑΣΤΗΡΙΟ ΙΧΘΥΟΛΟΓΙΑΣ

Διαειδικές διαφορές στη λεπτή δομή των ωοκυττάρων και στη δυναμική της ωογένεσης σε πελαγικούς ιχθύες

ΔΙΔΑΚΤΟΡΙΚΗ ΔΙΑΤΡΙΒΗ

ΚΑΤΕΡΙΝΑ ΧΑΡΙΤΩΝΙΔΟΥ

Πτυχιούχος Τμήματος Βιολογίας ΑΠΘ

Το έργο συγχρηματοδοτείται από την Ελλάδα και την Ευρωπαϊκή Ένωση (Ευρωπαϊκό Κοινωνικό Ταμείο) μέσω του Επιχειρησιακού Προγράμματος «Ανάπτυξη Ανθρώπινου Δυναμικού, Εκπαίδευση και Διά Βίου Μάθηση», στο πλαίσιο της Πράξης «Ενίσχυση του ανθρώπινου ερευνητικού δυναμικού μέσω της υλοποίησης διδακτορικής έρευνας – 2ος Κύκλος» (MIS-5000432), που υλοποιεί το Ίδρυμα Κρατικών Υποτροφιών (ΙΚΥ).

Ευρωπαϊκή Ένωση
Ευρωπαϊκό Κοινωνικό Ταμείο

Επιχειρησιακό Πρόγραμμα
Ανάπτυξη Ανθρώπινου Δυναμικού,
Εκπαίδευση και Διά Βίου Μάθηση
Με τη συγχρηματοδότηση της Ελλάδας και της Ευρωπαϊκής Ένωσης

ΕΣΠΑ 2014-2020
ανάπτυξη - εργασία - αλληλεγγύη

ΘΕΣΣΑΛΟΝΙΚΗ 2023

The approval of this dissertation by the School of Biology, Faculty of Sciences, Aristotle University of Thessaloniki does not imply acceptance of the author's opinions according to Law 5343/1932, article 202, paragraph 1.

Η έγκριση της παρούσας διατριβής από το Τμήμα Βιολογίας της Σχολής Θετικών Επιστημών του Αριστοτελείου Πανεπιστημίου Θεσσαλονίκης δεν υποδηλώνει αποδοχή των γνωμών του συγγραφέως, σύμφωνα με τον Ν. 5343/1932, άρθρο 202, παράγραφος 1.

I hereby certify that I am the author of this dissertation and that I have cited or referenced, explicitly and specifically, all sources from which I have used data, ideas, suggestions or words, whether they are precise quotes (in the original or translated) or paraphrased.

Βεβαιώνω ότι είμαι ο συγγραφέας της παρούσας εργασίας και ότι έχω αναφέρει ή παραπέμψει σε αυτήν, ρητά και συγκεκριμένα, όλες τις πηγές από τις οποίες έκανα χρήση δεδομένων, ιδεών, προτάσεων ή λέξεων, είτε αυτές μεταφέρονται επακριβώς (στο πρωτότυπο ή μεταφρασμένες) είτε παραφρασμένες.

Cite this dissertation as follows:

Charitonidou K (2023). Interspecies differences in oocyte fine structure and dynamics of oogenesis in pelagic fishes. Doctoral dissertation. Laboratory of Ichthyology, Department of Zoology, School of Biology, Aristotle University of Thessaloniki, Thessaloniki, Greece

Research funding:

This research is co-financed by Greece and the European Union (European Social Fund- ESF) through the Operational Programme «Human Resources Development, Education and Lifelong Learning» in the context of the project "Strengthening Human Resources Research Potential via Doctorate Research – 2nd Cycle" (MIS-5000432), implemented by the State Scholarships Foundation (IKY).

Advisory committee:

Dr. Konstantinos Ganias, Associate Professor, School of Biology, Department of Zoology, Aristotle University of Thessaloniki, Greece

Dr. Kjesbu Olav Sigurd, Chief Scientist, Institute of Marine Research, Norway

Dr. Emmanuel Panteris, Associate Professor, School of Biology, Department of Botany, Aristotle University of Thessaloniki, Greece

Examination committee:

Dr. Antonopoulou Efthimia, Associate Professor, School of Biology, Department of Zoology, Aristotle University of Thessaloniki, Greece

Dr. Somarakis Stylianos, Senior Researcher, Hellenic Centre for Marine Research, Greece

Dr. Rosario Dominguez-Petit, Tenured scientist, Spanish Institute of Oceanography (IEO), Spain

Dr. Martha Kaloyianni, Professor, School of Biology, Department of Zoology, Aristotle University of Thessaloniki, Greece

Αφιερωμένο στην οικογένειά μου,
που με στηρίζει σε κάθε βήμα

Table of contents

List of abbreviations 9
Glossary 12
Summary 14
Περίληψη 16
Acknowledgements 18
Chapter 1: Introduction 19
1.1. Reproductive strategies in fishes 19
1.2. Oocyte development during oogenesis and ovarian organization 19
1.3. Fecundity type 22
1.4. Implications of oogenesis and fecundity type to spawning stock biomass assessment (SSB) estimates through egg production methods 23
1.5 Species selection and the main scientific questions 25
Chapter 2: Methodology 29
2.1 Samples collection 29
2.2 Samples processing 31
2.3 Histological procedure 31
2.4 Whole-mount procedure 32
2.5 Confocal laser scanning microscopy (CLSM) procedure 33
2.6 Transmission electron microscopy (TEM) procedure 34
2.7 Statistical analysis 35
Chapter 3: Description of oocyte development during early oogenesis and investigation of the oogonial proliferation and early oocyte dynamics throughout the reproductive cycle in Clupeiform fishes 36
3.1 Specific objectives 36
3.2 Specific methodology 36
3.3 Results and Discussion 38
3.3.1 Oogonia and early (chromatin nucleolus stage) oocytes 38
3.3.2 Primary growth phase 39
3.3.3 Secondary growth phase 42
3.3.4 Changes in mitochondrial morphology in relation with organization of other organelles during oocyte development 47
3.3.5 Variation of oogonial proliferation and meiotic activity between reproductive phases 55
3.4 Conclusion 59
Chapter 4: Secondary phase of oogenesis: Ovarian dynamics and their link with the spawning dynamics at the interspecies level 61

4.1 Specific objectives 61
4.2 Specific methodology 62
4.2.1 Recruitment pattern from primary to secondary growth oocytes 62
4.2.2 Investigation of the secondary growth oocytes dynamics 62
4.2.3 Clustering algorithms for identification of fish oocyte cohorts based on the characteristics of cytoplasmic structures 62
4.2.4 Examination of POFs dynamics 66
4.3 Results and Discussion 67
4.3.1 Dynamics of the secondary growth oocytes 67
4.3.2 POF dynamics in sardine and mackerel 74
4.4 Conclusion 80
Chapter 5: General Discussion and Conclusions 81
5.1 Answers to the main scientific questions 82
5.2 Main findings 84
5.3 New knowledge acquired 85
5.4 Implications in DEPM application 87
5.5 Conclusions and future recommendations 88
5.5 Main conclusions in bullets 90
Literature cited 92
Cover picture 112
Annexes 113
Annex 1: Reproductive phases of ovary 113
Annex 2: Stereological method 114
Annex 3: Oocyte packing density theory 116
Annex 4: Estimates of threshold between primary and secondary growth oocytes 118
Annex 5: Estimates of relative number of primary, and secondary growth oocytes and relative batch fecundity 120
Annex 6: Morphological measurements in mitochondria 121
Annex 7: Bhattacharya method 122
Annex 8: Postovulatory follicles (POFs) 123
Publications 124

List of abbreviations

AEPM= annual egg production method

AM= advanced mode

Bb = Balbiani body

CA= cortical alveolar oocyte developmental stage

CA1 = primary cortical alveolar oocyte developmental stage. Few cortical alveoli in the cytoplasm, mainly at the periphery of the oocyte

CA2 = secondary cortical alveolar oocyte developmental stage. Increased number of cortical alveoli appearing throughout the cytoplasm, from the periphery of the oocyte to the nucleus

CA3 = final cortical alveolar oocyte developmental stage. Cytoplasm is filled with cortical alveoli before the presence of yolk globules

CLSM= confocal laser scanning microscopy

DAPI = 4',6-diamidino-2-phenylindole

DEPM = daily egg production method

DEV = developing reproductive phase

DFRM = daily fecundity reduction method

$DiOC_6$ = 0.3% aqueous solution of 3,3'-dihexyloxacarbocyanine iodide

EPM = egg production methods

ESG = early secondary growth oocytes

ESG:LPG ratio = the numerical ratio of early secondary growth and late primary growth oocytes

f = spawning frequency

F_B = batch fecundity

F_{POF} = number of POFs

GSI = gonadosomatic index

GVBD = germinal vesicle break down oocyte developmental stage

GVM1 = early germinal vesicle migration oocyte developmental stage

GVM2 = late germinal vesicle migration oocyte developmental stage

HYD = hydration oocyte developmental stage

ISI = interspawning interval

LPG= late primary growth oocytes

NEA = *Northeast Atlantic*

$\mathbf{N_v}$ = postovulatory follicles density

OD = oocyte diameter

OGP = oocyte growth period

OPD = oocyte packing density

OSFD = oocyte size frequency distributions

OV = ovary volume

OW = gonad weight

OWs = Subsamples of gonad tissue

PBS = phosphate buffered saline

$\mathbf{PC_{ACT}}$ = significant PCA scores served as an activity index

PFA = paraformaldehyde

PG= primary growth

POF method = postovulatory follicle method

$\mathbf{POF_{DA}}$ = postovulatory follicle diameter

POFPD = the adjusted for POFs packing density method

POFs = postovulatory follicles

REST = resting reproductive phase

$\mathbf{RF_{AM}}$ = the mean values of advanced mode relative batch fecundity

$\mathbf{RF_B}$ = the relative batch fecundity (oocytes*g^{-1})

$\mathbf{RF_{ci}}$ = cohort specific fecundity

$\mathbf{RF_{POF}}$ = relative POF fecundity

$\mathbf{RN_{PG}}$ = the relative number of primary growth oocytes (oocytes*g^{-1})

RN_{SG} = the relative number of secondary growth oocytes (oocytes*g^{-1})

S = daily spawning fraction

SG = secondary growth

SPC = spawning capable reproductive phase

SSB = spawning stock biomass

TEM = transmission electron microscopy

V_i = volume fraction of postovulatory follicles

VTG = vitellogenic

VTG1 = early vitellogenic oocyte developmental stage

VTG2 = secondary vitellogenic oocyte developmental stage

VTG3 = final vitellogenic oocyte developmental stage

W_{ev} = eviscerated weight

W_T = total weight

W_v = viscerated weight (without gonads)

Yg = yolk granules

Glossary

Balbiani body = a structure exhibiting cytoplasmic asymmetry during primary growth phase

Capital breeding strategy = species whose reproduction (gamete development, reproductive behaviuor, spawing migrations, etc.) is based on the energy acquired before spawning

Determinate fecundity type = the recruitment of the secondary growth oocytes is completed before the onset of the spawning activity

Fecundity type = the way and timing of the production of oocytes to be spawned

Income breeding strategy = species whose reproduction (gamete development, reproductive behaviuor, spawing migrations, etc.) is based on the energy acquired during spawning

Indeterminate fecundity type = the recruitment of the secondary growth oocytes also occurs after the onset of the spawning activity

Iteroparous reproductive strategy = two or more reproductive cycles occur during lifetime

Multiple batch spawners= fish that spawn more than one batches of oocytes during a spawning period

Oogenesis = the morphological and functional processes that lead to the production of fertilizable eggs

Oogonia = germ cells that may divide mitotically to maintain their population within the germinal epithelium or may enter meiosis and give rise to oocytes

Oogonial proliferation = mitotic division of an oogonium into two new oogonia

Postovulatory follicle = follicular layers that remain in the ovary after the release of the ovum during spawning

Postovulatory follicle cohort = all postovulatory follicles originated from a single spawning event

Reproductive cycle = the period from the onset of secondary growth recruitment till the completion of spawning activity of a fish stock

Reproductive phases = Maturity phases of the ovary considered along the reproductive cycle

Semelparous reproductive strategy = a single reproductive cycle occurs in lifetime

SG recruitment = recruitment of new oocytes from the primary growth to the secondary growth phase of oogenesis

Spawning fraction = the percentage of females spawned per day

Spawning frequency = the number of spawning events per unit time, the time lag between two successive spawning events

Spawning interval = the time lag between subsequent spawning events

Spawning period = the period between the release of the first and the last batch of eggs by the females of a fish stock

Total oocyte release strategy = all mature oocytes are released in a single spawning event within the spawning period

Vitellogenesis = accumulation of yolk protein in the oocyte cytoplasm

Summary

Fish species have a high diversity of reproductive traits in order to survive in their habitats and successfully reproduce increasing the survival of offspring. Extended knowledge of their reproductive traits is provided by the connection between oocyte dynamics during oogenesis and spawning throughout time. The fish fecundity type (determinate, indeterminate) is defined by the pattern of oocyte recruitment according to the spawning period. The fecundity type is an important parameter in fisheries management for selecting the appropriate egg production method (EPM) for estimating spawning-stock biomass (SSB). However, many details concerning the fecundity type of many fish stocks are still unclear or controversial. In that respect, the principal aim of this study was to shed light on previously undiscovered aspects of different phases of oogenesis in highly commercial pelagic fish species with distinct spawning dynamics and to show the link between the spawning and ovarian dynamics as well as how both shape the fecundity type of species and their impact on the applicability of egg production methods.

The fish species in this study were selected mainly based on their distinct spawning dynamics. Specifically, the early phase of oogenesis was studied throughout the reproductive cycle in the Mediterranean sardine, *Sardina pilchardus*, and the European anchovy, *Engraulis encrasicolus*, two closely related phylogenetic species with different spawning frequency and feeding strategies. The secondary phase of oogenesis was investigated using the Atlantic sardine, *Sardina pilchardus*, the Atlantic horse mackerel, *Trachurus trachurus*, and the Atlantic mackerel, *Scomber scombrus*, examining the ovarian dynamics of those species with different spawning dynamics. Thus, the selected species provided the opportunity to investigate the early phase of oogenesis in indeterminate spawners, and to examine the link between ovarian and spawning dynamics in the secondary phase of oogenesis, and its impact on egg production methods application.

Three main scientific questions were explored in the present study. The chapters were organized based on the phases of oogenesis, beginning with the early phase of oogenesis and continuing with the secondary phase of oogenesis. Specifically, the fine structure of early oocytes during their development, as well as the oogonial proliferation and early oocyte dynamics were investigated in *S. pilchardus* and *E. encrasicolus* in chapter 3. In chapter 4, the dynamics of secondary growth oocytes were studied in different ovarian stages of three commercially important fish species with indeterminate fecundity but distinct spawning dynamics, *S. pilchardus*, *T. trachurus*, and *S. scombrus*. Furthermore, the dynamics of released egg remnants in the ovary (postovulatory follicles, POFs) were investigated in two fish species, *S. pilchardus*, and *S. scombrus*, with different spawning frequency.

In conclusion, this study provided important answers for each one of the main scientific questions. Specifically, the pattern of oogonial proliferation and early oocyte dynamics was different throughout the reproductive cycle among indeterminate spawners, and the cytoplasmic development of primary and early secondary growth oocytes varied among closely related phylogenetic fish species indicating differences in the functional path during the development of their oocytes. In addition, the intensity

of oocyte recruitment from the primary to secondary growth phase as well as the secondary growth oocyte dynamics differed among indeterminate species with distinct spawning dynamics, showing that the fecundity type is flexible from determinacy to indeterminacy along a continuum. Moreover, POF dynamics varied among species with distinct spawning intervals, showing that sardine, with long spawning interval, had only a single daily POF cohort in the ovaries, whereas mackerel, with shorter spawning interval, exhibited co-occurrence of multiple daily POF cohorts. The coexistence of multiple daily POF cohorts in ovaries is an obstacle in the proper assessment of important parameters, such as spawning fraction, used in the application of the daily egg production method (DEPM).

Περίληψη

Τα διάφορα είδη ιχθύων έχουν αναπτύξει μεγάλη ποικιλότητα στα αναπαραγωγικά χαρακτηριστικά, προκειμένου να επιβιώσουν στα ενδιαιτήματα και να αναπαραχθούν με επιτυχία, αυξάνοντας την επιβίωση των απογόνων. Η εις βάθος γνώση των αναπαραγωγικών τους χαρακτηριστικών προϋποθέτει τη σύνδεση μεταξύ της δυναμικής των ωοκυττάρων, κατά τη διάρκεια της ωογένεσης, και της ωοτοκίας κατά τη διάρκεια του χρόνου. Ο τύπος γονιμότητας των ιχθύων (καθορισμένη, ακαθόριστη) ορίζεται από το μοτίβο στρατολόγησης των ωοκυττάρων ανάλογα με την περίοδο ωοτοκίας. Ο τύπος γονιμότητας είναι μια σημαντική παράμετρος στη διαχείριση της αλιείας, για την επιλογή της κατάλληλης μεθόδου παραγωγής αυγών (EPM) με σκοπό την εκτίμηση της βιομάζας του αποθέματος αναπαραγωγής (SSB). Ωστόσο, πολλές λεπτομέρειες σχετικά με τον τύπο γονιμότητας πολλών αποθεμάτων ιχθύων είναι ακόμη ασαφείς ή αμφιλεγόμενες. Έτσι, ο κύριος στόχος αυτής της μελέτης ήταν να διαλευκάνει προηγούμενες άγνωστες πτυχές των διαφορετικών φάσεων της ωογένεσης σε είδη πελαγικών ιχθύων με υψηλό εμπορικό ενδιαφέρον, που έχουν διαφορετική δυναμική ωοτοκίας, και να δείξει τη σχέση μεταξύ της δυναμικής της ωοτοκίας και των ωοθηκών, καθώς και το πώς αυτή η σχέση διαμορφώνει τον τύπο γονιμότητας των ειδών και τον αντίκτυπό της στην εφαρμογή των μεθόδων παραγωγής αυγών.

Τα είδη ιχθύων αυτής της μελέτης επιλέχθηκαν κυρίως με βάση τη διαφορετική δυναμική ωοτοκίας τους. Συγκεκριμένα, η πρώιμη φάση της ωογένεσης μελετήθηκε καθ' όλη τη διάρκεια του αναπαραγωγικού κύκλου στη Μεσογειακή σαρδέλα, *Sardina pilchardus*, και στον Ευρωπαϊκό γαύρο, *Engraulis encrasicolus*, δύο φυλογενετικά στενά συγγενικά είδη με διαφορετική συχνότητα ωοτοκίας και στρατηγικές διατροφής. Η δευτερογενής φάση της ωογένεσης διερευνήθηκε στη σαρδέλα του Ατλαντικού, *Sardina pilchardus*, το γκριζοσαύριδο του Ατλαντικού, *Trachurus trachurus* και το σκουμπρί του Ατλαντικού, *Scomber scombrus*, εξετάζοντας τη δυναμική των ωοθηκών στα τρία είδη που έχουν διαφορετική δυναμική ωοτοκίας. Έτσι, τα επιλεγμένα είδη παρείχαν την ευκαιρία να διερευνηθεί η πρώιμη φάση της ωογένεσης σε είδη με απροσδιόριστο τύπο γονιμότητας και να εξεταστεί σε διαειδικό επίπεδο η σχέση μεταξύ της δυναμικής των ωοθηκών και της δυναμικής της ωοτοκίας στη δευτερογενή φάση της ωογένεσης και η επίδρασή της στην εφαρμογή των μεθόδων παραγωγής αυγών.

Τρία κύρια επιστημονικά ερωτήματα διερευνήθηκαν στην παρούσα μελέτη. Τα κεφάλαια οργανώθηκαν με βάση τις φάσεις της ωογένεσης, ξεκινώντας από την πρώιμη φάση της ωογένεσης και συνεχίζοντας με τη δευτερογενή φάση. Συγκεκριμένα, η λεπτή δομή των πρώιμων ωοκυττάρων κατά τη διάρκεια της ανάπτυξής τους, καθώς και ο πολλαπλασιασμός των ωογονίων και η δυναμική των πρώιμων ωοκυττάρων στα είδα *S. pilchardus* και *E. encrasicolus* αναλύονται στο κεφάλαιο 3. Στο κεφάλαιο 4, εξετάζεται η δυναμική των ωοκυττάρων δευτερογενούς ανάπτυξης σε διαφορετικά στάδια της ωοθήκης τριών εμπορικά σημαντικών ειδών ιχθύων με απροσδιόριστο τύπο γονιμότητας αλλά διαφορετική δυναμική ωοτοκίας, *S. pilchardus*, *T. trachurus* και *S. scombrus*. Επιπλέον, διερευνήθηκε η δυναμική των υπολειμμάτων από τα απελευθερωμένα αυγά (κενά ωοθυλάκια, POFs) στην ωοθήκη, σε δύο είδη ιχθύων, *S. pilchardus* και *S. scombrus*, με διαφορετική συχνότητα ωοτοκίας.

Συνοψίζοντας, από αυτή τη μελέτη εξάγονται γενικά συμπεράσματα για κάθε ένα από τα κύρια επιστημονικά ερωτήματα. Συγκεκριμένα, το μοτίβο πολλαπλασιασμού των ωογονίων και η δυναμική των πρώιμων ωοκυττάρων διέφεραν σε όλο τον αναπαραγωγικό κύκλο μεταξύ των δύο ειδών με απροσδιόριστο τύπο γονιμότητας, και η κυτταροπλασματική ανάπτυξη μεταξύ των ωοκυττάρων πρωτογενούς και πρώιμης δευτερογενούς ανάπτυξης διέφερε μεταξύ ειδών ιχθύων με στενή φυλογενετική σχέση, υποδεικνύοντας διαφορές στα λειτουργικά μονοπάτια κατά τη διαδικασία ανάπτυξης των ωοκυττάρων τους. Επίσης, το ποσοστό των ωοκυττάρων που από την πρωτογενή εισέρχονται στη δευτερογενή φάση ανάπτυξης, καθώς και η δυναμική των δευτερογενών ωοκυττάρων δεν ήταν η ίδια μεταξύ των τριών ειδών με απροσδιόριστο τύπο γονιμότητας αλλά με διαφορετική δυναμική ωοτοκίας, δείχνοντας ότι ο τύπος γονιμότητας είναι ευέλικτος από προσδιορισμένο σε απροσδιόριστο με ποικίλλες ενδιάμεσες καταστάσεις. Επιπλέον, η δυναμική των κενών ωοθυλακίων (POF) ήταν διαφορετική μεταξύ των ειδών με διαφορετικά διαστήματα ωοτοκίας, δείχνοντας ότι η σαρδέλα, με μεγάλο διάστημα ωοτοκίας, είχε μόνο μία ημερήσια κοόρτη POF στην ωοθήκη, ενώ το σκουμπρί, με μικρότερο διάστημα ωοτοκίας, εμφάνισε συνύπαρξη πολλαπλών ημερήσιων κοορτών POF. Η συνύπαρξη πολλαπλών ημερήσιων κοόρτων POF στις ωοθήκες αποτελεί εμπόδιο στη σωστή εκτίμηση σημαντικών παραμέτρων, όπως το κλάσμα ωοτοκίας, που χρησιμοποιείται στην εφαρμογή της μεθόδου ημερήσιας παραγωγής αυγών (DEPM).

Acknowledgements

A long journey of years has come to an end. Like all trips, this one was rich in experiences, collaborations, analysis, containing days with storms but also pleasant moments full of satisfaction. All this would not have been possible without the contribution of several people during these years. First of all, nothing would have started without the contribution of my supervisor and mentor Prof. Ganias, whom I would like to thank for everything he taught me for the experience he gave me and for the opportunity to start this beautiful research journey. A warm thank you also to the colleagues of the laboratory, Foivos, Maria, Alexandra, for their support and advice, and to all the undergraduate and postgraduate students who were part of the team all these years.

Furthermore, I would like to thank my co-supervisor Dr. Olav for the hospitality he offered me in his group in Bergen, and for the knowledge and experience and endless research discussions we had throughout the PhD and while I was there. Of course, a warm thank you to the whole team that was there, and because I don't want to forget any names, I won't mention them by name. Next, I would like to thank Anders Thorsen for giving me the opportunity to participate in the egg survey in the Atlantic, which was one of the incredible experiences I have ever had.

Going back to the Aristotle University of Thessaloniki, I would like to thank my co-supervisor Prof. Panteris for introducing me to the cellular world, for the many hours of observations in confocal laser scanning microscopy and for the knowledge and expertise he taught me. In addition, I would like to express my gratitude to the team of Prof. Panteris' laboratory.

In addition, I would like to thank Prof. Kaloyianni, Prof. Antonopoulou, Dr. Somarakis, and Dr. Rosario who accepted to participate in the seven-member committee of my PhD, thank you for your time and the advice you gave me. At this point, I would also like to thank the European research centers, AZTI, IEO, IPMA, IMARES, and Rosario Dominguez-Petit, Dolores Garabana, Maria Albisua Korta, Maria Santos, Cindy J.G. van Damme, Cristina Nunes, and Maria Manuel Angelico, for their cooperation and the material from the Atlantic that they sent us.

However, none of this would have been possible without the support of my family, my father, my mother, my sister and Polykarpos, who have been by my side all these years through the hard times and the easy times, helping me in any way they can, thank you for everything and for your patience. Also, at this point I would like to thank my old and new friends who are by my side and support me.

"Βίρα τις άγκυρες λοιπόν, στο επόμενο ταξίδι!!!"

Chapter 1: Introduction

1.1. Reproductive strategies in fishes

Fish species exhibit a large variety in their reproductive strategies to adapt and inhabit the different marine habitats as well as to ensure the survival of their offspring (Wootton 1990; Murua and Saborido-Rey 2003; Patzner 2008). To cope with fluctuations in the environment, fishes display a wide variety of universal reproductive tactics or traits that occur in four temporal scales, 1) lifetime (e.g., sexual maturity, number of breeding opportunities), 2) annual (e.g., spawning seasonality, reproductive cycle), 3) intraseasonal (e.g., birthdate dynamics, spawning interval in batch spawners), and 4) diel (e.g., egg hydration, mating behaviour, spawning events) (Wootton 1984, 1990; Roff 1996; Murua and Saborido-Rey 2003; Lowerre-Barbieri et al. 2011). The majority of marine teleosts are highly fecund producing either pelagic or demersal eggs (oviparity, in which eggs are released at spawning and embryos develop outside the ovary) and they primarily use the r-strategy, which involves increasing the number of offspring while decreasing parental care, enhancing the likelihood that the offspring will survive (Wootton 1994; Murua and Saborido-Rey 2003). They are also iteroparous, which means that they spawn more than once during their lives in multiple reproductive cycles (Murua and Saborido-Rey 2003). However, there are fish species that spawn only once in their lives and then die exhibiting the semelparity type, such as the Pacific salmonids (*Oncorhynchus* sp.), capelin (*Mallotus villosus*), and eels (*Anguilla* sp.) (Murua and Saborido-Rey 2003). Fish species can either be total or batch spawners depending on the spawning pattern during the reproductive cycle. Iteroparous species which spawn in batches are the most common type among species, they develop and release multiple batches of eggs during a spawning period (Hunter and Macewicz 1985; Murua and Saborido-Rey 2003). Both iteroparous and semelparous species can be total spawners, which means that they spawn all their mature oocytes either in one event or over a short period (Pavlov et al. 2009; Lowerre-Barbieri et al. 2011). Fish species exhibit either a determinate or an indeterminate fecundity type depending on the pattern of oocyte recruitment during the spawning period (intraseasonal scale) (see **Section 1.3**). The connection between ovarian development and spawning over time provides extended knowledge of the reproductive traits in fishes.

1.2. Oocyte development during oogenesis and ovarian organization

Oogenesis is a complex process, including the transformation of oogonia into oocytes and their development to mature eggs, ready for fertilization (Grier et al., 2009). The general pattern of oogenesis in fish species is described briefly below. Oogonia are the descendants of primordial germ cells, derived from stem cells of the female germinal lineage (Grier, 2000; Nakamura et al., 2010; Nakamura et al., 2011). In mammals, oogonial proliferation occurs during the foetus stage (gestation) indicating that very few oogonia are formed after birth; the postnatal ovary is thought to include a fixed and non-renewing number of oocytes (Smith et al., 2014; Zou et al., 2009). In non-mammalian vertebrates, there are two oogonial proliferation patterns. Lampreys, almost all elasmobranchs, some teleosts, some reptiles and birds have oogonial proliferation limited to the embryonic or larval period. Unlike other vertebrates, in most teleosts, amphibians and reptiles, oogonia undergo periodic

proliferation throughout some part of the reproductive cycle (Tokarz, 1978). Focusing on fishes, in several species, proliferating oogonia are most abundant during the post-spawning period (Tokarz, 1978). Oogonia divide mitotically to self-renew or produce germline cysts, whereas some oogonia undergo reabsorption (Nakamura et al., 2010; Nakamura et al., 2011; Quagio-Grassiotto et al., 2011). After a few synchronized mitotic divisions, oogonia inside the cysts (nests) transform into oocytes entering meiosis (chromatin nucleolus stage) (Grier et al., 2009; Nakamura, 2010; Nakamura et al., 2011) (**Fig.1.1**). All oocytes of each nest develop synchronously during the chromatin nucleolus stage of oogenesis. This stage lasts from the onset of meiotic prophase I division through diplotene, then meiosis ceases and cytoplasmic basophilia indicates the beginning of the primary growth phase (PG) (Grier 2000).

During primary growth phase, nuclei multiply and assume a perinuclear position (one-nucleolus, multiple nucleoli, perinucleolar stage) (**Fig. 1.1**). Also, an asymmetry is established in the cytoplasm of oocytes with the formation of the so-called Balbiani body (Bb). The Bb appears as a distinct spherical structure in the most teleosts (e.g., Beams and Kessel 1973; Dominguez-Castanedo and Uribe 2019; Elkouby et al. 2016; Elkouby 2017; Fusco et al. 2000; Grier 2012; Grier et al. 2018; Lyman-Gingerich and Pelegri 2007; Marlow and Mullins 2008; Zhang et al. 2008; Zelazowska and Halajian 2019), similarly to *Xenopus laevis* (Kloc et al. 2001, 2004; Kloc and Etkin 2005), however, its morphology and composition vary among species. It consists mainly of mitochondria, nuage (aggregation of RNA and proteins, generally thought to carry determinants of the germline, such as ribosomal RNA (rRNA), nucleolar proteins, mRNAs, Piwi-interacting RNAs), and proteins which are precursors of germplasm. It also contains localized maternal messenger ribonucleic acids (mRNAs), and in some cases, lipid droplets and lysosome-like organelles, endoplasmic reticulum, Golgi bodies, and membranous vesicles (Bilinski et al. 2004; Kloc et al. 2001; Kloc et al. 2004; Kloc and Etkin 2005; Kloc et al. 2007; Kloc et al. 2008; Marlow and Mullins 2008; Selman and Wallace 1989; Tworzydlo et al. 2014, 2016). The oocytes' fate is influenced by the functions of the Bb. First of all, it plays a role in germline specification and oocyte polarity determination as it forms the animal-vegetal polarity, which is critical for embryonic development due to the stabilization of the embryonic axis (Coloza and De Robertis 2014; Elkouby et al. 2016; Langdon and Mullins 2011). Also, it transports the germplasm determinants to the vegetal pole (Marlow and Mullins 2008; Saito et al. 2014; Škugor et al. 2016) and contains gene products required for RNA processing and storage, as well as transposon suppression (Marlow and Mullins 2008). In addition, it plays a role in follicular cell polar differentiation at the vegetal pole (Iwamatsu and Nakashima 1996). It is involved in the removal of malfunctioning mitochondria from oocytes, as well as the formation, multiplication, and accumulation of organelles in the cytoplasm (Bilinski et al. 2017; Tworzydlo et al. 2016). Remarkably, the connection of oocyte cytoplasmic dynamics, such as the formation of the Bb, with the reproductive period of fish species can be useful in applied fisheries reproductive biology. For example, in Atlantic cod and Atlantic herring, the appearance of a circumnuclear ring - a structure which has been characterized as homologous to the Bb (Sorokin 1957; Shirokova 1977; Kjesbu and Kryvi 1989; Kjesbu et al. 2011; McPherson and Kjesbu 2012)- in the cytoplasm of primary growth oocytes is considered a marker of maturity as well as the onset of the reproductive period (Kjesbu et al. 2011; McPherson and Kjesbu 2012).

The secondary growth phase (SG) is gonadotropin-dependent and starts with the appearance of cortical alveoli or/and oil droplets (CA1, CA2, CA3 stages), followed by the vitellogenesis process, with the accumulation of yolk in the cytoplasm and the increase of oocyte size (VTG1, VTG2, VTG3 stages) (Lubzens et al. 2010; Luckenbach et al. 2008; Wallace and Selman 1981; Brown-Peterson et al. 2011). Then, the oocyte maturation begins with the migration of the nucleus to the animal pole (GVM1 and GVM2 stages), and the first meiotic division resumes (Grier 2000). After that, the germinal vesicle breakdown (GVBD) and the hydration phase (HYD) take place before the ovulation (Grier 2000) (**Fig.1.1**). This process is especially pronounced in species that spawn pelagic eggs (Murua and Saborido-Rey 2003). In ovulation, the eggs are released from the follicular complex into the ovarian lumen, and the second meiotic division is performed (Grier 2000). The dynamics and the recruitment pattern of oocytes in the ovary range among fish species.

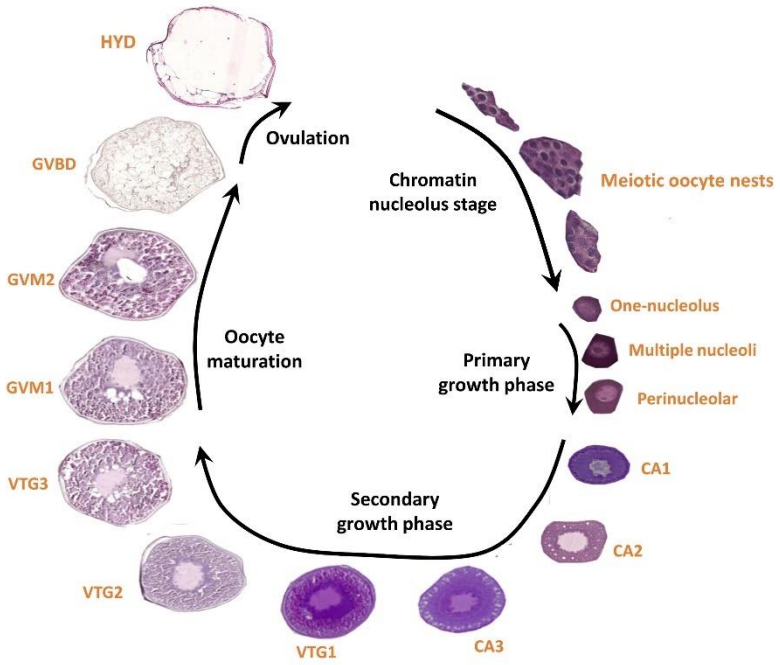

Figure 1.1. *Sardina pilchardus*. Phases of development (black colour) and oocyte stages (orange colour) during oogenesis.

Εικόνα 1.1. *Sardina pilchardus*. Φάσεις ανάπτυξης (μαύρο χρώμα) και στάδια ωοκυττάρων (πορτοκαλί χρώμα) κατά τη διάρκεια της ωογένεσης.

The dynamics of oogonia and early oocytes during the reproductive cycle have received little attention, despite the evidence that primary growth oocytes regulate fish fecundity (Tokarz, 1978; Wildner et al. 2013; Thome et al. 2012; dos Santos Schmidt et al. 2017). Furthermore, little attention has been given to the seasonal recruitment pattern from early (chromatin nucleolus stage) oocytes to PG oocytes. The majority of research has focused on PG oocytes dynamics and SG oocytes recruitment (e.g., Greer- Walker et al. 1994; Kjesbu 2009; Korta et al. 2010; Kjesbu et al. 2011; Schismenou et al. 2012; Grier et al. 2018; Mouchianitis et al. 2019; Mouchianitis et al. 2020; Serrat et al. 2019). Methods,

such as the oocyte packing density method (OPD) (Thorsen and Kjesbu 2001; Kurita and Kjesbu 2009; Korta et al. 2010), facilitated the quantification of smaller oocytes, mainly PG oocytes, but the quantitative study of chromatin nucleolus oocytes remained difficult due to their large accumulations within the oocyte nests. On the other hand, the SG oocyte dynamics have been extensively examined at several temporal scales and in many different fish species (e.g., Ganias et al. 2004; Murua and Motos 2006; Ganias et al. 2017).

1.3. Fecundity type

An important process during oogenesis is the time that the oocytes are recruited from the PG to the SG phase according to the spawning period, which defines the fecundity type of fish (determinate vs indeterminate) (Hunter et al. 1992; Kjesbu 2009; Pavlov et al. 2009; Ganias 2013) (see below **Section 1.4**). Specifically, in fish with determinate fecundity type, the oocyte recruitment from PG to SG phase is completed before the onset of the spawning period (**Fig. 1.2**), whereas in fish with indeterminate fecundity type, new oocytes are recruited to the SG phase throughout the spawning period and during the spawning activity, resulting in an overlap of the secondary growth oocytes recruitment and the spawning period to some extent (**Fig. 1.2**).

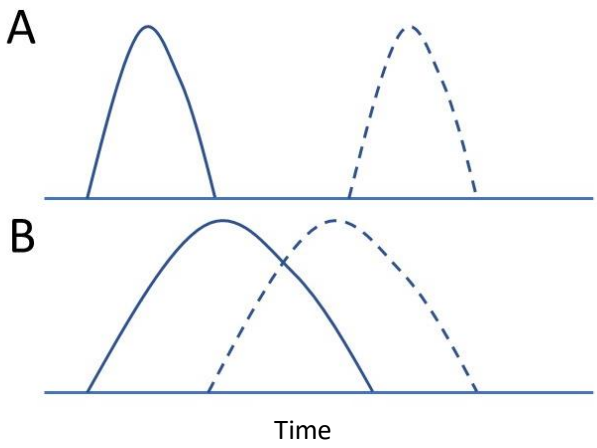

Figure 1.2. Temporal correlation between oocyte recruitment from primary to secondary growth phase (solid line) and spawning period (dashed line). A) clear temporal distinction determines the determinate fecundity type, and B) temporal overlap defines the indeterminate fecundity type. Adapted from Ganias (2013).

Εικόνα 1.2. Χρονική συσχέτιση μεταξύ εισδοχής ωοκυττάρων από την πρώιμη στη δευτερογενή φάση ανάπτυξης (συμπαγής γραμμή) και την περίοδο ωοτοκίας (διακεκομμένη γραμμή). Α) πλήρης χρονικός διαχωρισμός ορίζει το καθορισμένο τύπο γονιμότητας, και Β) χρονική επικάλυψη ορίζει τον απροσδιόριστο τύπο γονιμότητας. Προσαρμοσμένο από Ganias (2013).

Total spawners have determinate fecundity type since all SG oocytes to be spawned develop at the same time. On the contrary, batch spawners spawn multiple times throughout a spawning period, and fecundity type is often defined by the ratio of the oocyte growth period (OGP) to the spawning period (Rideout et al. 2005; Ganias et al. 2015; Ganias and Lowerre-Barbieri 2018) (see below **Section 1.4**).

Assessing the relationship between OGP and the duration of the spawning period, simulations of fecundity type demonstrated that both water temperature and latitudinal distributions have an impact on OGP and spawning period and that SG oocyte recruitment patterns on their own are not indicative of fecundity type (Ganias et al. 2015; Ganias and Lowerre-Barbieri 2018). This has significant consequences as waters warm under climate change scenarios in northern climates resulting in shorter OGPs and potential shifts in fecundity type.

1.4. Implications of oogenesis and fecundity type to spawning stock biomass assessment (SSB) estimates through egg production methods

The fecundity type is an important parameter for estimating fish stock reproductive potential and selecting the appropriate egg production method (EPM) for estimating spawning-stock biomass (SSB). SSB is widely used for the determination of stock- recruit curves and for the estimates of SSB trends to investigate the threshold point where the population recruitment is weakened (Hunter et al. 1985; Alheit 1993; Lo et al. 1993; Marshall et al. 1999; Stratoudakis et al. 2006; Armstrong and Witthames 2012) (see **BOX-1**). For fish with planktonic eggs, three egg production methods have been developed (see Armstrong and Witthames 2012; Stratoudakis et al. 2006), the Daily Egg Production Method (DEPM; Parker 1980), the Annual Egg Production Method (AEPM; Lockwood et al. 1981; Saville 1964), and the Daily Fecundity Reduction Method (DFRM; Lo et al. 1992, 1993). All of the aforementioned methods can be used on determinate spawners selected based on their reproductive biology, but only DEPM is intended for use on indeterminate species. The primary distinction between DEPM and the other two methods is the estimation of fecundity. For species with determinate fecundity type, the potential annual fecundity is assessed based on the total number of developing oocytes before the commencement of the spawning, since the recruitment of oocytes to the vitellogenic pool ended before the spawning period (Murua and Saborido-Rey 2003). In species with indeterminate fecundity, where oocyte recruitment is continuous during the spawning period, potential annual fecundity is estimated by parameters such as the number of oocytes spawned per batch (i.e., batch fecundity, F_B), the spawning fraction (i.e., the percentage of females spawned per day), and the duration of the spawning period (Parker 1980; Hunter et al. 1985; Murua and Saborido-Rey 2003). The spawning fraction is a population parameter and the most widely used for estimates of spawning frequency (f; i.e., the number of spawning events per unit time) in DEPM applications. Spawning frequency can be also assessed through an individual parameter, spawning interval (ISI; i.e., the time lag between subsequent spawning events; Wootton 1974).

The most common method for calculating spawning fraction in multiple spawning fish is through the postovulatory follicle method (POF method) (Parker 1980). For the application of the POF method, POFs must be aged (time lag between spawning and sampling) and grouped into daily cohorts to identify the number of recent spawners, whose averaged fraction in the mature population provides an estimate of spawning fraction (Hunter and Macewicz 1985; Ganias 2013). Despite its popularity, the method can be quite inaccurate when its criteria are applied to other species and populations without prior validation (Stratoudakis et al. 2006; Ganias 2012). New approaches and procedures have been developed for the improvement of the application of egg production methods, especially in

technical aspects (Stratoudakis et al. 2006). However, expanding the knowledge and evaluating the parameters, such as oocyte growth rate, spawning fraction, and spawning interval in species with indeterminate fecundity, is important for proper application of DEPM for more accurate SSB estimates (e.g., Ganias et al. 2011; Uriarte et al. 2012).

BOX-1. Methods for the spawning stock biomass (SSB) estimates

The most frequently used method to estimate SSB in fish species with planktonic eggs is egg production methods (EPM) by combining egg production estimations from ichthyoplankton surveys with estimations of fecundity per unit biomass from a representative sampling of mature fish at the proper time (Hunter and Lo 1993). Despite their high accuracy, egg production methods are expensive to use, and in order to avoid biases, certain guidelines must be followed, including careful survey design and data collection, and the selection of the appropriate method based on the reproductive biology and behaviour of the target species (Hunter and Lo 1992, 1993). For the precise definition of the fecundity type and the application of the most suitable egg production method for each fish species, knowledge of oocyte growth and development as well as the reproductive biology of fish is particularly important.

Despite the extensive utilization of the fecundity type in fisheries management, the fecundity type of many fish stocks remains controversial. Four lines of evidence have traditionally been used to assess fish fecundity type, i.e., whether it is determinate or indeterminate (Hunter et al. 1989; Hunter et al. 1992; Greer Walker et al. 1994; Murua and Saborido-Rey 2003; Armstrong and Witthames 2012). Briefly, these criteria include, i) the presence (determinacy) or absence (indeterminacy) of a hiatus between PG and SG oocytes in mature ovaries (SG recruitment), ii) the seasonal dynamics in the number and size of advanced vitellogenic oocytes, iii) the co-occurrence of recent and imminent spawning markers and iv) the intensity of atresia along the spawning period (depending on when it appears one or the other strategy is considered). Recent methodological advancements in the quantification of PG oocytes (Kurita and Kjesbu 2009; Korta et al. 2010; Kjesbu et al. 2011; Ganias et al. 2015; Mouchlianitis et al. 2019; Serrat et al. 2019; Anderson et al. 2020) not only have improved our general understanding of oocyte recruitment processes in both indeterminate (e.g., European hake, *Merluccius merluccius*; Korta et al. 2010) and determinate (e.g., cod, *Gadus morhua*; Kjesbu et al. 2010) spawners, but have remarkably contributed in revising the aforementioned criteria. For instance, after their detailed assessment of PG oocytes, Serrat et al. (2019) concluded that indeterminacy in European hake is ambiguous as the pool of late previtellogenic oocyte stages corresponds to the potential fecundity which is a characteristic of determinate spawners. Ganias et al. (2017) used a revised set of criteria to show that horse mackerel, *Trachurus trachurus*, ceases SG recruitment during the latter part of the spawning period, reflecting its controversial fecundity pattern (Karlou-Riga and Economidis 1996). The cessation of SG recruitment during the spawning period has also been observed in Gulf menhaden, *Brevoortia patronus* (Brown-Peterson et al. 2017), in blueback

herring, *Alosa aestivalis* (Mouchlianitis et al. 2020) and in picarel, *Spicara smaris* (Karlou-Riga et al. 2020). Schismenou et al. (2012) showed for the European anchovy, *Engraulis encrasicolus*, another indeterminate spawner, that recruitment during the ovulatory cycle occurs in pulses of very short duration, replenishing ovulated oocytes and maintaining a dynamic balance between spawned and recruited oocyte batches. Mouchlianitis et al. (2020) similarly suggested a pulsating oocyte recruitment pattern for the Macedonian shad, *Alosa macedonica* that is triggered by the hydration of the spawning batch. All these assessments show the complexity of fish spawning dynamics that has been ignored until recently.

Moreover, both biological and ecological mechanisms that lead to one or the other fecundity type remain unknown. In general, fecundity type is a dynamic characteristic influenced by many factors. The most accepted theory combines the fecundity type of fish species with its latitudinal distribution (Hunter et al. 1985; Ganias 2013; Ganias et al. 2015; Ganias and Lowerre-Barbieri 2018). Specifically, Hunter et al. (1985) suggested that species with boreal geographic distributions exhibit determinate fecundity type, whereas species from tropical and temperate environments display indeterminate fecundity type. This theory was also supported by other studies (e.g., Witthames and Greer-Walker 1995; Wuenschel et al. 2013; McBride et al. 2016). Another theory correlates the fecundity types with seasons, such as determinate spawners spawn during the winter, while the indeterminate spawners during the summer (Rijnsdorp and Witthames 2005; Kjesbu 2009; Ganias and Lowerre-Barbieri 2018). Another approach reveals that the strategy of allocating energy to reproduction determines the type of fecundity (Rijnsdorp and Witthames 2005; Kjesbu and Witthames 2007; Kjesbu 2009; Armstrong and Witthames 2012). Capital breeders, for example, require food resources ahead of time in preparation for offspring production, whereas income breeders, who consume food concurrently with offspring production and do not store food in reservoirs, typically demonstrate indeterminate fecundity. Therefore, fecundity type is well recognized as an ecophenotypic reaction to environmental conditions. However, other factors contribute to fecundity type regulation, such as genetic drivers (Kjesbu and Witthames 2007; Ganias 2013), hence this issue requires further research.

1.5 Species selection and the main scientific questions

The purpose of this study was to shed light on previously undiscovered aspects of different phases of oogenesis in highly commercial pelagic fish species with distinct spawning dynamics and to show the link between the spawning and ovarian dynamics, as well as how both shape the fecundity type of species and their impact on the applicability of current egg production methods. Oogenesis was split into two phases for the sake of this study: early oogenesis (**Chapter 3**), including the oogonia and early oocytes dynamics up to the secondary growth phase, and secondary oogenesis (**Chapter 4**), containing dynamics of the secondary growth oocytes up to ovulation (**Fig. 1.3**).

Specifically, in the early phase of oogenesis (**Chapter 3**), the fine structure of early oocytes during development as well as the oogonial proliferation and the early oocytes dynamics throughout the reproductive cycle were investigated in two pelagic fish species, the Mediterranean sardine (*Sardina*

pilchardus) and European anchovy (*Engraulis encrasicolus*) with indeterminate fecundity type and opposite spawning periods. These species were selected due to a lack of prior study on their oogonial proliferation and early oocyte dynamics, as well as their cytoplasmic development. The early phase of oogenesis has been received little attention especially in indeterminate fish species because of the complexity of their ovarian dynamics and the continuous recruitment from PG to SG oocytes. Thus, these two species were selected as both are indeterminate spawners as well as multiple batch spawners, releasing many oocyte batches during the spawning period. Despite the common fecundity type, these two species were also selected to contrast the early oogenesis dynamics as they exhibit distinct spawning interval (**sardine**: ~10-11 days, Ganias et al. 2011; **anchovy**: ~2-4 days, Somarakis et al. 2004; Somarakis et al. 2012), opposite spawning periods [**sardine**: autumn to spring (Bandarra et al. 2018; Ganias et al. 2007b; Stratoudakis et al. 2007; Ganias 2009); **anchovy**: spring to autumn (Somarakis et al. 2004; Somarakis 2005)], and different feeding strategies (**sardine**: capital breeder; **anchovy**: income breeder). In particular, sardine restores energy for the spawning period, indicating a capital breeding strategy (Ganias et al. 2007b; Mustac and Sinovcic 2009; Nunes et al. 2011; Zwolinski et al. 2001). Besides stored energy, little evidence demonstrates direct energetic transfer from food to reproduction, taking opportunistic advantage of food availability during spawning, especially in the Mediterranean Sea, which is a highly oligotrophic habitat (Garrido et al. 2008; Ganias 2009). Anchovy reproduces during the warm months of the year (spring to autumn) when the food supplies are abundant, and exhibit an income feeding strategy, allocating energy directly to reproduction (Somarakis et al. 2004; Somarakis 2005).

To investigate the secondary phase of oogenesis (**Chapter 4**), the ovarian dynamics (including oocytes and postovulatory follicles dynamics) were examined in the Atlantic sardine (*Sardina pilchardus*), the Atlantic mackerel (*Scomber scombrus*), and the Atlantic horse mackerel (*Trachurus trachurus*)—three pelagic fish species with different spawning dynamics. The Atlantic sardine was selected because it has well-known ovarian and spawning dynamics (spawning interval= ~10-11 days, Ganias et al. 2011; Oocyte growth rate= 45 days, Ganias et al. 2014a; Spawning period= 90 days, Stratoudakis et al. 2007). Sardine exhibits an indeterminate fecundity type, matching all the traditional criteria (**Section 1.4**). The Atlantic mackerel was chosen due to its short spawning interval (~1.6-5 days, Priede and Watson 1993), the low oocyte growth rate (OGP=140-150 days, Greer- Walker et al. 1994; more than 200 days ICES 2012), spawning period equal to 90 days (Costa et al. 2006) and the lack of knowledge regarding its ovarian dynamics (Priede and Watson 1992; Ganias et al. 2018; dos Santos Schmidt et al. 2021). Mackerel has been considered a determinate spawner so far (Greer- Walker et al. 1994), however, recent studies show evidence of indeterminacy (Ganias et al. 2018; dos Santos Schmidt et al. 2021). The Atlantic horse mackerel was chosen since it has an intermediate spawning interval compared to the other two species (~6 days, Karlou-Riga and Economidis 1997), a short oocyte growth period (OGP), a spawning period of 180 days (Costa 2009; Ganias et al. 2017), and its ovarian dynamics have received little attention (Macer 1974; Karlou-Riga and Ekonomidis et al. 1997; Gordo et al. 2008; van Damme et al. 2014; Ganias et al. 2017). The horse mackerel has a controversial fecundity type that exhibits varied traits (**Section 1.4**; Macer 1974; Karlou-Riga and Ekonomidis et al. 1997; Gordo et al. 2008, van Damme et al. 2014, Ganias et al. 2017). Until 2004, horse mackerel was considered a

determinate spawner, and its SSB was estimated using AEPM (ICES 1993, 1994, 2002). However, evidence suggests that horse mackerel fecundity is most probably indeterminate (Karlou-Riga and Economidis 1997; Gordo et al. 2008; Ndjaula et al. 2009; Ganias et al. 2017), and the method used for SSB estimations has been re-evaluated using the DEPM since 2007 (ICES 2003, 2012; Goncalves et al. 2009).

The main scientific questions are summarized below:

Q1. Are there differences in the fine structure of oocytes during the primary and early secondary growth phases in closely related phylogenetic fish species?
Q2. Are the dynamics of oogonial proliferation and early oocytes throughout the reproductive cycle identical in fish species with the same fecundity type?
Q3. What is the relationship between spawning and ovarian dynamics, (SG oocytes and postovulatory follicles (POFs) cohorts dynamics), and how do they affect fecundity type and other fecundity parameters in fish species with distinct spawning dynamics?

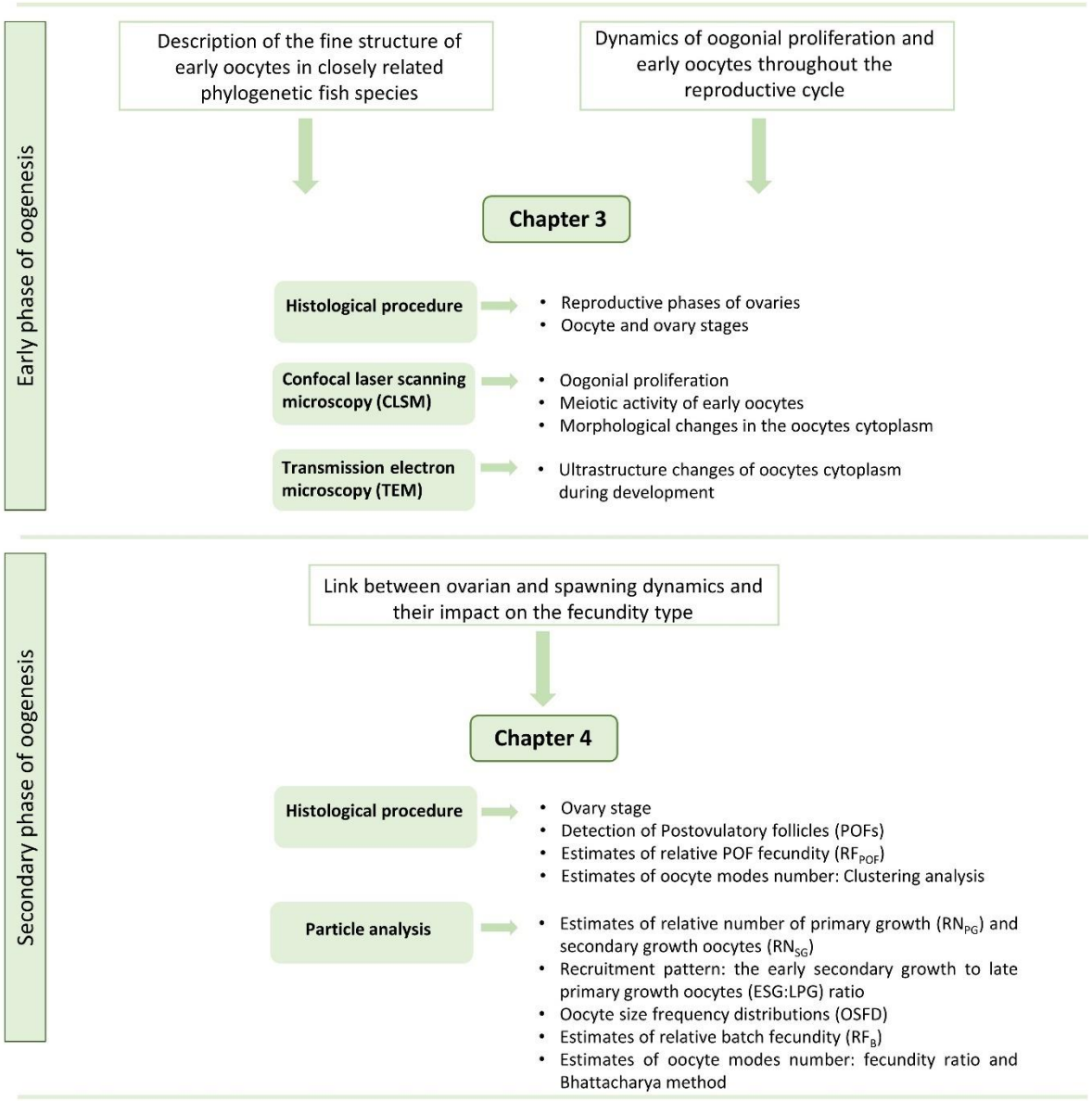

Figure 1.3. Summary of the thesis structure, showing the methodology followed in each chapter to answer the main scientific questions (Q1-3; White boxes) investigating the two phases of oogenesis.

Εικόνα 1.3. Σύνοψη της δομής της διδακτορικής μελέτης, που δείχνει τη μεθοδολογία που ακολουθήθηκε σε κάθε κεφάλαιο για να απαντηθούν τα κύρια επιστημονικά ερωτήματα (Q1-3; Λευκά πλαίσια) που διερευνούν τις δύο φάσεις της ωογένεσης.

Chapter 2: Methodology

2.1 Samples collection

For **Chapter 3**, a total of 240 female anchovies, *Engraulis encrasicolus*, and 320 female sardines, *Sardina pilchardus*, were collected from the local commercial purse seine fishery in the North Aegean Sea during one-year monthly samplings (2019- 2020) (**Fig. 2.1**).

Figure. 2.1. Sampling areas (green colour) of European anchovy, *Engraulis encrasicolus*, and Mediterranean sardine, *Sardina pilchardus* in the North Aegean Sea.

Εικόνα 2.1. Περιοχές δειγματοληψίας (πράσινο χρώμα) του ευρωπαϊκού γαύρου, *Engraulis encrasicolus,* και της Μεσογειακής σαρδέλας, *Sardina pilchardus* στο βόρειο Αιγαίο.

For **Chapter 4**, ovarian samples of Atlantic sardine, *Sardina pilchardus*, Atlantic horse mackerel, *Trachurus trachurus*, and Atlantic mackerel, *Scomber scombrus,* fixed in 10% neutral buffered formalin, were provided by European fisheries research institutes (**Table 2.1**) collected in the Northeast Atlantic (off Portugal and the Bay of Biscay) at or near their spawning peak as part of national egg production surveys (**Fig. 2.2**). Specifically, the Atlantic sardine was collected from March to May (spawning peak between March and April; Stratoudakis et al. 2007), the Atlantic horse mackerel from March to April (spawning peak between February and April; Borges and Gordo 1991), and the Atlantic mackerel samples from February to April (spawning peak from March to June; Olafsdottir et al. 2019).

Table 2.1. The number of samples of each species sent by the European fisheries research institutes.

Πίνακας 2.1. Αριθμός δειγμάτων κάθε είδους τα οποία στάλθηκαν από Ευρωπαικά ερευνητικά ινστιτούτα αλιείας.

Institute	Number of samples	Species
AZTI	79	Atlantic sardine *Sardina pilchardus*
	10	Atlantic mackerel *Scomber scombrus*
IEO	72	Atlantic sardine *Sardina pilchardus*
	72	Atlantic mackerel *Scomber scombrus*
IPMA	81	Atlantic sardine *Sardina pilchardus*
	91	Atlantic horse mackerel *Trachurus trachurus*
IMARES	76	Atlantic mackerel *Scomber scombrus*

AZTI: Ciencia y technologia marina y alimentaria
IEO: Instituto Español de Oceanografía
IPMA: Portuguese Institute for Sea and Atmosphere
IMARES: Wageningen Marine Research (Institute for Marine Resources and Ecosystem Studies)

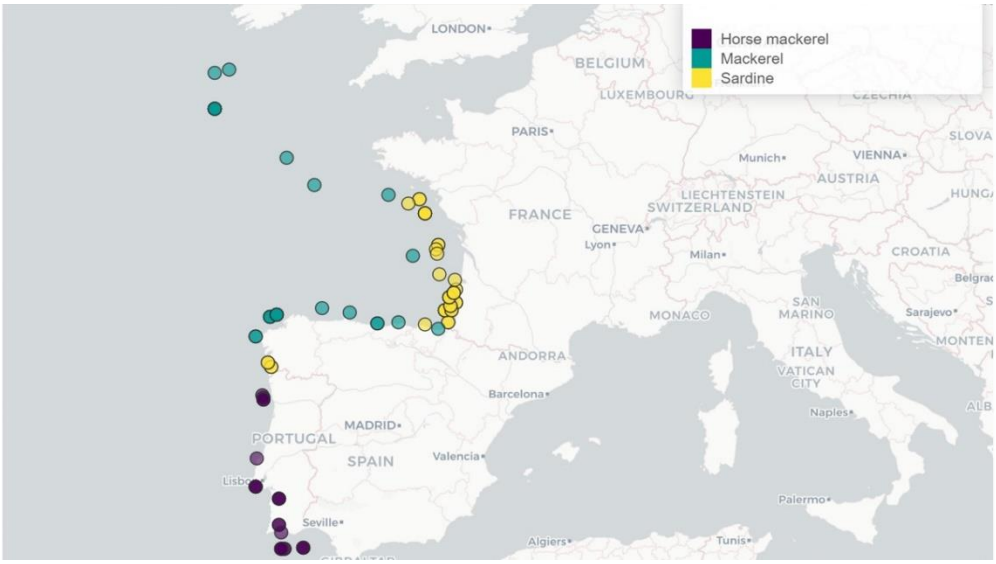

Figure 2.2. Sampling area of Atlantic sardine, *Sardina pilchardus*, Atlantic horse mackerel, *Trachurus trachurus*, and Atlantic mackerel, *Scomber scombrus*. The different species are indicated with different colours.

Εικόνα 2.2. Περιοχές δειγματοληψίας της σαρδέλας του Ατλαντικού, *Sardina pilchardus*, του γκριζοσαύριδου του Ατλαντικού, *Trachurus trachurus* και του σκουμπριού του Ατλαντικού, *Scomber scombrus.* Τα διάφορα είδη υποδεικνύονται με διαφορετικά χρώματα.

2.2 Samples processing

Fishes were collected and immediately after capture, were sexed and females were measured for total weight (W_T, 0.1 g), eviscerated weight ($W_{ev.}$, 0.1 g), viscerated weight (without gonads) (W_v, 0.1g) and gonad weight (OW, 0.1 g). Ovarian samples were fixed for histological analysis, confocal laser scanning microscopy (CLSM), and transmission electron microscopy (TEM) observations.

2.3 Histological procedure

The ovaries were fixed in 10% neutral buffered formalin for histological analysis. In the laboratory, a small piece of tissue was removed from the center of one ovarian lobe and was then subjected to histological analysis using paraffin embedding (sections~4 mm) and haematoxylin/eosin or haematoxylin/eosin/safran staining.

For **Chapter 3**, a total of 186 ovarian subsamples were processed histologically (embedded in paraffin, sectioned at 4 µm thickness, and stained with haematoxylin/eosin staining). The histological slides were digitized into high-resolution (2.3 MP) pictures using a Basler acA1920-40uc microscopy camera (Ahrensburg, Germany) mounted on a Zeiss Axio Lab. A1 light microscope (Jena, Germany) and Microvisioneer's manualWSI software (Esslingen am Neckar, Germany) (**Fig. 2.3A and C**). This analysis was carried out at the Aristotle University of Thessaloniki. Histological micrographs were used to assess the reproductive phase of each ovary (i.e., developing, spawning-capable, etc) (Grier et al. 2009; Brown-Peterson et al. 2011) (see **Annex 1**), as well as the oocyte stages and ovary stages (see details in **Section 1.1**).

In **Chapter 4**, the ovarian samples were processed histologically (sardine and mackerel: paraffin, 4 µm sections, haematoxylin/eosin staining; horse mackerel: historesin, 4 µm sections, haematoxylin/ eosin/ safran staining). Histological sections were scanned in high-resolution micrographs using a digital slide scanner (NanoZoomer S60 Digital Slide Scanner, Hamamatsu) (**Fig. 2.3A and B**). This procedure was performed at the laboratory facilities of the Institute of Marine Research (IMR) in Bergen. The ovaries were classified into stages based on the most advanced cohort of oocytes according to Brown-Peterson et al. (2011) (see details in **Section 1.1**) and those belonging to vitellogenic (VTG), germinal vesicle migration (GVM), germinal vesicle breakdown (GVBD), and hydration (HYD) stages were selected for further analysis. In total, 41 sardine, 22 horse mackerel, and 27 mackerel ovaries were used for the estimation of secondary growth oocytes cohorts. For POFs analysis, ovaries from 152 Atlantic sardines and 158 Atlantic mackerels were analysed. Specimens containing POFs were selected for further scrutiny and measured for the cross-sectional area of each

individual POF (POF_{xsa}, μm^2). The number of POFs cohorts for both species was investigated through detailed screening of histological slides for possible co-occurrence of different POF stages. The volume fraction of POFs (V_i) and the POFs density (N_v) were estimated through histological slides, for the calculation of relative POF fecundity (number of POFs per gram eviscerated body weight; $RF_{POF} = F_{POF}/W_{EV}$). Two methods were applied the Weibel method (Weibel et al. 1966) and the adjusted for POFs packing density method (POFPD) (Kjesbu et al. 2011) (see **ANNEX 2** and **3**).

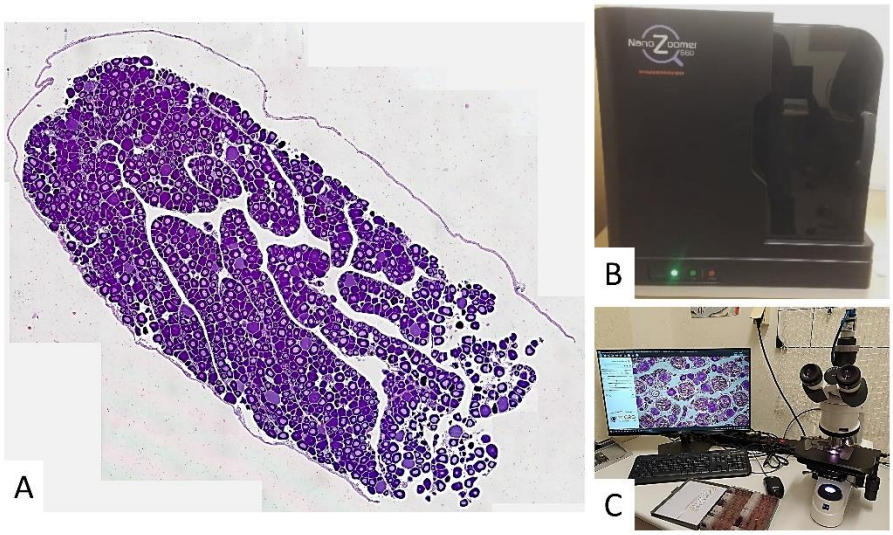

Figure 2.3. Equipment for histological analysis. A) Photomicrograph of an ovarian histological section, B) NanoZoomer S60 slide scanner, and C) BASLER acA1920-40uc camera and Zeiss Axio Lab.A1 microscope image capturing system.

Εικόνα 2.3. Εξοπλισμός για Ιστολογική ανάλυση. Α) Φωτομικρογραφία ιστολογικής τομής ωοθήκης, Β) NanoZoomer S60 σαρωτής ιστολογικών τομών, και C) Σύστημα λήψης εικόνας με κάμερα BASLER acA1920-40uc και μικροσκόπιο Zeiss Axio Lab.A1.

2.4 Whole-mount procedure

In **Chapter 4**, the ovarian samples were analysed through whole mount procedures. Subsamples of ovarian tissue of 0.05–0.1 g, depending on the ovarian stage, were dissected and weighed (OWs, 0.001 g). Oocytes were separated ultrasonically (Vibra-Cell VCX 130FSJ, Sonics & Materials Inc., US: 130 Watt, 50% amplitude, for 10 s; see also Anderson et al. 2020) (**Fig. 2.4A**), sieved (50 µm mesh) to discard oogonia and very small primary growth oocytes and stained with toluidine blue. The whole mount was captured under a Jenoptik Progress C3 camera and a Euromex NZ 80 stereomicroscope (**Fig. 2.4B**). This procedure was performed at the Institute of Marine Research (IMR) in Bergen. The oocyte number and diameter were automatically measured using the open-source image analysis program ImageJ (v. 1.52, https://imagej.nih.gov/ij/) with the plugin ObjectJ (https://sils.fnwi.uva.nl/bcb/objectj/) and an adapted variant of the elliptical oocytes project (https://sils.fnwi.uva.nl/bcb/objectj/examples/oocytes/Oocytes.htm) (see Thorsen and Kjesbu 2001; Ganias et al. 2010; Ganias et al. 2014b; Anderson et al. 2020). Oocyte size frequency distributions were

generated and the threshold diameter values between primary and secondary growth oocytes were determined for each species (see **Annex 4**) to estimate the relative number of primary growth oocytes (RN_{PG}, oocytes*g^{-1}), the relative number of secondary growth oocytes (RN_{SG}, oocytes*g^{-1}) and the relative batch fecundity (RF_B, oocytes*g^{-1}) using the gravimetric method (see **Annex 5**). Also, the advanced mode (AM) of each oocyte size frequency distribution was determined, and the batch fecundity (F_B) was assessed through the advanced mode (AM) corresponding to the spawning batch.

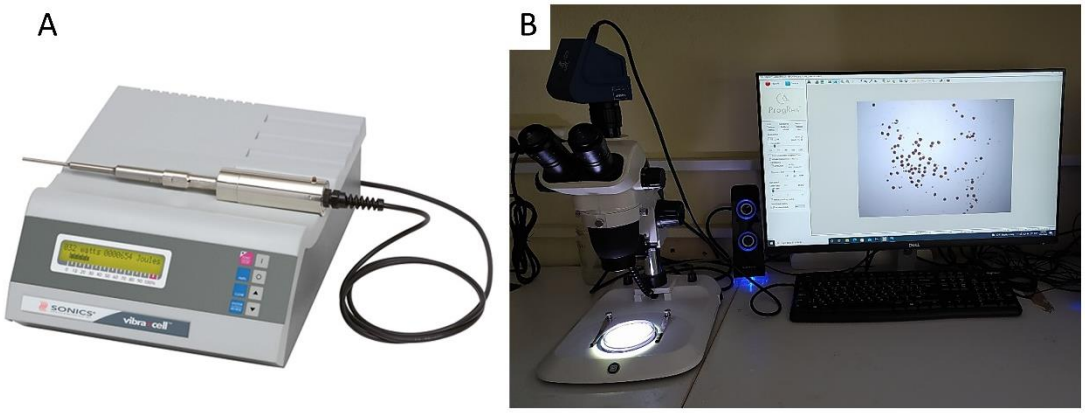

Figure 2.4. Equipment for particle analysis. A) Ultrasonic system Vibra-Cell VCX 130FSJ for separation of oocytes, B) Stereomicroscope image capturing system consisted of a Jenoptik Progress C3 camera and a Euromex NZ 80 stereo microscope.

Εικόνα 2.4. Εξοπλισμός για ανάλυση σωματιδίων. Α) Σύστημα υπερήχων Vibra-Cell VCX 130FSJ για διαχωρισμό ωοκυττάρων, Β) Σύστημα λήψης φωτογραφιών αποτελούμενο από κάμερα Jenoptik Progress C3 και στερεοσκόπιο Euromex NZ 80.

2.5 Confocal laser scanning microscopy (CLSM) procedure

In **Chapter 3**, a total of 186 ovarian samples were processed for CLSM observations carried out at the Aristotle University of Thessaloniki. Specifically, an ovarian subsample from the centre of each lobe was fixed in 8% paraformaldehyde (PFA) in phosphate buffered saline (PBS) (pH 7.2) for 2 h, and then stored in PBS at 4°C in preparation for CLSM observations. The ovarian samples were first washed in PBS. Then, the stored samples were first incubated in a 0.3% aqueous solution of 3,3'-dihexyloxacarbocyanine iodide ($DiOC_6$) (Panteris et al. 2004) for 1 h in the dark and washed 3 times in PBS for staining of membranous structures (mitochondria, endoplasmic reticulum, etc.). They were then immersed in DAPI [0.9 mM stock solution of 4',6-diamidino-2-phenylindole in DMSO and further diluted 1:1000 in PBS (Pappas et al. 2020)] for 2 h in the dark and washed 3 times in PBS to stain DNA (tubulin protein). The subsamples were mounted between the microscope slide and coverslip with a PBS and glycerol mixture (1:2 v/v) supplemented with 0.5% (w/v) p-phenylenediamine as an anti-fade agent. Ovarian subsamples were examined under a Zeiss Observer.Z1 (Carl Zeiss AG, Munich, Germany) microscope, equipped with the Zeiss LSM780 CLSM module, with suitable filters for each

stain (**Fig. 2.5**). ZEN2011 software was used, according to the manufacturer's instructions. This technique provides a 3D representation of the oocytes.

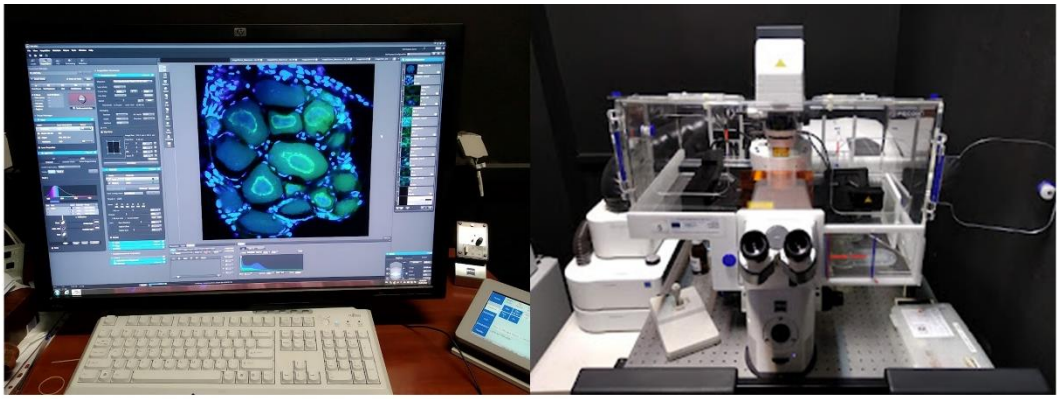

Figure 2.5. Confocal laser scanning microscope (CLSM): Zeiss Observer.Z1 inverted microscope, equipped with Zeiss LSM780 CLSM module.

Εικόνα 2.5. Συνεστιακό μικροσκόπιο σάρωσης laser (CLSM): ανάστροφο μικροσκόπιο Zeiss Observer.Z1, εξοπλισμένο με τη μονάδα Zeiss LSM780 CLSM.

CLSM was used to examine the following: 1) the dynamics of oogonial proliferation as well as the meiotic activity of early oocytes throughout the reproductive cycle, and 2) changes in the oocyte cytoplasmic morphology during early oogenesis.

2.6 Transmission electron microscopy (TEM) procedure

In **Chapter 3**, a total of 8 subsamples were prepared for TEM observations performed (Aristotle University of Thessaloniki). In particular, small pieces of the ovaries were fixed overnight in 3% (v/v) glutaraldehyde in 50 mM sodium cacodylate buffer, pH 7. The samples were then post-fixed in 1% (w/v) osmium tetroxide in the same buffer at 4°C for 3.5 h, dehydrated in an acetone series, and embedded in Durcupan resin (Sigma, Taufkirchen, Germany). Ultrathin sections (70–90 nm) were contrasted with uranyl acetate and lead citrate and observed with a JEOL JEM 1011 TEM (JEOL Ltd., Tokyo, Japan) at 80 kV. Electron micrographs were acquired with a Gatan ES500W (Gatan, Pleasanton, CA, USA) digital camera with Digital Micrograph 3.11.2 software. Transmission electron micrographs were processed using Adobe Photoshop CC 2015.

TEM was used to examine the changes in the fine structure of oocytes during their development in early oogenesis. Specifically, the cytoplasmic asymmetry was examined focusing on the development of the Balbiani body in the primary growth phase and the cytoplasmic zonation observed during the early secondary growth phase. In addition, changes in the morphology of mitochondria were studied during the early development of oocytes. These changes were contrasted between species.

2.7 Statistical analysis

All statistical analyses were carried out in RStudio 1.1.456 (R Core Team 2020). In all Chapters, data visualization was carried out with ggplot2 (Wickham 2016), ggpubr (Kassambara 2019), ggjoy (Wilke 2018), and factoextra (Kassambara and Mundt 2020) packages.

In **Chapter 3**, the prevalence (presence/absence) of each marker of oogonial proliferation (mitotic divisions, oogonia nests) and meiotic divisions (leptotene, zygotene, pachytene, diplotene) was recorded in the ovaries among the reproductive phases. Principal component analysis (PCA) was used to synthetically examine the activity of cell divisions (mitosis/meiosis). Specifically, PCA was used to examine the potential correlation between the distribution pattern of the markers and reproductive phases. The packages dplyr (Wickham et al. 2023) and factoMineR (Le et al. 2008) were used to perform PCA analysis. If present, intrinsic patterns in the multidimensional swarm of different markers would emerge within a plot of the first two or three components. A component was considered to explain a significant proportion of the variance in the multidimensional data set when its associated eigenvalue was greater than 1.0. These significant PCA scores served as an activity index (PC_{ACT}) of cell divisions throughout the reproductive cycle. Non-parametric statistical comparisons of PC_{ACT} among the three reproductive phases were performed through the Kruskal Wallis test (Kruskal and Wallis 1952) and Dunn's test in conjunction with the Bonferroni post-hoc adjustment (Dunn 1961). The prevalence of each marker of oogonial proliferation and meiotic divisions was compared among the three reproductive phases using the Chi-square test.

In **Chapter 4**, the oocytes size frequency distribution plots were visualized using the ggjoy package. The clustering analysis was performed with the Stats (R Core Team 2020) package, which used the K-means algorithm (see **Section 4.2.3**). To estimate the best number of groups for the K-means analysis, the NbClust (Charrad et al. 2014) package was utilized. For the Silhouette analysis, the Cluster package was used to evaluate clustering results. The normality of data was tested using the Shapiro test (Shapiro and Wilk 1965). Pairwise comparisons with corrections for multiple testing were done. Specifically, for parametric data, a one-way ANOVA test (Girden 1992) was implemented, and if the results were significant, Tukey's test (Tukey 1949) was applied. For non-parametric data, the Kruskal Wallis test (Kruskal and Wallis 1952) was applied, and when results were significant, a Pairwise Wilcoxon Rank Sum Test (Wilcoxon 1945) was performed in conjunction with the Benjamini–Hochberg post hoc adjustment (Benjamini and Hockberg 1995), and in some cases the Welch's test (Welch 1947) was applied.

Chapter 3: Description of oocyte development during early oogenesis and investigation of the oogonial proliferation and early oocyte dynamics throughout the reproductive cycle in Clupeiform fishes

These results have been published in the scientific articles:
Charitonidou K., Panteris E., Ganias K. (2022a). Ultrastructural changes in mitochondria during oogenesis in two phylogenetically close fish species. *Journal of Morphology*, 283: 502-509.

Charitonidou K., Panteris E., Ganias K. (2022c). Balbiani body formation and cytoplasmic zonation during early oocyte development in two Clupeiform fishes. *Journal of Fish Biology*, 100: 1223-1232.

Charitonidou K, Panteris E, Ganias K. (2022d). Oogonial proliferation and early oocyte dynamics during the reproductive cycle of two Clupeiform fish species. *Journal of Fish Biology*, 102: 44-52.

3.1 Specific objectives

This chapter presents aspects of oocyte developmental changes during early oogenesis in two Clupeiform fish species, the European anchovy, *Engraulis encrasicolus*, and the Mediterranean sardine, *Sardina pilchardus*, which can be utilized as markers for oocyte recruitment and dynamics identification. Light microscopy, transmission electron microscopy (TEM), and confocal laser scanning microscopy (CLSM) observations were used to investigate and compare changes in fine structure of oocytes throughout the early development in the two species. In particular, the mitotic and meiotic divisions of chromosomes were investigated in chromatin nucleolus oocytes, as well as the cytoplasmic asymmetry [Balbiani body (Bb) formation] that develops in primary growth oocytes, and the cytoplasmic zonation that appears after the disassembly of the Balbiani body in the onset of secondary growth phase were examined. To further understand the requirements of their developmental processes, various oocyte stages were used to study the organization of other organelles as well as the modifications in mitochondria. Furthermore, the different phases of prophase I meiotic divisions of chromosomes in oocyte nests (leptotene, zygotene, pachytene, diplotene), as well as the presence or absence of mitosis and oogonia nests were noted in order to describe the dynamics of both oogonial proliferation and early oocytes throughout the reproductive cycle. The major hypothesis predicts identical developmental changes in the oocytes of the two studied species due to their close phylogenetic relationship. Moreover, because both species have indeterminate fecundity, ongoing recruitment from oogonia to early oocytes is expected.

3.2 Specific methodology

A total of 94 anchovy and 92 sardine ovaries at various reproductive phases (**Table 3.1**) were used for the analysis. **Figure 3.1** summarizes the monthly evolution of the gonadosomatic index (GSI = 100 *

OW / $W_{ev.}$) and the prevalence of each reproductive phase (developing, spawning-capable, and resting; see **Annex 1**) for a total of 240 anchovies and 320 sardines throughout the sampling period.

Table 3.1. The number of ovaries in different reproductive phases was analysed in two fish species, anchovy, *Engraulis encrasicolus,* and sardine, *Sardina pilchardus*, using light microscope and confocal laser scanning microscope (Charitonidou et al. 2022d).

Πίνακας 3.1. Ο αριθμός των ωοθηκών σε διαφορετικές αναπαραγωγικές φάσεις που αναλύθηκε σε δύο είδη ιχθύων, στο γαύρο, *Engraulis encrasicolus* και στη σαρδέλα, *Sardina pilchardus,* με τη χρήση οπτικού και συνεστιακού μικροσκοπίου (Charitonidou et al. 2022d).

	Developing	Spawning-capable	Resting
Anchovy	9	55	30
Sardine	13	44	35

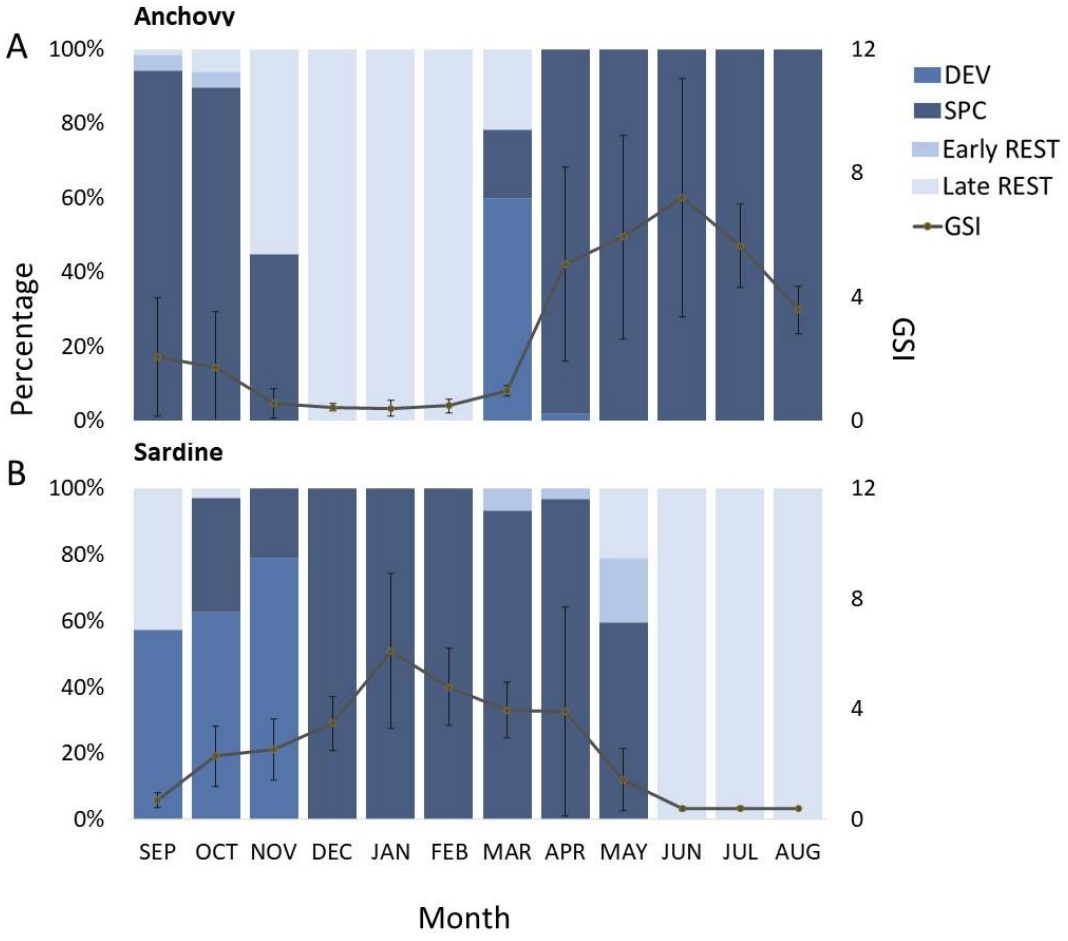

Figure 3.1. Percentage of fish individuals in various reproductive phases, including developing (DEV), spawning-capable (SPC), and early and late resting phase (early REST and late REST). The line represents the monthly

average of the gonadosomatic index (GSI). The 95% confidence interval is represented by bars. A total of 240 anchovies and 320 sardines were analysed. A) anchovy, *Engraulis encrasicolus*, and B) sardine, *Sardina pilchardus* (Charitonidou et al. 2022d).

Εικόνα 3.1. Ποσοστό ατόμων ψαριών σε διάφορες φάσεις ανάπτυξης της ωοθήκης, συμπεριλαμβανομένης της αναπτυσσόμενης (DEV), της αναπαραγωγικά ικανής (SPC) και της πρώιμης και όψιμης φάσης απενεργοποίησης (early REST and late REST). Η γραμμή αντιπροσωπεύει τον μηνιαίο μέσο όρο του γοναδοσωματικού δείκτη (GSI). Το διάστημα εμπιστοσύνης 95% παρουσιάζεται με ράβδους. Συνολικά 240 άτομα γαύρου και 320 άτομα σαρδέλας αναλύθηκαν. Α) γαύρος, *Engraulis encrasicolus* και Β) σαρδέλα, *Sardina pilchardus* (Charitonidou et al. 2022d).

Light microscopy, CLSM, and TEM micrographs were used to evaluate the developmental changes of oocytes at various stages. Oocytes' mitochondrial ultrastructure and cytoplasmic composition were closely examined using TEM (see details in **Annex 6**). Light microscopy and CLSM micrographs were used to study the dynamics of oogonial proliferation and early meiotic oocyte nests.

3.3 Results and Discussion

3.3.1 Oogonia and early (chromatin nucleolus stage) oocytes

Mitotic and prophase I meiotic divisions occurred in oogonia and early oocytes, respectively. In both species, oogonia divided mitotically in nests (**Fig. 3.2A**). After completion of mitosis, they remained in the nests (**Fig. 3.2B**) before transforming into oocytes at the onset of meiosis, entering in leptotene of prophase I. Chromosomes appeared as thin threads, while nucleoli were observed at the periphery of the nucleus (**Fig. 3.2C**). A "bouquet" of chromosomes was observed at zygotene, as the chromosomes appeared aggregated at one side of the nucleus (**Fig. 3.2D**). This bouquet configuration disappeared at pachytene (**Fig. 3.2E**), as chromosomes were evenly distributed in the nucleus. At early diplotene, the homologous chromosomes appeared thinner than in previous meiotic phases (**Fig. 3.2A, D**). At this time point, the oocytes were no longer restricted within nests. Meiosis pauses at diplotene and resumes at the oocyte maturation stage. The analysis of the prophase I meiotic divisions using confocal microscopy in fish oocytes was also studied in Zebrafish in the study of Elkouby and Mullins (2017).

Both mitotic and meiotic divisions as well as oogonia nests were utilized as markers to study the dynamics of oogonia and early oocytes during the reproductive cycle (see **Section 3.3.5**).

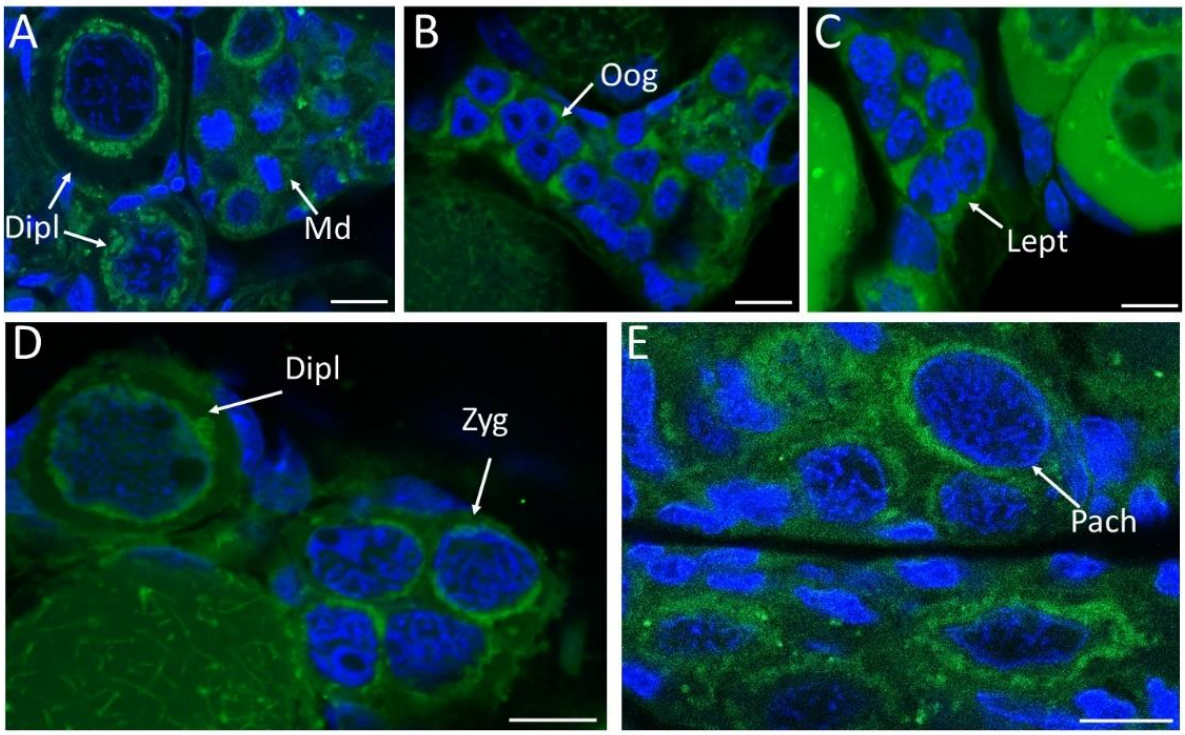

Figure 3.2. Single CLSM sections depicting mitotic and meiotic divisions in ovaries of *Sardina pilchardus* and *Engraulis encrasicolus*, after $DiOC_6$ (green) and DAPI (blue) staining. A) *S. pilchardus.* Mitotic divisions of oogonia (Md) and oocytes at diplotene (Dipl), B) *E. encrasicolus.* Oogonia nest (Oog), C) *E. encrasicolus.* Oocyte nest at leptotene (Lept), D) *E. encrasicolus.* Oocyte at diplotene (Dipl) and oocyte nest at zygotene (Zyg), E) *S. pilchardus.* Oocyte at pachytene (Pach). Scale bars= 10μm (Charitonidou et al. 2022d).

Εικόνα 3.2. Εικόνες απλών CLSM τομών που απεικονίζουν μιτωτικές και μειωτικές διαιρέσεις στις ωοθήκες της σαρδέλας, *Sardina pilchardus*, και του γαύρου, *Engraulis encrasicolus*, μετά από χρώση με $DIOC_6$ (πράσινο) και DAPI (μπλε). Α) *S. pilchardus*. Μιτωτικές διαιρέσεις ωογονίων (Md) και ωοκύτταρα στο στάδιο της διπλοταινίας (Dipl), Β) *E. encrasicolus*. Φωλεά ωογονίων (Oog), C) *E. encrasicolus*. Φωλεά ωοκυττάρων στο στάδιο της λεπτοταινίας (Lept), D) *E. encrasicolus*. Φωλεά ωοκυττάρων στο στάδιο της διπλοταινίας (Dipl) και φωλιά ωοκυττάρων στο στάδιο της ζυγοταινίας (Zyg), Ε) *S. pilchardus*. Ωοκύτταρο στο στάδιο της παχυταινίας (Pach). Κλίμακες = 10μm (Charitonidou et al. 2022d).

3.3.2 Primary growth phase

Meiosis pauses at diplotene and resumes at the oocyte maturation stage. During the primary growth phase, oocytes exhibited changes in their cytoplasm with the appearance of cytoplasmic asymmetry. Specifically, in the multiple nucleoli, and perinucleolar stage of primary growth oocytes, both sardine, and anchovy oocytes exhibited a distinct, almost spherical fluorescent structure in the cytoplasm, stained by $DiOC_6$, which detects membranous structures, such as mitochondria, endoplasmic reticulum, membranous vesicles, etc. (**Fig. 3.3A, B**). This structure was a compartment of Balbiani body (Bb), which by TEM appeared to consist of electron-dense membranous threads with curl or loop

configuration, escorted by mitochondria (**Fig. 3.3C, D**). Due to their high electron density, these threads were not conventional membranous ones. However, their overall appearance and the fact that they were stained by $DiOC_6$ explained the membranous nature of these threads. This structure was located near the nucleus during the start of the primary growth phase (**Fig. 3.3D**), migrating subsequently to the periphery at the future vegetal pole, where it disassembles. Furthermore, in sardine oocytes, the spherical structure coexisted with another compartment of Bb, a dense perinuclear zone (**Fig. 3.3A, E**), consisting of mitochondria, nuage, and small vesicles (**Fig. 3.3E**). In anchovy, this ring was thinner (**Fig. 3.3B, F**), being more pronounced in small oocytes and consisting of nuage and mitochondria complexes (**Fig. 3.3F**) that gradually migrated to the periphery during oocyte development (**Table 3.2**). The Atlantic herring, *Clupea harengus*, which is also a clupeoid, has a circumnuclear ring that appeared initially in the perinuclear region and subsequently dispersed to the periphery, however, without the presence of a spherical compartment of Bb in the cytoplasm (Kjesbu et al. 2011; McPherson and Kjesbu 2012). Primary growth oocytes from *Labeobarbus marequensis*, a Cypriniform species that belongs to Clupeocephala group (Hughes et al. 2018), the same group as both studied species, contain Bb as a spherical structure called a yolk nucleus, and a perinuclear nuage with mitochondria complexes (Zelazowska and Halajian 2020).

The morphology of the Bb is not a phylogenetic feature of species and its morphology (e.g., spherical, or perinuclear ring, etc.) differs not only among species of different families but also between species within the same family (Dymek et al. 2021a; Dymek et al. 2021b). Dymek et al. (2021a, 2021b) showed diversity in early oocyte development between Osteoglossiform fishes. Despite the different phylogeny among both species studied (Clupeocephala) and *O. latipes* (Percomorphaceae) (Kobayasi and Iwamatsu 2000), the Bb appears to contain similar components. Kobayasi and Iwamatsu (2000) showed that oocytes of *Oryzias latipes* (Beloniformes, Adrianichthyidae) also contain a spherical Bb, which appears as a mass of granular threads, identified as vacuoles consisting of a single lamella with bilayers of ribosomes or ribonucleoprotein-like particles. In addition, a perinuclear zone of basophilic cytoplasm coexisted with the Bb in this species, but their functional and structural similarities are yet unknown (Kobayasi and Iwamatsu 2000).

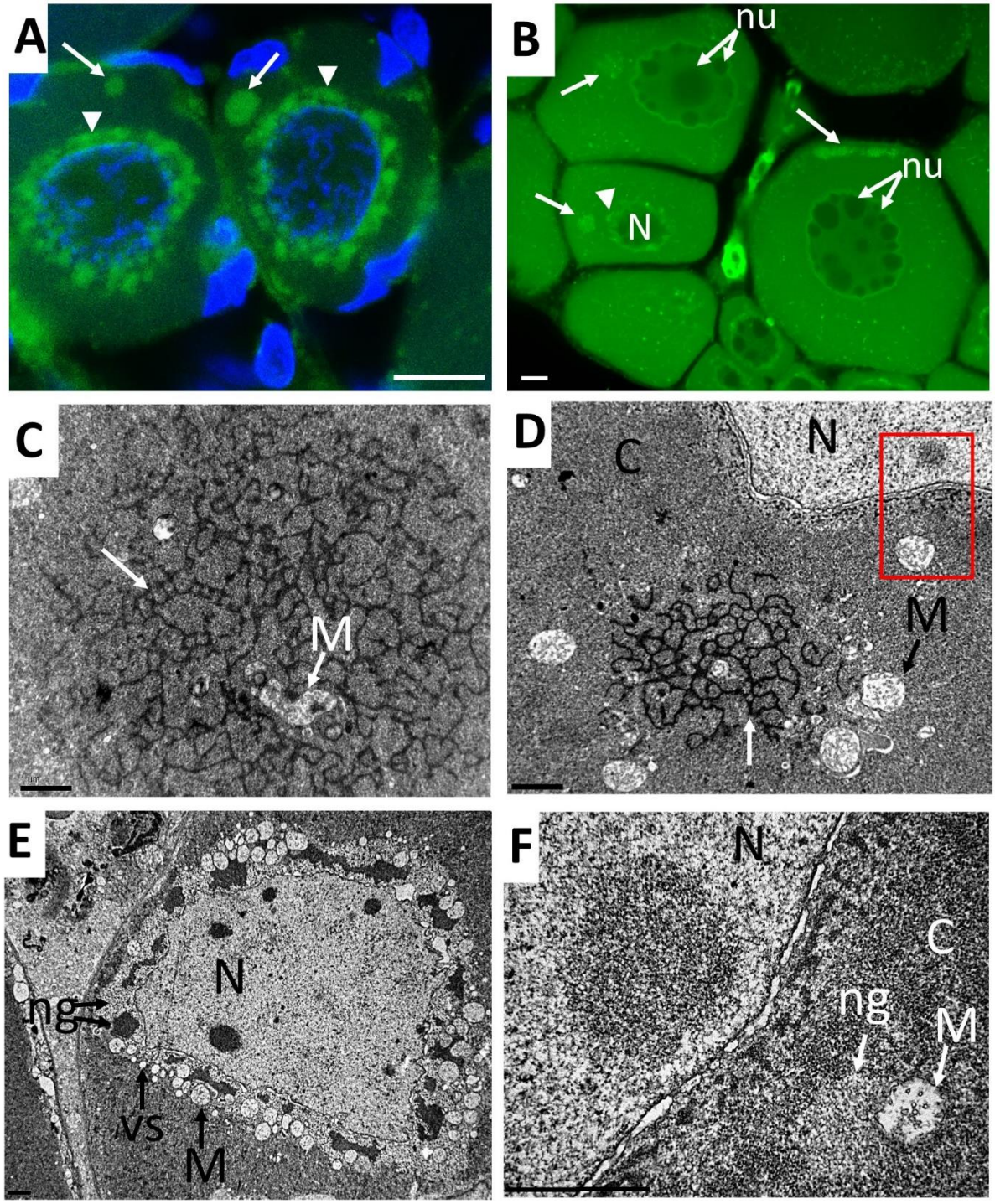

Figure 3.3. Observations of Balbiani body in primary growth oocytes, at multiple nucleoli, and perinucleolar stages. A) Single CLSM section of *Sardina pilchardus* whole mount ovarian samples, after staining with $DiOC_6$ (green) and DAPI (blue). A prominent thick fluorescent ring (arrowheads) in the perinuclear region and an almost spherical Balbiani body (arrows) can be observed in the cytoplasm of primary growth oocytes at multiple nucleoli stage. Scale bar= 10 µm. B) *Engraulis encrasicolus.* Single CLSM section after $DiOC_6$ staining. The Balbiani body in the cytoplasm of oocytes at various developmental stages of primary growth phase (multiple nucleoli stage, perinucleolar stage), and early secondary growth phase (cortical alveoli stage) can be observed at different locations (arrows). A perinuclear (N= nucleus) fluorescent ring can also be observed (arrowhead). Scale bar= 10 µm. C) *Sardina pilchardus,* TEM micrograph. The Balbiani body consists of electron-dense membranous threads

(white arrow) and mitochondria (M) in the cytoplasm of primary growth oocyte at multiple nucleoli stage. Scale bar= 1 μm. D) *Engraulis encrasicolus* TEM micrograph of primary growth oocyte in multiple nucleoli stage. Balbiani body consists of electron-dense membranous threads (white arrow) escorted by mitochondria (M). The red frame indicates an area similar to that presented at higher magnification in (F). Nucleus (N), Cytoplasm (C). Scale bar= 1 μm. E) *Sardina pilchardus,* TEM micrograph of primary growth oocyte at multiple nucleoli stage. The perinuclear ring (nucleus= N) consists of mitochondria (M), nuage (ng), ribosomes and small vesicles (vs). Scale bar= 1 μm. F) *Engraulis encrasicolus* TEM micrograph of primary growth oocyte at multiple nucleoli stage. Mitochondria (M) and nuage (ng) occur in the perinuclear ring, simultaneously with the Balbiani body in the cytoplasm. Nucleus (N), Cytoplasm (C). Scale bar= 1μm (Charitonidou et al. 2022c).

Εικόνα 3.3. Παρατηρήσεις της δομής του σωματίου Balbiani σε ωοκύτταρα πρωτογενούς ανάπτυξης, στο στάδιο πολλαπλών πυρηνίσκων και στο περιπυρηνικό στάδιο. Α) Απλή CLSM τομή από ωοθήκη σαρδέλας, *Sardina pilchardus,* μετά από χρώση με $DiOC_6$ (πράσινο) και DAPI (μπλε). Διακρίνονται ένας ευρύς φθορίζων δακτύλιος (κεφαλές βέλους) στην περιπυρηνική περιοχή και ένα σχεδόν σφαιρικό σωμάτιο Balbiani (βέλη) στο κυτταρόπλασμα των ωοκυττάρων πρωτογενούς ανάπτυξης στο στάδιο των πολλαπλών πυρήνων. Κλίμακα= 10 μm. Β) *Engraulis encrasicolus*. Απλή τομή CLSM μετά από χρώση $DiOC_6$. Το σωμάτιο Balbiani μπορεί να παρατηρηθεί σε διαφορετικές θέσεις (βέλη) στο κυτταρόπλασμα των ωοκυττάρων σε διάφορα αναπτυξιακά στάδια της πρωτογενούς φάσης ανάπτυξης (στάδιο πολλαπλών πυρηνίσκων, περιπυρηνικό στάδιο) και πρώιμης δευτερογενούς φάσης ανάπτυξης (στάδιο κυψελίδων του φλοιού). Επίσης παρατηρείται ένας περιπυρηνικός (N= πυρήνας) φθορίζων δακτύλιος (κεφαλή βέλους). Κλίμακα= 10 μm. C) *Sardina pilchardus*, Ηλεκτρονιογραφία TEM. Το σωμάτιο Balbiani αποτελείται από ηλεκτρονιόπυκνα μεμβρανώδη νήματα (λευκό βέλος) και μιτοχόνδρια (M) στο κυτταρόπλασμα του ωοκυττάρου πρωτογενούς ανάπτυξης στο στάδιο πολλαπλών πυρηνίσκων. Κλίμακα= 1 μm. D) *Engraulis encrasicolus,* Ηλεκτρονιογραφία TEM ωοκυττάρου πρωτογενούς ανάπτυξης στο στάδιο πολλαπλών πυρηνίσκων. Το σωμάτιο Balbiani αποτελείται από ηλεκτρονιόπυκνα μεμβρανώδη νήματα (λευκό βέλος) που συνοδεύονται από μιτοχόνδρια (M). Το κόκκινο πλαίσιο υποδεικνύει μια περιοχή παρόμοια με αυτή που παρουσιάζεται σε μεγαλύτερη μεγέθυνση στο (F). Πυρήνας (N), Κυτταρόπλασμα (C). Κλίμακα= 1 μm. Ε) *Sardina pilchardus*, ηλεκτρονιογραφία TEM ωοκυττάρου πρωτογενούς ανάπτυξης στο στάδιο πολλαπλών πυρηνίσκων. Ο περιπυρηνικός δακτύλιος (πυρήνας= N) αποτελείται από μιτοχόνδρια (M), «νέφος» (nuage, ng), ριβοσώματα, και μικρά κυστίδια (vs). Κλίμακα= 1 μm. F) *Engraulis encrasicolus* ηλεκτρονιογραφία TEM ωοκυττάρου πρωτογενούς ανάπτυξης στο στάδιο πολλαπλών πυρηνίσκων. Τα μιτοχόνδρια (M) και το νέφος (ng) εμφανίζονται στον περιπυρηνικό δακτύλιο, ταυτόχρονα με το σωμάτιο Balbiani στο κυτταρόπλασμα. Πυρήνας (N), Κυτταρόπλασμα (C). Κλίμακα = 1μm (Charitonidou et al. 2022c).

3.3.3 Secondary growth phase

After the primary growth phase and dispersion of the Bb components into the peripheral area of the oocytes, a prominent cytoplasmic zonation was established in the cytoplasm of the early secondary oocytes, which contained cortical alveoli in their cytoplasm, up to early vitellogenesis, which included early yolk globules in their cytoplasm, in both species, extending from the nucleus to the periphery (**Fig. 3.4**). In sardine oocytes, the first zone was a perinuclear ring, consisting of nuage and abundant ribosomes (**Fig. 3.4A**). The second zone was broader, containing abundant endoplasmic reticulum elements (**Fig. 3.4A**). The third zone was characterized by aggregations of mitochondria, also

containing rough endoplasmic reticulum sacks, peroxisomes, cortical alveoli, and oil droplets (**Fig. 3.4B**). The 4th zone at the periphery appeared as an area rich in ribosomes and vesicles (**Fig. 3.4B**).

The cytoplasmic zonation of anchovy oocytes differed from that of sardine (**Table 3.2**). The first zone was perinuclear, containing, apart from nuage and ribosomes, some endoplasmic reticulum elements (**Fig. 3.4C**). The second zone included a significant aggregation of mitochondria, which appeared like a broad ring around the 1st zone (**Fig. 3.4C**), while the frequency of mitochondria decreased toward the periphery, where endoplasmic reticulum, yolk globules, and other vesicles were present (**Fig. 3.4D**). The 4th zone was similar to that of sardine oocytes (**Fig. 3.4D**).

The above cytoplasmic zonation in oocytes of sardine and anchovy faded as vitellogenesis progressed, and mitochondria, endoplasmic reticulum, and other organelles became dispersed throughout the cytoplasm.

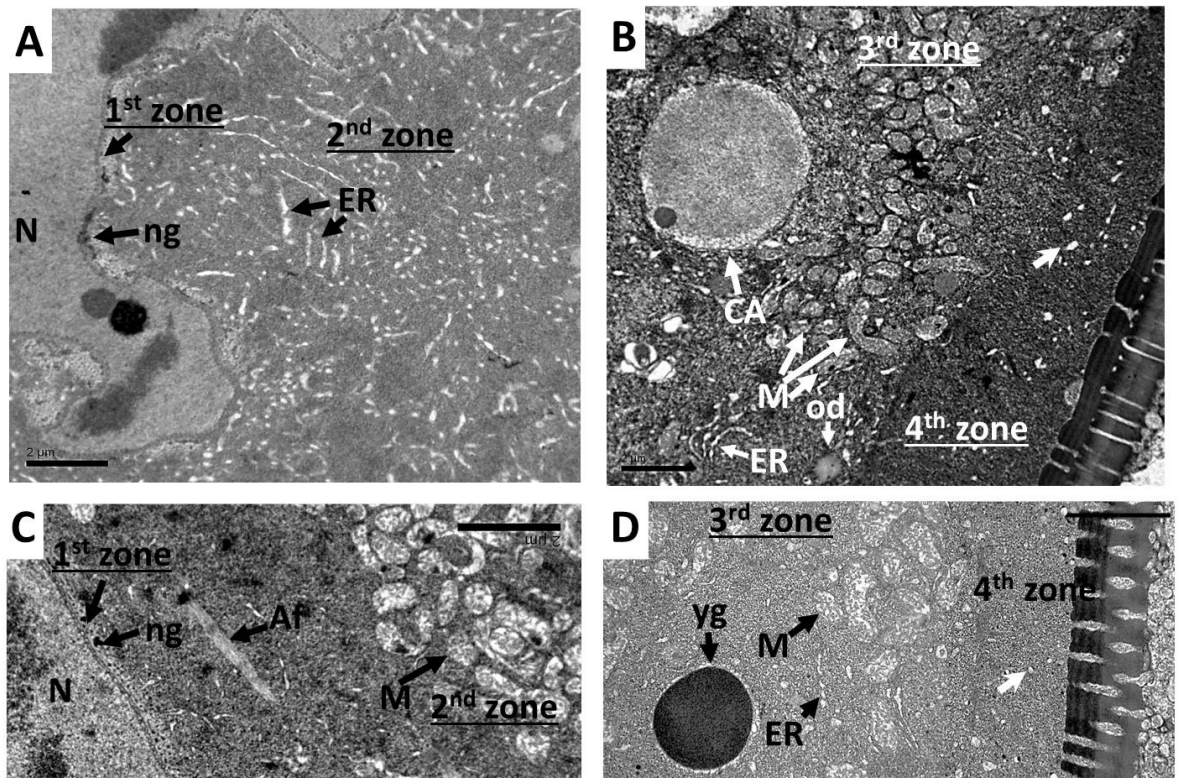

Figure 3.4. TEM micrographs depicting the cytoplasmic zonation, established from the nucleus (N) to the periphery, in an early secondary growth oocyte, cortical alveoli stage, in *Sardina pilchardus* (A, B), and an early vitellogenic oocyte in *Engraulis encrasicolus* (C, D). A) *Sardina pilchardus.* Cytoplasmic zonation of an early secondary growth oocyte: 1st zone: a perinuclear zone consisting of nuage (ng) and abundant ribosomes. 2nd zone: a broad zone containing numerous endoplasmic reticulum sacks (ER). Nucleus (N). Scale bar= 2 µm. B) *Sardina pilchardus.* Cytoplasmic zonation of an early secondary growth oocyte: 3rd zone: endoplasmic reticulum sacks (ER), mitochondria (M), cortical alveoli (ca) and oil droplets (od). 4th zone: many ribosomes and small vesicles (white arrow). Scale bar= 2 µm. C) *Engraulis encrasicolus.* Cytoplasmic zonation of an early vitellogenic

oocyte: 1st zone: nuage (ng), endoplasmic reticulum sacks (ER), actin filament bundles (Af) around the nucleus (N), 2nd zone: numerous mitochondria (M) surround the 1st zone. Scale bar= 2 μm. D) *Engraulis encrasicolus.* Cytoplasmic zonation of an early vitellogenic oocyte: 3rd zone: endoplasmic reticulum sacks (ER), yolk globules (Yg), mitochondria (M) and other vesicles. 4th zone: many ribosomes and small vesicles (white arrow). Scale bar= 2 μm (Charitonidou et al. 2022c).

Εικόνα 3.4. Ηλεκτρονιογραφίες TEM που απεικονίζουν την κυτταροπλασματική ζώνωση, που σχηματίζεται από τον πυρήνα (N) προς την περιφέρεια, σε ένα ωοκύτταρο πρώιμης δευτερογενούς ανάπτυξης, στο στάδιο των κυψελίδων του φλοιού, στη σαρδέλα, *Sardina pilchardus* (A, B) και σε ένα πρώιμο λεκιθικό ωοκύτταρο στο γαύρο, *Engraulis encrasicolus* (C, D). A) *Sardina pilchardus*. Κυτταροπλασματική ζώνωση ενός ωοκυττάρου πρώιμης δευτερογενούς ανάπτυξης: 1η ζώνη: μια περιπυρηνική ζώνη που αποτελείται από νέφος (ng) και πολυάριθμα ριβοσώματα. 2η ζώνη: μια ευρεία ζώνη που περιέχει πολυάριθμους σάκους ενδοπλασματικού δικτύου (ER). Πυρήνας (N). Κλίμακα= 2 μm. B) *Sardina pilchardus*. Κυτταροπλασματική ζώνωση ενός ωοκυττάρου πρώιμης δευτερογενούς ανάπτυξης: 3η ζώνη: σάκοι ενδοπλασματικού δικτύου (ER), μιτοχόνδρια (M), κυψελίδες του φλοιού (ca) και σταγονίδια ελαίου (od). 4η ζώνη: πολυάριθμα ριβοσώματα και μικρά κυστίδια (λευκό βέλος). Κλίμακα= 2 μm. C) *Engraulis encrasicolus*. Κυτταροπλασματική ζώνωση ενός πρώιμου λεκιθικού ωοκυττάρου: 1η ζώνη: νέφος (ng), σάκοι ενδοπλασματικού δικτύου (ER), δέσμες νηματίων ακτίνης (Af) γύρω από τον πυρήνα (N), 2η ζώνη: πολυάριθμα μιτοχόνδρια (M) περιβάλλουν την 1η ζώνη. Κλίμακα= 2 μm. D) *Engraulis encrasicolus*. Κυτταροπλασματική ζώνωση ενός πρώιμου λεκιθικού ωοκυττάρου: 3η ζώνη: σάκοι ενδοπλασματικού δικτύου (ER), σφαιρίδια λεκίθου (Yg), μιτοχόνδρια (M) και κυστίδια. 4η ζώνη: πολυάριθμα ριβοσώματα και μικρά κυστίδια (λευκό βέλος). Κλίμακα= 2 μm (Charitonidou et al. 2022c).

The perinuclear ring of sardine primary growth oocytes, which was detected by TEM (**Fig. 3.3E and 3.5A**), was not discernible by light microscopy in paraffin-haematoxylin/eosin histological sections (**Fig. 3.5C**). However, it was apparent in semithin sections of samples embedded in Durcupan, stained with Toluidine blue (**Fig. 3.5E**). Nonetheless, the mitochondria-rich ring, detected by TEM in anchovy secondary growth oocytes (**Fig. 3.4C and 3.5B**), was obvious in histological sections stained either with haematoxylin/eosin (**Fig. 3.5D**) or Toluidine blue (**Fig. 3.5F**). The detection of the Balbiani body and cytoplasmic zonation using standard procedures could be useful for distinguishing immature individuals in routine light microscopy observations, either from histological sections or from whole mounts with immunostaining. Specifically, the existence of these markers throughout the reproductive cycle offers important information about maturity and the imminent spawning period (Kjesbu et al. 2011; McPherson and Kjesbu 2012). McPherson and Kjesbu (2012) showed that the circumnuclear (perinuclear) ring in Atlantic herring (*Clupea harengus*) is a predictor of first oocyte maturation and an indicator of imminent spawning. A circumnuclear ring was also used for the classification of early oocytes into stages. Serrat et al. (2019) classified European hake (*Merluccius merluccius*) oocytes into phases based on the circumnuclear ring to calculate the specific number of oocytes across oocyte stages to investigate the seasonal pattern of oocyte recruitment. Furthermore, these markers provide information on the onset of secondary growth and, thus, on the forthcoming reproductive period; with this information, the oocyte growth rate for each species, as well as other important parameters for the applied fisheries reproductive biology, such as the spawning fraction, can be estimated (Ganias et al. 2014a).

Table 3.2. Summary of the differences between the oocytes of sardine (*Sardina pilchardus*) and anchovy (*Engraulis encrasicolus)* in the development of Balbiani body (Bb) during the primary growth phase and the cytoplasmic zonation at the onset of the secondary growth phase, after the disassembly of Bb (Charitonidou et al. 2022c).

Πίνακας 3.2. Σύνοψη των διαφορών μεταξύ των ωοκυττάρων της σαρδέλας (*Sardina pilchardus*) και του γαύρου (*Engraulis encrasicolus*) στην ανάπτυξη του σωμάτιου Balbiani (Bb) κατά τη διάρκεια της πρωτογενούς αναπτυξιακής φάσης και της κυτταροπλασματικής ζώνωσης στην αρχή της δευτερογενούς φάσης ανάπτυξης, μετά την διάλυση του δωμάτιου Bb (Charitonidou et al. 2022c).

	Sardina pilchardus	*Engraulis encrasicolus*
Bb formation	**Structure**: distinct spherical structure combined with a thick perinuclear ring **Content**: spherical structure: electron dense membranous threads with curl or loop forms, and mitochondria perinuclear ring: mitochondria, nuage, and vesicles.	**Structure:** distinct spherical structure and perinuclear complexes **Content**: spherical structure: electron dense membranous threads with curl or loop forms, and mitochondria. perinuclear complexes: complexes of nuage and mitochondria
Cytoplasmic zonation after Bb disassembly	**1st zone**: a perinuclear zone consisting of nuage and abundant ribosomes. **2nd zone**: broad zone including endoplasmic reticulum. **3rd zone**: it contains endoplasmic reticulum, mitochondria, peroxisomes, cortical alveoli and oil droplets. **4th zone**: peripheral zone with many ribosomes and vesicles.	**1st zone**: a perinuclear zone, which contains nuage, endoplasmic reticulum and ribosomes. **2nd zone**: a ring of aggregated mitochondria **3rd zone**: fewer mitochondria and more endoplasmic reticulum elements are present together with yolk globules and other vesicles. **4th zone**: peripheral zone with many ribosomes and vesicles.

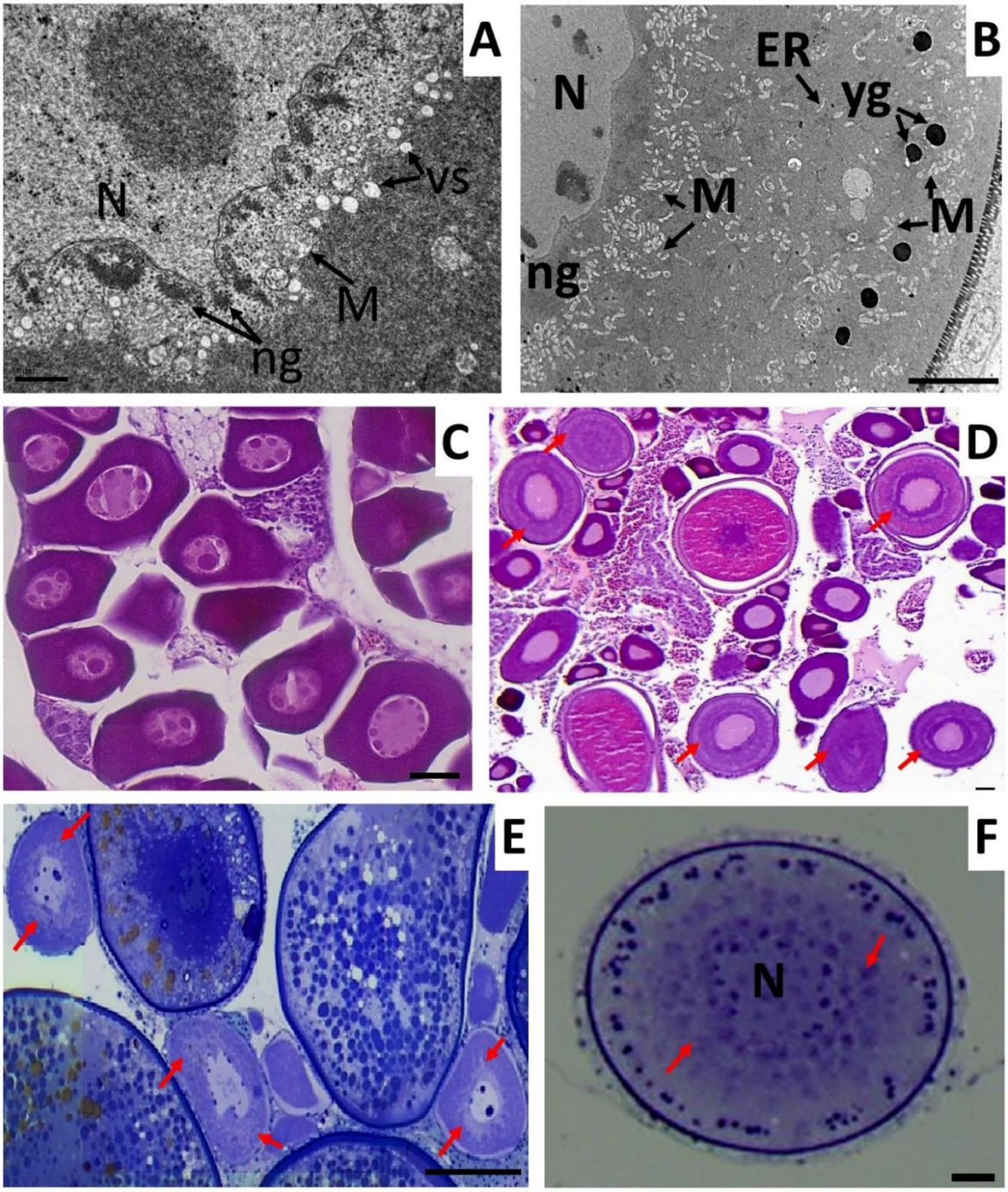

Figure 3.5. Different methods for displaying the perinuclear ring of primary growth oocytes, at multiple nucleoli and perinucleolar stage, in sardine (A, C, E), and the mitochondria-rich ring of early secondary growth oocytes, at cortical alveoli stage, and early vitellogenic stage, in anchovy (B, D, F). A) *Sardine pilchardus,* TEM micrograph of primary growth oocytes, at multiple nucleoli stage. The perinuclear ring (nucleus= N) consists of mitochondria (M), nuage (ng), ribosomes and small vesicles (vs). Scale bar= 1 µm. B) *Engraulis encrasicolus,* TEM micrograph of secondary growth oocyte at early vitellogenic stage. An overall view of the cytoplasmic zonation in an early vitellogenic oocyte (see also **Fig. 3.4C, D**). During this stage, the mitochondria-rich ring begins to expand toward the periphery. Nuage (ng), endoplasmic reticulum sacks (ER), yolk globules (yg), mitochondria (M). Scale bar= 10 µm. C) *Sardina pilchardus,* primary growth oocytes, at multiple nucleoli and perinucleolar stage. Histological section of sample embedded in paraffin and stained with haematoxylin/eosin. The perinuclear ring and the

spherical Bb are not discernible in primary growth oocytes at different development stages. Scale bar= 30 μm. D) *Engraulis encrasicolus,* early secondary growth oocytes, at cortical alveoli stage, and early vitellogenic stage. Histological section of sample embedded in paraffin and stained with haematoxylin/eosin. The mitochondria-rich ring is observed around the nucleus of early secondary growth and early vitellogenic oocytes (arrows). Scale bar= 30 μm. E) *Sardina pilchardus,* primary growth oocytes, at multiple nucleoli and perinucleolar stage. Semithin section (2 μm) of sample embedded in Durcupan resin and stained with Toluidine blue. The perinuclear ring of primary growth oocytes is demonstrated (arrows). Scale bar= 30 μm. F) *Engraulis encrasicolus,* secondary growth oocyte at early vitellogenic stage. Semithin section (2 μm) of sample embedded in Durcupan resin and stained with Toluidine blue. The mitochondria-rich ring of early secondary growth oocytes is demonstrated (arrows). Scale bar= 30 μm (Charitonidou et al. 2022c).

Εικόνα 3.5. Εντοπισμός με διάφορες μεθόδους του περιπυρηνικού δακτυλίου των ωοκυττάρων πρωτογενούς ανάπτυξης, στο στάδιο των πολλαπλών πυρηνίσκων και το περιπυρηνικό στάδιο, στη σαρδέλα (A, C, E) και το πλούσιο σε μιτοχόνδρια δακτύλιο των ωοκυττάρων πρώιμης δευτερογενούς ανάπτυξης, στο στάδιο των κυψελίδων του φλοιού και στο πρώιμο λεκιθικό στάδιο, στο γαύρο (B, D, F). A) *Sardine pilchardus*, ηλεκτρονιογραφία TEM ωοκυττάρων πρωτογενούς ανάπτυξης, σε στάδιο πολλαπλών πυρηνίσκων. Ο περιπυρηνικός δακτύλιος (πυρήνας= N) αποτελείται από μιτοχόνδρια (M), νέφος (ng), ριβοσώματα και μικρά κυστίδια (vs). Κλίμακα= 1 μm. B) *Engraulis encrasicolus*, ηλεκτρονιογραφία TEM ωοκυττάρου δευτερογενούς ανάπτυξης στο πρώιμο στάδιο της λεκιθογένεσης. Συνολική εικόνα της κυτταροπλασματικής ζώνωσης σε ένα πρώιμο λεκιθικό ωοκύτταρο (βλ. επίσης **Εικόνα 3.4C, D**). Κατά τη διάρκεια αυτού του σταδίου, ο πλούσιος σε μιτοχόνδρια δακτύλιος αρχίζει να επεκτείνεται προς την περιφέρεια. Νέφος (ng), σάκοι ενδοπλασματικού δικτύου (ER), σφαιρίδια λεκίθου (yg), μιτοχόνδρια (M). Κλίμακα= 10 μm. C) *Sardina pilchardus*, ωοκύτταρα πρωτογενούς ανάπτυξης, στα στάδια πολλαπλών πυρηνίσκων και περιπυρηνικό. Ιστολογική τομή δείγματος εγκλεισμένου σε παραφίνη, με χρώση αιματοξυλίνης/ηωσίνης. Ο περιπυρηνικός δακτύλιος και το σφαιρικό Bb δεν είναι ευδιάκριτα στα πρωτογενή ωάρια ανάπτυξης σε διαφορετικά στάδια ανάπτυξης. Κλίμακα= 30 μm. D) *Engraulis encrasicolus*, ωοκύτταρα πρώιμης δευτερογενούς ανάπτυξης, στο στάδιο των κυψελίδων του φλοιού και στο πρώιμο στάδιο της λεκιθογένεσης. Ιστολογική τομή δείγματος εγκλεισμένου σε παραφίνη, με χρώση αιματοξυλίνης/ηωσίνης. Ο πλούσιος σε μιτοχόνδρια δακτύλιος παρατηρείται γύρω από τον πυρήνα της πρώιμης δευτερογενούς ανάπτυξης και των πρώιμων λεκιθικών ωοκυττάρων (βέλη). Κλίμακα= 30 μm. E) *Sardina pilchardus*, ωοκύτταρα πρωτογενούς ανάπτυξης, στα στάδια πολλαπλών πυρηνίσκων και στο περιπυρηνικό.στάδιο. Ημίλεπτη τομή (2 μm) δείγματος εγκλεισμένου σε ρητίνη Durcupan, με χρώση κυανό τολουιδίνης. Παρατηρείται ο περιπυρηνικός δακτύλιος των ωοκυττάρων πρωτογενούς ανάπτυξης (βέλη). Κλίμακα= 30 μm. F) *Engraulis encrasicolus*, ωοκύτταρο δευτερογενούς ανάπτυξης στο πρώιμο λεκιθικό στάδιο. Ημίλεπτη τομή (2 μm) δείγματος εγκλεισμένου σε ρητίνη Durcupan, με χρώση κυανό τολουιδίνης. Εντοπίζεται ο πλούσιος σε μιτοχόνδρια δακτύλιος των ωοκυττάρων πρώιμης δευτερογενούς ανάπτυξης (βέλη). Κλίμακα= 30 μm (Charitonidou et al. 2022c).

3.3.4 Changes in mitochondrial morphology in relation with organization of other organelles during oocyte development

During the early phases of oocyte development, the structural features of mitochondria were similar in both species. In the chromatin nucleolus oocytes in both species, mitochondria were localized in the perinuclear area and represented 10.5% of the cytoplasm volume; they were large, with a median

diameter of 2.17 (±1.07) μm, with few cristae, with density in mitochondria about 6.9% (**Fig. 3.6 and 3.7**).

In primary growth oocytes of both species, the area fraction of mitochondria is 10.3%, similar to that of previous developmental phases. Mitochondria appear significantly smaller (Pairwise Wilcoxon Rank Sum test, $p<0.05$), with a median diameter of 1.10 (±0.25) μm, oval/elongated in shape, containing more cristae, with density in mitochondria 13.5% in sardine and 22% in anchovy (**Fig. 3.6 and 3.7b**). Mitochondria in sardine oocytes were concentrated in the perinuclear region at the beginning of the primary growth phase, expanding later throughout the whole cytoplasm. This distribution pattern was not observed in anchovy oocytes, where mitochondria formed a ring around the nucleus at the end of the primary growth phase. Few mitochondria were observed in the Balbiani body component (**Fig. 3.3**). In the oocytes of the common snook, *Centropomus undecimalis*, modifications in the structure of mitochondria and their cristae were also observed during the transition from the chromatin nucleolus to the primary growth phase (Grier 2000). Specifically, mitochondria of zygotene oocytes (chromatin nucleolus oocytes) were ovoid, electro-lucent, and had few lamellar cristae, while mitochondria of primary growth oocytes became ovoid to elongate, electron-dense, and had numerous cristae (Grier 2000).

The modifications of mitochondrial cristae in secondary growth oocytes differed between the two species, despite their close phylogenetic relationship (**Fig. 3.6**). In sardine, the proportion of mitochondria in the cytoplasm of early secondary growth oocytes was lower than that of anchovy, at 13.37%, but it was similar to the percentage of mitochondria in the cytoplasm of primary growth oocytes. Mitochondria were smaller than in earlier phases, though not significantly (Pairwise Wilcoxon Rank Sum test, $p >0.05$), with a median diameter of 0.83 (±0.27) μm and an ovoid/elongate shape, with cristae density ~43.9% (**Fig. 3.6 and 3.7c**). Mitochondria were found at the periphery of the cell. In anchovy, mitochondria of early secondary growth oocytes occupied a greater fraction (~25.09%) of the cytoplasm than those in primary growth oocytes. They exhibited a median diameter of 1.13 (±0.43) μm, were ovoid/ elongate in shape, and had fewer cristae (density of cristae in mitochondria 14.4%) than mitochondria at previous developmental phases (**Fig. 3.6 and Fig. 3.7e**). The perinuclear mitochondrial ring spreads throughout the cytoplasm at this phase. In the middle of the secondary growth phase, sardine oocytes contained numerous mitochondria, accounting for 31.56% of the cytoplasm, which was significantly higher than at earlier phases of development, though mitochondria were now significantly smaller (Pairwise Wilcoxon Rank Sum test, $p<0.05$), measuring 0.52 (±0.18) m in diameter. Mitochondria appeared ovoid/elongated with deformed cristae and were dispersed throughout the cytoplasm (**Fig. 3.7d**). The cristae density in mitochondria was lower, compared to previous ovarian phases (~6.6%; **Fig. 3.6**). In anchovy oocytes, in the middle of the secondary growth phase, mitochondria occupied 17.72% of the cytoplasm, significantly lower than in the previous oocyte phase. The mitochondria were even smaller than those at previous phases of anchovy oocytes, with a median diameter of 0.93 (±0.25) μm, no significant difference from that of previous phases (Pairwise Wilcoxon Rank Sum test, $p>0.05$). Mitochondria were dispersed throughout the whole cytoplasm and their shape was comparable to that of earlier oocyte phases. They contained many cristae, with a

density of 28.4%, in contrast to mitochondria at the preceding phase (**Fig. 3.6 and 3.7f**). The difference in structure and abundance of mitochondria between primary and secondary growth oocytes has been also observed in *Pampus argenteus* (Yang et al. 2021). As the oocytes develop, the percentage of mitochondria in the cytoplasm increases, while their individual size decreased, augmenting therefore their number in the cytoplasm. Apart from this, modifications in cristae development were also observed. Differences in the structure of mitochondria between primary and secondary growth oocytes have been observed in many species, such as the guppy, *Lebistes reticulatus*, where early oocyte mitochondria were large and contain tubular and shelf-like cristae, whereas after the onset of secondary growth oocytes, mitochondria became thinner in diameter and increased in number, while tubular cristae disappeared (Droller and Roth 1966).

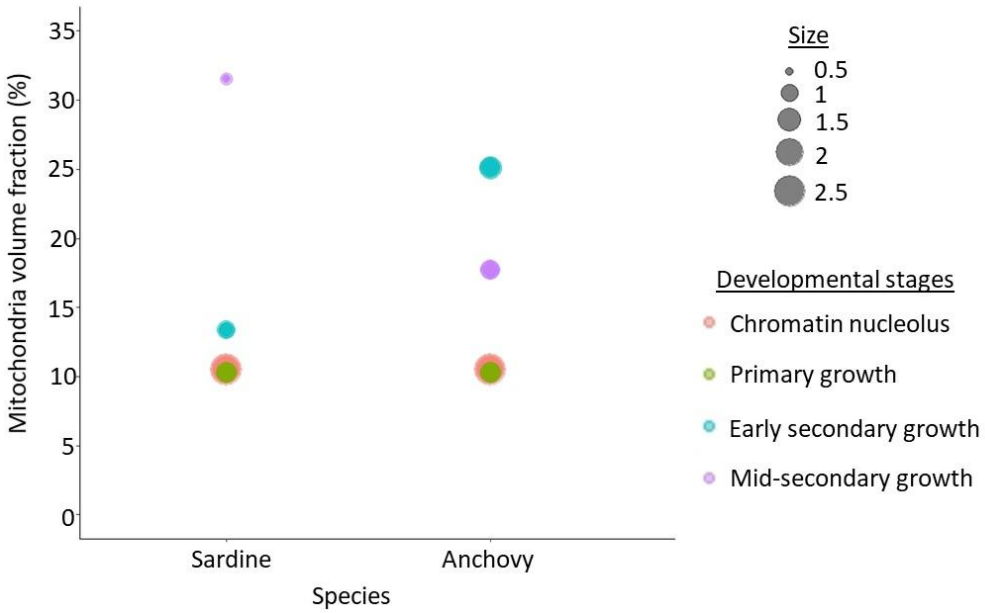

Figure 3.6. The area fraction of mitochondria (%) in the cytoplasm of oocytes in different developmental phases (presented by different colours) in sardine, *Sardina pilchardus,* and anchovy, *Engraulis encrasicolus*, is indicated. The average mitochondria size in different oocyte developmental phases is shown with the bubble sizes.

Εικόνα 3.6. Κλάσμα εμβαδού των μιτοχονδρίων (%) στο κυτταρόπλασμα των διαφορετικών φάσεων ανάπτυξης ωοκυττάρων (παρουσιάζονται με διαφορετικά χρώματα) στη σαρδέλα, *Sardina pilchardus,* και στο γαύρο *Engraulis encrasicolus*. Το μέσο μέγεθος των μιτοχονδρίων σε διαφορετικές φάσεις ανάπτυξης των ωοκυττάρων αντιπροσωπεύεται από τα μεγέθη των σφαιριδίων.

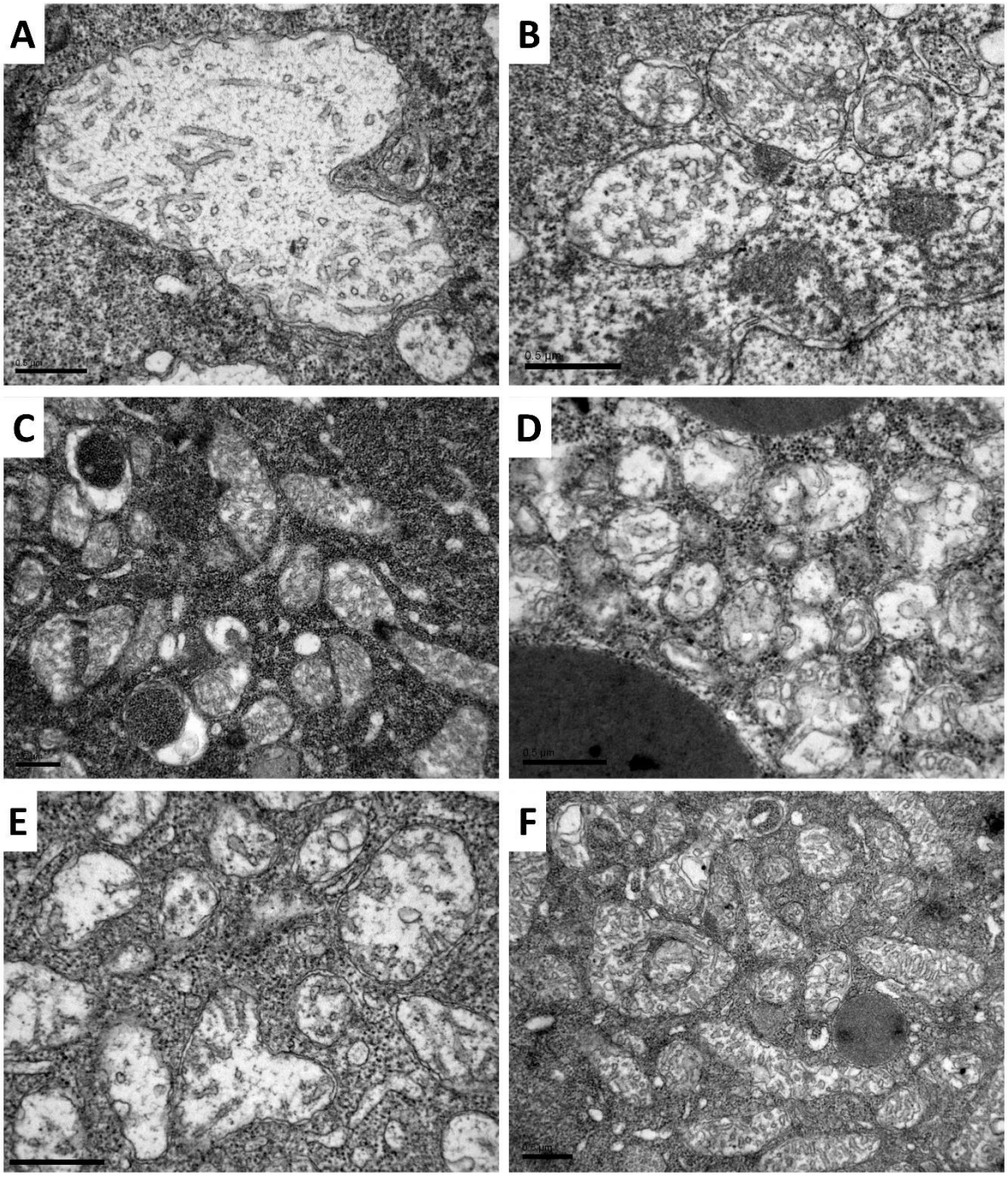

Figure 3.7. Transmission electron micrographs depicting the morphology of oocyte mitochondria at various developmental phases of the oocytes. A) *E. encrasicolus*. Mitochondria of oocytes at the chromatin nucleolus phase appear swollen with few cristae. Scale bar = 0.5 µm. B) *S. pilchardus*. Mitochondria of oocytes in primary growth exhibit various shapes and contain numerous tubular cristae. Scale bar = 0.5 µm. C) *S. pilchardus*. At the onset of secondary growth phase, mitochondria of oocytes are smaller and more numerous than those at earlier oocyte phases, also containing many cristae. Scale bar = 0.5 µm. D) *S. pilchardus*. At the middle of secondary growth phase, the cristae of mitochondria appear distorted. Scale bar = 0.5 µm. E) *E. encrasicolus*. At the onset of secondary growth phase, mitochondria contain few underdeveloped cristae. Scale bar = 0.5 µm. F) *E. encrasicolus*. At the middle of secondary growth phase, mitochondria contain numerous cristae. Scale bar = 0.5 µm (Charitonidou et al. 2022a).

Εικόνα 3.7. Ηλεκτρονιοφραφίες TEM που απεικονίζουν τη μορφολογία των μιτοχονδρίων των διαφορετικών αναπτυξιακών φάσεων των ωοκυττάρων. Α) *E. encrasicolus*. Τα μιτοχόνδρια των ωοκυττάρων σε φάση χρωματίνης-πυρηνίσκου εμφανίζονται διογκωμένα με περιορισμένη ανάπτυξη ακρολοφίων. Κλίμακα = 0,5 μm. Β) *S. pilchardus*. Τα μιτοχόνδρια των ωοκυττάρων της πρωτογενούς αναπτυξιακής φάσης έχουν διάφορα σχήματα και περιέχουν πολυάριθμες σωληνοειδείς ακρολοφίες. Κλίμακα = 0.5 μm. C) *S. pilchardus*. Κατά την έναρξη της δευτερογενούς ανάπτυξης των ωοκυττάρων, τα μιτοχόνδρια είναι μικρότερα και πιο πολλά από εκείνα των προηγούμενων φάσεων των ωοκυττάρων, και περιέχουν επίσης πολλές ακρολοφίες. Κλίμακα = 0.5 μm. D) *S. pilchardus*. Στα μισά της δευτερογενούς ανάπτυξης, οι ακρολοφίες των μιτοχονδρίων εμφανίζονται παραμορφωμένες. Κλίμακα = 0.5 μm. E) *E. encrasicolus*. Κατά την έναρξη της δευτερογενούς ανάπτυξης των ωοκυττάρων, τα μιτοχόνδρια περιέχουν λίγες υπανάπτυκτες ακρολοφίες. Κλίμακα = 0.5 μm. F) *E. encrasicolus*. Στα μισά της δευτερογενούς ανάπτυξης των ωοκυττάρων, τα μιτοχόνδρια περιέχουν πολυάριθμες ακρολοφίες. Κλίμακα = 0.5 μm (Charitonidou et al. 2022a).

In some species, modified mitochondria appeared during late vitellogenesis and participate in the formation of multivesicular bodies involved in the formation of yolk granule precursors (Chung et al. 2009; Jun et al. 2018; Kunz 2004; Pfannestiel and Grünig 1982). In sturgeon and paddlefish, mitochondria with various degrees of cristae distortion were assumed to play a role in the formation of lipid droplets in previtellogenic oocytes (Zelazowska and Fopp-Bayat 2019; Zelazowska and Kilarski 2009).

In sardine, the close relation of endoplasmic reticulum, and the electron translucent yolk bodies (YB1; **Fig. 3.8A and B**) in middle secondary growth oocytes, as well as the absence of YB1 (**Fig. 3.8C**), when more advanced electron-dense yolk bodies (YB2) and yolk granules develop in the cytoplasm, together with the presence of mitochondria with distorted cristae during the appearance of crystalline content in the yolk granules (**Fig. 3.8D**), lead to the assumption that mitochondria are involved in yolk granule formation. However, additional research, apart from TEM observations, is required to corroborate these assumptions. Yang et al. (2021) showed that mitochondria with well-developed cristae, Ca^{2+}-ATPase enzymatic activity, and the transcript levels of mitochondrial fission factor (mff) increased during vitellogenesis, suggesting the possible participation of mitochondria in the formation of vitellogenesis in the silver pomfret *Pampus argenteus*.

The decrease in mitochondrial percentage between early and mid-secondary growth oocytes in anchovy, as well as the simultaneous increase in cristae abundance, allow the assumption that they might be involved in a metabolic process during these phases. In addition, the absence of oil droplets from anchovy oocytes, as well as the presence of vacuoles containing small vesicles in early secondary growth oocytes (**Fig. 3.9A, B**) and the presence of vacuoles with fragmented membranes close to small vesicles (**Fig. 3.9C**), as well as the numerous peroxisomes (**Fig. 3.9D**) in later phases of oocyte development, are indicative of lipidation processes. Hence, the existence of altered mitochondrial cristae during this developmental phase (**Fig. 3.7E, F**) may indicate that mitochondria play a role in this metabolic pathway of lipid synthesis. Also, the presence of mitochondria with increased cristae density, after this phase, indicates the elevated energy demands during vitellogenesis. Both the Golgi

apparatus and endoplasmic reticulum are involved in the development of yolk generating vacuoles, which contributes to the expansion of the yolk globule size (Anderson 1968). In particular, the routes for transferring free fatty acids (FFA, lipid precursors) from the extracellular space to the cytoplasm through the plasma membrane have been described (Lubzens et al. 2017; Thompson et al. 2010). In brief, the FFA bind to certain receptors and is carried to endocytotic vesicles, where they are delivered by specific proteins to other subcellular organelles or structures including endosomes, peroxisomes, endoplasmic reticulum, mitochondria, and the nucleus. Some FFA captured by specialized receptors are used to create lipid droplets, while the majority of FFA enter the cell and are delivered to subcellular organelles with the assistance of a specific protein, for further metabolism (e.g., oxidation and biosynthesis of lipids, membranes, and lipoproteins) or signalling functions (Lubzens et al. 2017; Thompson et al. 2010). Furthermore, some studies have shown that mitochondria and multivesicular structures play a role in the production of yolk granule precursors (Chung et al. 2009; Jun et al. 2018).

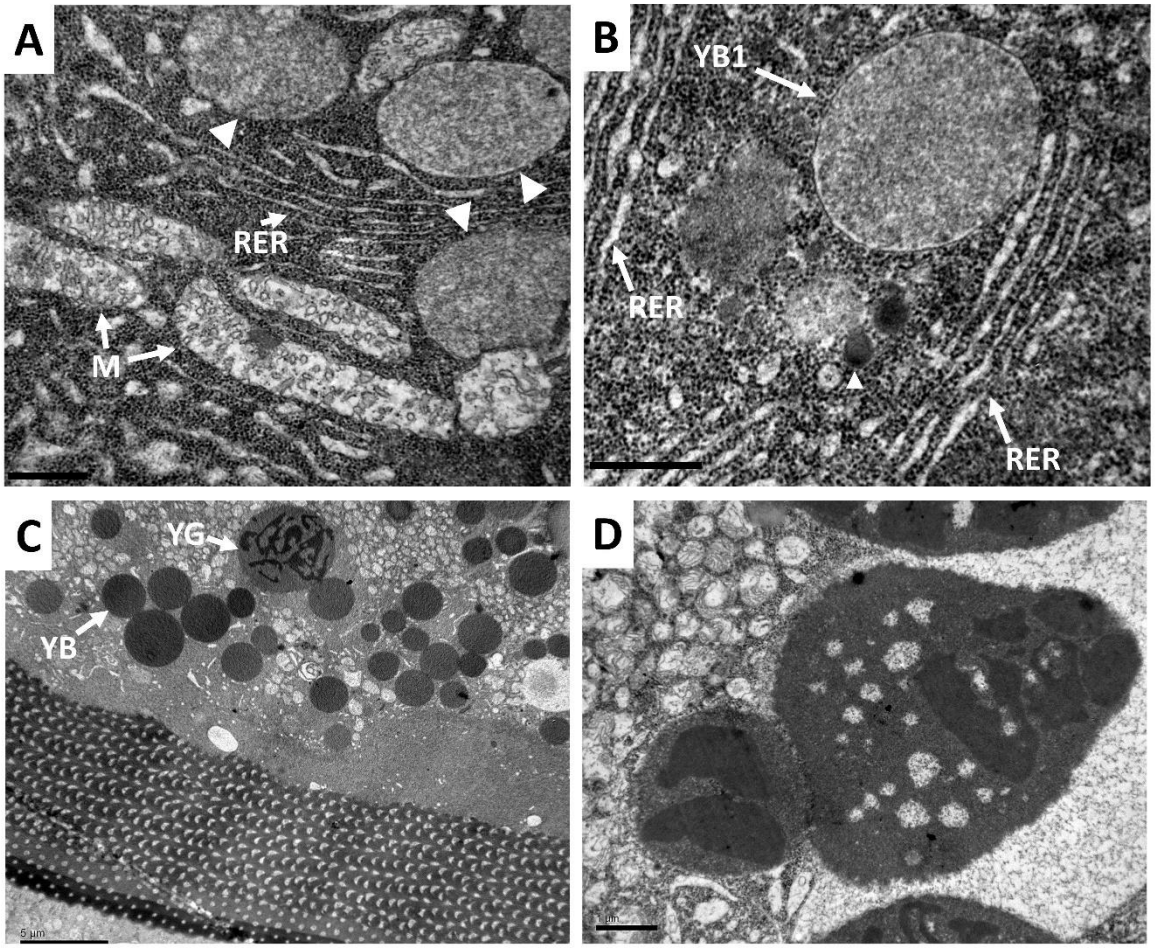

Figure 3.8. Transmission electron micrographs of *S. pilchardus* oocytes. A) Secondary oocytes with yolk bodies (YB1) (arrowheads) close to rough endoplasmic reticulum (RER) and mitochondria (M). Scale bar = 0.6 µm. B) Secondary oocytes with tiny electron-dense yolk bodies (YB0) (white arrowhead) and small yolk bodies (YB1) close to rough endoplasmic reticulum (RER). Scale bar = 0.5 µm. C) Middle secondary growth oocyte with developed yolk bodies (YB) and yolk granules with crystalline content (YG). Scale bar = 5 µm. D) Yolk granules

with crystalline content close to mitochondria with distorted cristae (at the left). Scale bar = 1 μm (Charitonidou et al. 2022a).

Εικόνα 3.8. Ηλεκτρονιογραφίες TEM των ωοκυττάρων σαρδέλας, *S. pilchardus*. Α) Ωοκύτταρα δευτερογενούς ανάπτυξης με λεκιθικά σωμάτια (YB1) (Κεφαλή βέλους) κοντά σε αδρό ενδοπλασματικό δίκτυο (RER) και μιτοχόνδρια (M). Κλίμακα = 0.6 μm. Β) Ωοκύτταρα δευτερογενούς ανάπτυξης με μικρά ηλεκτρονιόπυκνα λεκιθικά σωμάτια (YB0) (λευκή κεφαλή βέλους) και μεγαλύτερα σώματα λεκίθου (YB1) κοντά σε αδρό ενδοπλασματικό δίκτυο (RER). Κλίμακα = 0.5 μm. C) ωοκύτταρο δευτερογενούς ανάπτυξης με αναπτυγμένα σωμάτια λεκίθου (YB) και λεκιθικά κοκκία με κρυσταλλικό περιεχόμενο (YG). Κλίμακα = 5 μm. D) Λεκιθικά κοκκία με κρυσταλλικό περιεχόμενο κοντά σε μιτοχόνδρια με παραμορφωμένες ακρολοφίες (στα αριστερά). Κλίμακα = 1 μm (Charitonidou et al. 2022a).

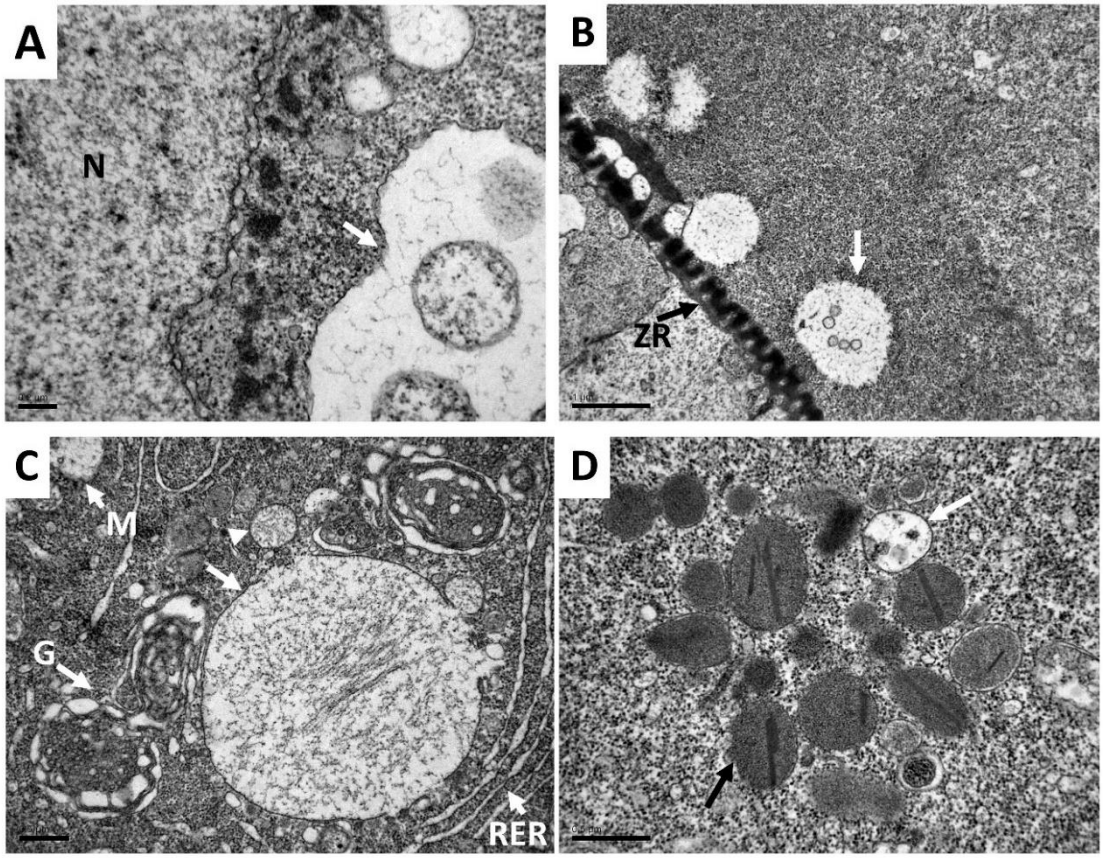

Figure 3.9. Transmission electron micrographs of *E. encrasicolus* oocytes. (A, B) Early secondary growth oocyte: Large vesicles (arrow) containing granule vacuoles are found close to the nucleus (N), A) scale bar = 0.2 μm and B) close to periphery, zona radiata (ZR), scale bar = 1 μm. C) Middle secondary growth oocyte: a vacuole (arrow) close to small vesicles containing granular content (arrowhead), mitochondria (M), Golgi apparatus (G), rough endoplasmic reticulum (RER), scale bar = 0.5 μm. D) Small vesicle with granular content (white arrow) close to peroxisomes (black arrow), scale bar = 0.5 μm (Charitonidou et al. 2022a).

Εικόνα 3.9. Ηλεκτρονιογραφίες TEM ωοκυττάρων του γαύρου, *E. encrasicolus*. Α, Β) Ωοκύτταρα πρώιμης δευτερογενούς ανάπτυξης: Μεγάλα κυστίδια (βέλος) που περιέχουν κοκκώδη κενοτόπια βρίσκονται κοντά στον πυρήνα (N), Α) Κλίμακα = 0.2 μm, και Β) κοντά στην περιφέρεια, zona radiata (Zr), κλίμακα = 1 μm. C) Ωοκύτταρο

μέσης δευτερογενούς ανάπτυξης: κενοτόπιο (βέλος) κοντά σε μικρά κυστίδια με κοκκιώδες περιεχόμενο (κεφαλή βέλους), μιτοχόνδρια (M), συσκευή Golgi (G) και αδρό ενδοπλασματικό δίκτυο (RER), Κλίμακα = 0.5 μm. D) Μικρό κυστίδιο με κοκκιώδες περιεχόμενο (λευκό βέλος) κοντά σε υπεροξειδιοσώματα (μαύρο βέλος), Κλίμακα = 0.5 μm (Charitonidou et al. 2022a).

Both species exhibit evidence of exogenous heterosynthesis of yolk. Specifically, oocytes absorb yolk components through pore canals of the thickened zona radiata, which includes long microvilli (**Fig. 3.10A, B**) and numerous actin filament bundles (**Fig. 3.10D**) that provide a more advanced level of controlled mobility (Kjesbu et al. 1996; Kobayashi 1985; Mooseker 1985). In addition, small endocytotic vesicles were found in the cytoplasm (**Fig. 3.10C**). Although the number of microvilli gradually increases during vitellogenesis (**Fig. 3.10A, B**), in mature oocytes the microvilli disappear, and the pits of zona radiata close, preventing the entrance of nutrients (Chung et al. 2009; Jun et al. 2018; Kjesbu et al. 1996).

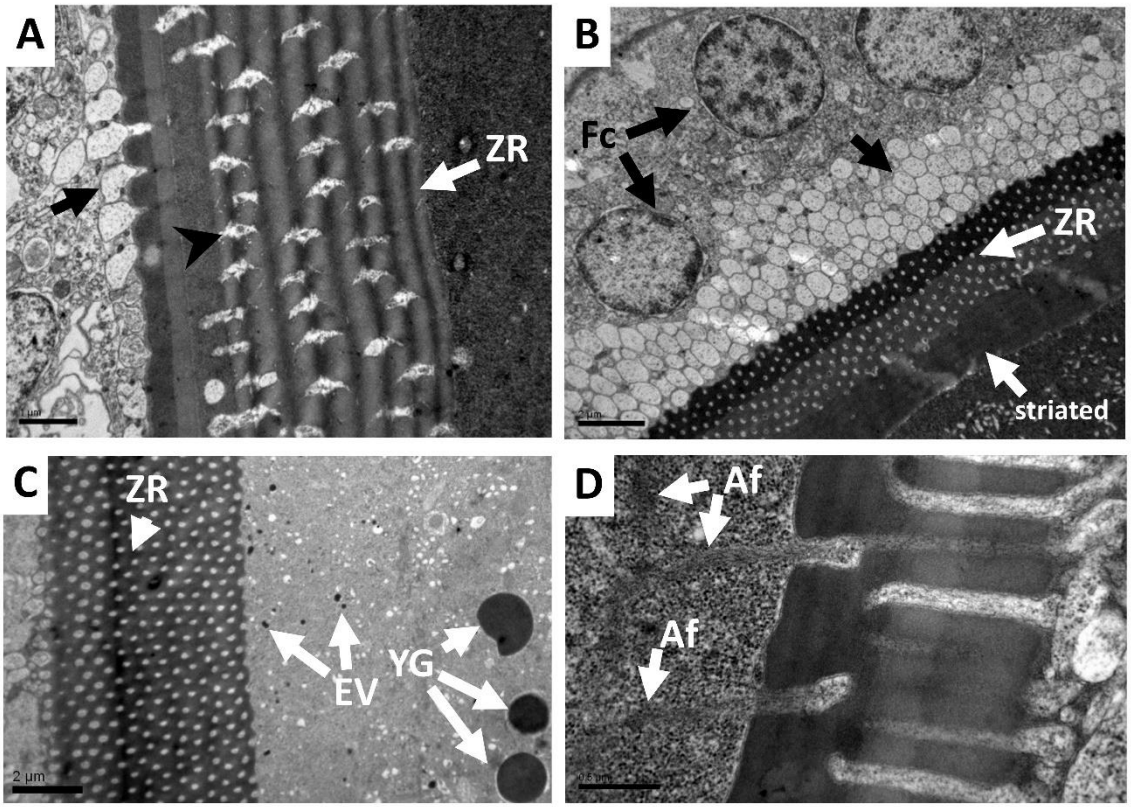

Figure 3.10. Transmission electron micrographs of vitellogenic oocytes. A) *S. pilchardus*. Vitellogenic oocyte with well-developed zona radiata (ZR), which contains pore canals (arrowhead) with few extending microvilli (black arrow). Scale bar = 1 μm. B) *S. pilchardus*. Oocyte at the middle of vitellogenesis: an increased number of microvilli (black arrow). Follicular cells (Fc). Scale bar = 2 μm. C) *E. encrasicolus*. Oocyte at middle vitellogenesis. Small endocytic vesicles (EV) appear in the cytoplasm due to the endocytosis of exogenous yolk proteins. Yolk globules (YG), zona radiata (ZR). Scale bar = 2 μm. D) *S. pilchardus*. The pore canals of zona radiata contain actin filaments bundles (Af). Scale bar = 0.5 μm (Charitonidou et al. 2022a).

Εικόνα 3.10. Ηλεκτρονιογραφίες TEM λεκιθικών ωοκυττάρων.Α) *S. pilchardus*. Λεκιθικό ωοκύτταρο με καλά ανεπτυγμένη *zona radiata* (ZR), που περιέχει κανάλια πόρων (κεφαλή βέλους) με λίγες εκτεινόμενες μικρολάχνες (μαύρο βέλος). Κλίμακα= 1 μm. Β) *S. pilchardus*. Ωοκύτταρο στο μέσο της λεκιθογένεσης: αυξημένος αριθμός μικρολαχνών (εργκάρσια τμημένων, μαύρο βέλος). Θυλακικά κύτταρα (Fc). Κλίμακα = 2 μm. C) *E. encrasicolus*. Ωοκύτταρο στο μέσο της λεκιθογένεσης. Μικρά ενδοκυτταρικά κυστίδια (EV) εμφανίζονται στο κυτταρόπλασμα λόγω της ενδοκυττάρωσης εξωγενών λεκιθικών πρωτεϊνών. Σφαιρίδια λεκίθου (YG), *zona radiata* (ZR). Κλίμακα = 2 μm. D) *S. pilchardus*. Τα κανάλια πόρων της *zona radiata* περιέχουν δέσμες νηματίων ακτίνης (Af). Κλίμακα = 0.5 μm (Charitonidou et al. 2022a).

3.3.5 Variation of oogonial proliferation and meiotic activity between reproductive phases

The eigenvalue of the first principal component of the PCA was greater than 1.0 in both species and thus its scores, PC_{ACT}, served as a synthetic index of oogonial proliferation and meiotic activity. The values of PC_{ACT} differed significantly among the three reproductive phases in both anchovy (Kruskal Wallis test, chi-squared=33.85, df=2, p-value < 0.05) and sardine (Kruskal Wallis test, chi-squared=9.9756, df=2, p-value < 0.05) (**Fig. 3.11**).

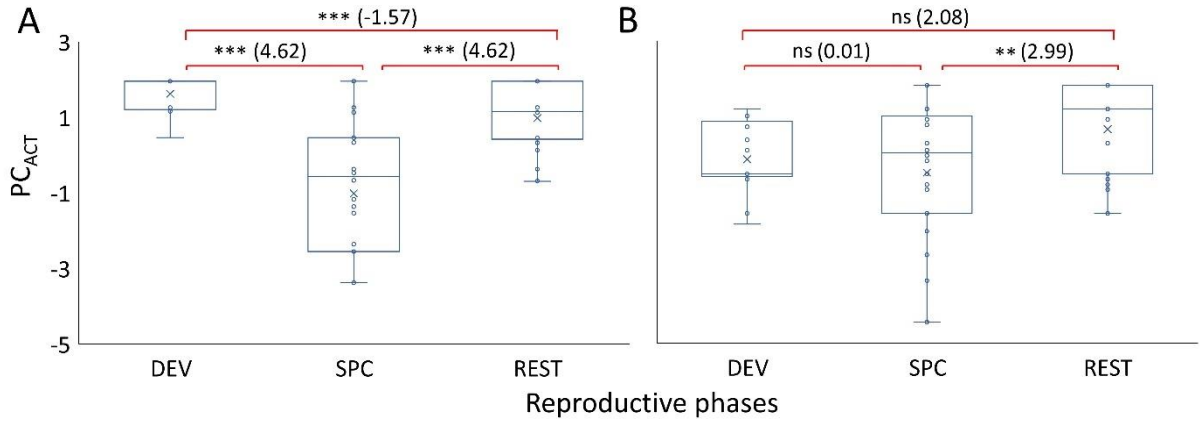

Figure 3.11. Box plots of contribution of oogonial proliferation and meiotic divisions in component 1 of Principal component analysis, (activity index, PC_{ACT}), in developing (DEV), spawning- capable (SPC) and resting (REST) reproductive phases of A) anchovy, *Engraulis encrasicolus,* and B) sardine, *Sardina pilchardus*. Details of the ovarian samples are presented in **Table 3.1**. Dunn's test results were also provided, z in brackets, the statistical significance is indicated by an asterisk (*); ns: non- significant difference; *: p-value < 0.05; ** p-value < 0.01; *** p-value < 0.001 (Charitonidou et al. 2022d).

Εικόνα 3.11. Θηκογράμματα της συμβολής του πολλαπλασιασμού των ωογονίων και των μειωτικών διαιρέσεων στη συνιστώσα 1 της ανάλυσης κύριας συνιστώσας (δείκτης δραστηριότητας, PC_{ACT}), σε αναπτυσσόμενες (DEV), αναπαραγωγικά ικανές (SPC) και απενεργοποιημένες (REST) ωοθήκες του Α) γαύρου, *E. encrasicolus*, και της Β) σαρδέλας, *S. pilchardus*. Λεπτομέρειες για τα δείγματα ωοθηκών παρουσιάζονται στον **Πίνακα 3.1**. Επίσης, αναφέρονται τα αποτελέσματα της δοκιμής Dunn, ο αριθμός z αναγράφεται σε

αγκύλες, η στατιστική σημαντικότητα υποδεικνύεται με αστερίσκο (*). ns: μη σημαντική διαφορά. *: p-value < 0.05; ** τιμή p < 0.01; *** p-value < 0.001 (Charitonidou et al. 2022d).

According to Dunn's test, the DEV phase in anchovy showed the highest activity in oogonial proliferation (80%), whereas the REST phase was situated in between the DEV and SPC phases (**Fig. 3.12A**). Oogonial proliferation in sardines, on the other hand, showed a particularly low prevalence of the two oogonial proliferation markers (mitosis and oogonia nests), but it was more constant throughout the three reproductive phases (**Fig. 3.12B**). The seasonal patterns of oogonial proliferation vary among fish species (**Table 3.3**). In several species, oogonial divisions are most frequent during the post-spawning phase (REST phase), although during spawning or even throughout the reproductive cycle in other species. In other fish species, oogonial proliferation commences at the end of one cycle (Tokarz 1978). No apparent correlation existed between oogonial dynamics and reproductive modes (e.g., oviparity, viviparity), species taxonomy (**Table 3.3**), or fecundity types whether new oocytes are reproduced continuously during the spawning period (indeterminacy) or are fixed at the onset of spawning (determinacy). In general, the higher rate of oogonial proliferation seems to occur during the post-spawning phase, regardless of the reproductive strategy, ensuring the availability of eggs for the new spawning event (de Jesus-Silva et al. 2018; Wildner et al. 2013) (**Table 3.3**). Species with a short annual spawning period, on the other hand, have a limited period of peak oogonial proliferation, whereas species with a longer annual spawning period exhibit “waves” of oogonial proliferation or continuous proliferation throughout the year (Tokarz 1978).

In anchovy, the SPC phase had considerably lower PC_{ACT} values than the other two reproductive phases (**Fig. 3.11A**). Except for diplotene, there was a significantly decreased prevalence of all meiosis (leptotene, zygotene, and pachytene) markers (**Fig. 3.12A**). Overall, the DEV phase in anchovy showed the highest activity: 100% in all meiotic markers, followed by the REST phase (**Fig. 3.12A**). In sardines, the PC_{ACT} values of the SPC phase were considerably lower than those of the REST phase but not of the DEV phase (**Fig. 3.11B**). Only pachytene and leptotene were found to be considerably reduced in the DEV and SPC periods (**Fig. 3.12B**). In the sturgeon, *Acipenser gueldenstaedtii,* after the first spawning, in the REST phase, the larger oocytes were in diplotene, and the smaller oocytes were in earlier phases of meiosis (Raikova 1976). In the indeterminate spawner *Serresalmus maculatus*, the DEV phase had more oocytes in the early phases of meiosis than oogonia nests (Wildner et al. 2013). In general, the meiotic oocyte nests are plenty in some fish species during or after the peak of oogonial proliferation throughout the reproductive cycle. The time interval between the last oogonial division and the beginning of meiosis is thought to be short (Eggert 1931; Yamazaki 1965). In several fish species, the existence of a significant number of meiotic oocyte nests after each spawning shows that oocytes are renewed in the ovary after ovulation (Barr 1963). Furthermore, no cyclic pattern of meiotic oocyte nests is observed in fish species that spawn sporadically throughout the year (Eggert 1931), while in species with no peaks in oogonial proliferation, the meiotic oocyte nests are present all year (Moser 1967).

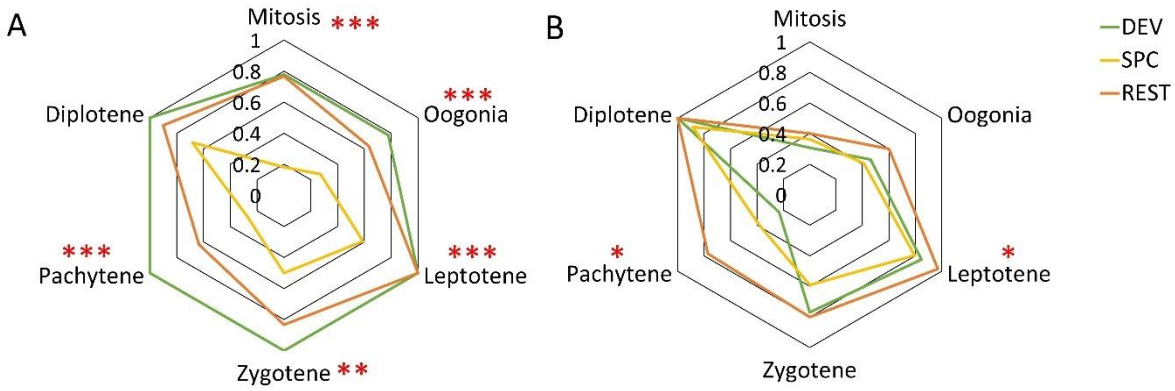

Figure 3.12. Mean values of the prevalence of different markers of oogonial proliferation (mitosis, oogonia nests) and meiotic divisions (leptotene, zygotene, pachytene, and diplotene) in different reproductive phases [developing (DEV), spawning- capable (SPC), and resting (REST)], A) anchovy, *Engraulis encrasicolus,* and B) sardine, *Sardina pilchardus* ovaries. Details of the ovarian samples are presented in **Table 3.1**. The confidence interval is 95%. The Chi-squared test's statistical results are provided, the statistical significance is indicated by an asterisk (*); *: p-value 0.05, ** p-value 0.01; *** p-value 0.001, no asterisk= non-significant difference. In all comparisons degree of freedom (df) was equal to 2 (Charitonidou et al. 2022d).

Εικόνα 3.12. Μέση τιμή της επικράτησης των διαφορετικών δεικτών του πολλαπλασιασμού των ωογονίων (μίτωσης, φωλεές ωογονίων) και των μειωτικών διαιρέσεων (λεπτοταινία, ζυγοταινία, παχυταινία, και διπλοταινία) σε διαφορετικές φάσεις της ωοθήκης [αναπτυσσόμενη (DEV), δυνατότητα ωοτοκίας (SPC), και ανάπαυσης (REST)], Α) γαύρος, *Engraulis encrasicolus* και Β) σαρδέλα, *Sardina pilchardus.* Λεπτομέρειες για τα δείγματα ωοθηκών παρουσιάζονται στον **Πίνακας 3.1**. Το διάστημα εμπιστοσύνης είναι 95%. Τα στατιστικά αποτελέσματα του στατιστικού τεστ X^2 παρέχονται, η στατιστική σημασία υποδεικνύεται με έναν αστερίσκο (*); *: p-value 0.05, ** p-value 0.01; *** p-value 0.001, χωρίς αστερίσκο= μη σημαντική διαφορά. Σε όλες τις συγκρίσεις ο βαθμός ελευθερίας (df) ήταν ίσος με 2 (Charitonidou et al. 2022d).

Table 3.3. Patterns of greatest oogonial proliferation during the reproductive cycle in several fish species, belonging in different superorders (Acanthopterygii, Ostariophysi, Protacanthopterygii) and with different reproductive traits (Oviparity, Ovoviviparity, Viviparity) (Charitonidou et al. 2022d).

Πίνακας 3.3. Μοτίβα του μέγιστου πολλαπλασιασμού των ωογονίων κατά τη διάρκεια της αναπαραγωγικής περιόδου σε διάφορα είδη ιχθύων, που ανήκουν σε διαφορετικές υπερτάξεις (Acanthopterygii, Ostariophysi, Protacanthopterygii) και με διαφορετικά αναπαραγωγικά χαρακτηρίστηκα (Oviparity, Ovoviviparity, Viviparity) (Charitonidou et al. 2022d).

Species	**Superorder**	**Reproductive traits**	**Period of greatest oogonial proliferation**	**Reference**
Cottus bairdii *Eucalia inconstans* *Fundulus heteroclitus* *Gasterosteus aculeatus* *Gillichthys mirabilis* *Pleuronectes platessa* *Acanthopagrus latus* *Dicentrarchus labrax* *Centropomus undecimalis* *Sciaenops ocellatus* *Oreochromis mossambicus*	Acanthopterygii	Oviparous	Postspawning	Hann 1927 Brackevelt and McMillan 1967 Matthews 1938 Craig-Bennett 1931 De Vlaming 1972 Barr 1963 Abou- Seedo et al. 2003 Mayer et al. 1988 Grier 2000 Grier 2012 Coward and Bromage 1998
Oryzias latipes		Oviparous	Spawning	Yamamoto 1962
Heterandria Formosa		Viviparous	Throughout the reproductive cycle	Uribe and Grier 2011
Syngnathus scovelli *Sebastodes paucispinis*		Ovoviviparous	Throughout the reproductive cycle	Begovac and Wallace 1988 Moser 1967
Periophthalmus chrysospilos *Periophthalmus vulgaris*		Oviparous	Throughout the reproductive cycle	Eggert 1931
Ilyodon whitei *Neotoca bilineata*		Viviparous	late gestation, shortly before birth	Nakamura et al. 2010 Mendoza 1943
Carassius auratus *Phoxinus laevis* *Pimelodus maculatus* *Serrasalmus maculatus*	Ostariophysi	Oviparous	Postspawning	Yamazaki 1965 Bullough 1942 Wildner et al. 2013 Wildner et al. 2013
Rhodeus ocellatus		Oviparous	Spawning	Yamamoto and Shirai 1962
Oncorhynchus mykiss	Protacanthopterygii	Oviparous	During and after spawning period	Grier et al. 2007

Overall, the pattern of cell division activity in sardine appeared to be more consistent than that of the anchovy throughout the reproductive cycle (**Fig. 3.11B**). Sardine has mainly a capital breeding strategy, accumulating food energy for spawning, allowing them to have energy support throughout their reproductive cycle (Ganias et al. 2007b; Mustac and Sinovcic 2009; Nunes et al. 2011; Zwolinski et al. 2001). In the case of anchovy, which has an income breeding strategy (Somarakis et al. 2004; Somarakis 2005), the ovaries are prepared for the next spawning period primarily prior to and after spawning, when food supplies have begun to recover and become plentiful (**Fig. 3.1**). The period of peaked oogonial proliferation occurs after the spawning period in the cases of *Fundulus heteroclitus* and *Gasterosteus aculeatus*, which are both indeterminate spawners and income breeders, like anchovy, whereas in *Oryzias latipes*, which is an indeterminate spawner exhibiting both income and capital breeding strategies, the peaked period of oogonial proliferation exists during the spawning (McBride et al. 2015; Tokarz 1978). The peak period of oogonial proliferation occurs after the spawning period in *Gillichtys mirabilis*, another indeterminate spawner with a mixed capital and income breeding strategy (McBride et al. 2015; Tokarz 1978). On the other hand, the oogonial proliferation is increased after the spawning period in *Pleuronectes platessa* and *Dicentrarchus labrax*, two species with determinate fecundity type and mainly capital breeding strategy (McBride et al. 2015; Tokarz 1978). In fishes, there is evidence of interspecific as well as intra-individual, ontogenetic variations in energy acquisition and allocation to reproduction (McBride et al. 2015). Both the fecundity type and the feeding strategy of species seem to shape the dynamics of oogonial proliferation; however, this assumption needs further investigation.

According to evidence, both oogonia and early oocytes regulate the configuration of the fecundity during oogenesis (dos Santos Schmidt et al. 2017; Higashino et al. 2002; Thome et al. 2012). Specifically, unfavourable environmental conditions, such as poor food supply, exert a negative impact on primary growth reservoirs and early oocyte recruitment, consequently affecting future fecundity (dos Santos Schmidt et al. 2017). Under favourable environmental circumstances (temperature, dissolved oxygen), oogonia are driven to enter meiosis, meiotic oocyte nests are produced, and apoptosis is minimal (Thome et al. 2012). When environmental conditions are unfavourable, oogonia proliferation occurs together with few meiotic oocyte nests and a high rate of apoptosis (Thome et al. 2012).

3.4 Conclusion

The current chapter describes the developmental changes in sardine and anchovy oocytes during early oogenesis, as well as the dynamics of oogonial proliferation and early oocytes. In particular, there were differences in the development of oocytes between sardines and anchovies. In both species, a spherical Bb with membranous threads and few mitochondria were seen in primary growth oocytes. In both species, a perinuclear ring was visible. A thick perinuclear zone of mitochondria, nuage, and small vesicles were found in sardines, whereas nuage and mitochondria complexes were seen in anchovies. In secondary growth oocytes, cytoplasmic zonation evolved differently in the two species after Bb was dissembled. Based on both differences in cytoplasmic dynamics of each studied species and mitochondrial alterations, it was assumed that mitochondria in sardines play a role in the

formation of yolk granules, whereas mitochondria in anchovies play a role in the lipid synthesis pathway. Both species showed exogenous heterosynthesis of yolk, through the process of pinocytosis in the zona radiata of oocytes. Both Bb and cytoplasmic zonation are visible using traditional histological processes and they could be employed as markers to differentiate between immature and mature fishes, as well as to indicate the onset of the reproductive phase, providing a valuable tool for applied fisheries biology. Changes in chromosomes due to the cell divisions were utilized as markers to identify oogonia and early oocyte recruitment and dynamics. Both mitotic and meiotic divisions were used as markers to analyse the dynamics of oogonial proliferation and early (chromatin nucleolus) oocytes in sardine and anchovy throughout the reproductive cycle. Our working hypothesis was confirmed because ongoing recruitment from oogonia to early oocytes occurred throughout the reproductive cycle in both species investigated. In anchovies, oogonial proliferation was higher both before (developing ovaries) and after (resting ovaries) spawning, whereas, in sardine, it was stable throughout the reproductive period. Before the spawning period, anchovy ovaries exhibited a higher rate of prophase I meiotic activity, whereas sardine ovaries had a higher rate after the spawning period. Understanding the early phases of oogenesis is crucial since the dynamics of oogonia and early oocytes appear to be affected by environmental conditions and have an impact on fecundity, a key parameter in applied fisheries.

Chapter 4: Secondary phase of oogenesis: Ovarian dynamics and their link with the spawning dynamics at the interspecies level

These results have been published in the scientific articles:
Charitonidou K., Kjesbu O.S., Dominguez-Petit R., Garabana D., Korta M.A., Santos M., van Damme C.J.G., Thorsen A., Ganias K. (2020). Contrasting post-ovulatory follicle production in fishes with different spawning dynamics. *Fisheries Research*, 231: 105710.

Charitonidou K., Ganias K. (2021). Using clustering algorithms for identification of fish oocyte cohorts based on the characteristics of cytoplasmic structures. *Theriogenology*: 170: 46-53.

Charitonidou K., Kjesbu O.S., Nunes C., Angelico M.M., Domingues-Petit R., Garabana D., Ganias K. (2022b). Linking the dynamic organization of the ovary with spawning dynamics in pelagic fishes. *Marine Biology*, 169: 47.

4.1 Specific objectives

The aim of this chapter was to analyze the ovarian dynamics of three fish species during the secondary phase of oogenesis. Specifically, the dynamics of secondary growth oocytes were studied in different ovarian stages of three commercially important fish species with indeterminate fecundity but distinct spawning dynamics, the Atlantic sardine, *Sardina pilchardus*, the Atlantic horse mackerel, *Trachurus trachurus*, and the Atlantic mackerel, *Scomber scombrus*. Furthermore, the dynamics of the remnants of the released egg (postovulatory follicles, POFs) were investigated in two fish species, the Atlantic sardine, and the Atlantic mackerel, with different spawning frequencies. POFs dynamics are of great importance since they are commonly implemented for spawning fraction estimated in the application of the daily egg production method (DEPM). Histological procedures and particle analysis were performed on the ovarian samples. Several methods were utilized to investigate secondary growth oocytes, including oocyte size frequency distribution, total fecundity ratio, number of oocyte cohorts, and recruitment of early secondary growth oocytes based on historic estimations of spawning frequency and oocyte growth rate. Additionally, a novel method was developed that used clustering analysis algorithms on the specific histological traits of secondary growth oocytes to estimate the number of oocyte cohorts in species with complex ovarian dynamics. Two methods were applied to investigate the dynamics of POFs, the Weibel method and the simple oocyte packing density method (OPD method) adjusted in POFs (POFPD method), estimating the relative number of POFs leading to the number of POFs cohorts. Interspecies variability in ovarian dynamics is expected due to the varied spawning attributes of the three species investigated. Because all of the fish analysed are indeterminate spawners, ongoing recruitment from primary growth to secondary growth oocytes is expected. Due to the high spawning interval, multiple POFs cohorts are likely to co-occur in the ovaries of the Atlantic mackerel.

4.2 Specific methodology

4.2.1 Recruitment pattern from primary to secondary growth oocytes

The oocyte recruitment pattern from primary to secondary growth phase was examined among ovarian stages of each species as well as between the three species. For this purpose, the numerical ratio of early secondary growth oocytes (ESG) to late primary growth oocytes (LPG) was used. For comparative purposes, a common size range was used for both the ESG (200–250 μm) and LPG (150–200 μm) oocytes in all three species. The size range of LPG oocytes followed pilot examinations of oocyte size frequency distributions in specimens containing only primary growth oocytes, i.e., prespawning fish and spent females (see also the study by Greer Walker et al. (1994) for mackerel). The size range of ESG oocytes was based on the findings of Ndjaula et al. (2009) for horse mackerel, assuming that there were no important interspecific differences in the size of these very early oocyte stages (see also Greer Walker et al. 1994).

4.2.2 Investigation of the secondary growth oocytes dynamics

The number of cohorts of secondary growth oocytes was estimated using three different methods: two methods based on whole mounts and one on histological procedures. The first method, based on whole mounts, was the 'fecundity ratio' calculated as the ratio of RN_{SG} to RF_B (Ganias et al. 2017; Mouchlianitis et al. 2020). The second method, based on histology, was a new innovative method for grouping secondary growth oocytes into different cohorts based on the application of the K-means clustering algorithm on the characteristics of cytoplasmic structures, such as the varying size and intensity of cortical alveoli and yolk granules in oocytes of different development. The method allowed the grouping of oocytes without the need of using oocyte diameter, and thus, a crucial histological bias dealing with the cutting angle and the orientation of reference points (e.g., nucleus) has been overcome (**Section 4.2.3**). The third method was based on the analysis of oocyte size frequency distributions (obtained from whole mounts) and the decomposition of overlapping oocyte size distributions (Bhattacharya 1967) to identify the number of different secondary growth oocyte modes. In addition, the relative fecundity of each oocyte cohort (cohort specific fecundity, RF_{ci}) was assessed gravimetrically (see **Annex 7**).

4.2.3 Clustering algorithms for identification of fish oocyte cohorts based on the characteristics of cytoplasmic structures

Clustering analysis was developed to identify the fish oocyte cohorts. According to this analysis, the oocytes of each ovary were classified into two groups based on whether the cortical alveoli (ca) (oocyte group I, OcGI) or the yolk granules (yg) (oocyte group II, OcGII) served as better indicators for their histological characterization. Specifically, the OcGI group included pre-vitellogenic oocytes with only cortical alveoli (**Fig. 4.1A**) and early vitellogenic oocytes with both cortical alveoli and oil droplets (**Fig. 4.1B**), as in sardine the oil droplets begin to appear in the cytoplasm during the early vitellogenic stage (Nejedli et al. 2004; Ganias et al. 2004). Oil droplets and cortical alveoli look like unstained vesicles in histological sections through conventional haematoxylin-eosin preparations (Forberg 1982;

Quagio-grassiotto et al. 2014). Given their similar histological appearance, they were both considered as cortical alveoli in subsequent encodings. In some early vitellogenic oocytes, i.e., those with a well-formed zona radiata and few smaller yolk granules, this assignment was more elaborate and was based on whether cortical alveoli were wholly discernible and thus measurable (OcGI, **Fig. 4.1B**) or whether they were obscured by overlaying yolk granules (**Fig. 4.1C**). In the latter case, oocytes were classified into the OcGII group (**Fig. 4.1D**) and thus yolk granules were utilized for their histological characterization. This procedure was performed in sardine for oocytes up to the end of VTG stage. The advanced oocyte mode from the GVM stage onwards was considered as a single, well-distinguishable cohort, which was subsequently manually added to the number of cohorts calculated by the clustering analysis.

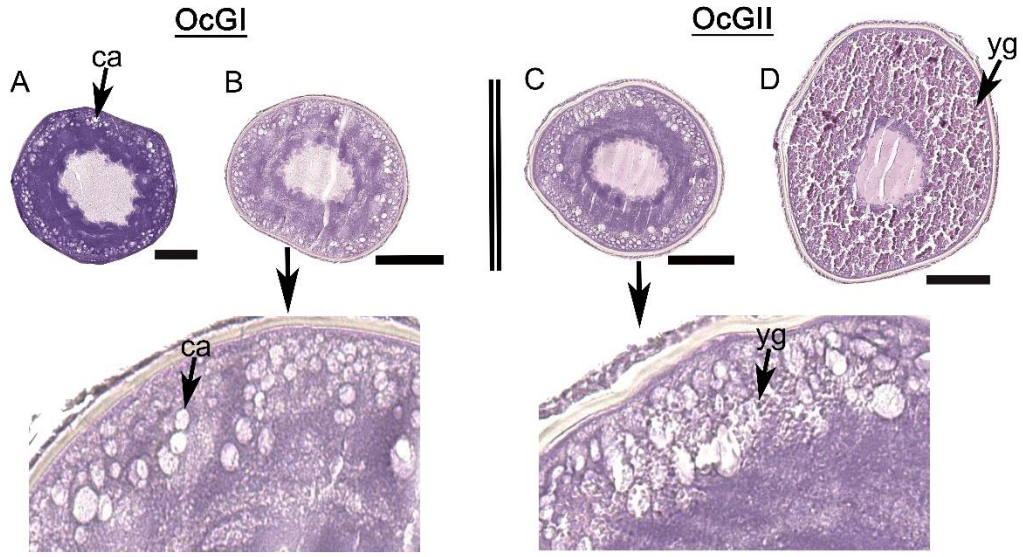

Figure 4.1. Characteristics of oocyte group I (OcGI) and oocyte group II (OcGII): A) oocytes with clearly defined, and measurable cortical alveoli (ca). Scale bar = 50 μm. B) early vitellogenic oocytes with a well-formed zona radiata with very small yolk granules and measurable cortical alveoli (ca). Scale bar = 100 μm. C) early vitellogenic oocytes with a well-formed zona radiata and larger yolk granules (yg) which overlap cortical alveoli. Scale bar = 100 μm. D) vitellogenic oocytes with clearly defined and measurable yolk granules (yg). Scale bars =100 μm (Charitonidou and Ganias 2021).

Εικόνα 4.1. Χαρακτηριστικά της ομάδας ωοκυττάρων I (OcGI) και της ομάδας ωοκυττάρων II (OcGII): Α) ωοκύτταρα με σαφώς καθορισμένες και μετρήσιμες κυψελίδες του φλοιού (ca). Κλίμακα = 50 μm. Β) πρώιμα λεκιθικά ωοκύτταρα με καλοσχηματισμένη *zona radiata* με πολύ μικρούς κόκκους λεκίθου και μετρήσιμες κυψελίδες του φλοιού (ca). Κλίμακα = 100 μm. C) πρώιμα λεκιθικά ωοκύτταρα με καλοσχηματισμένη *zona radiata* και μεγαλύτερους κόκκους λεκίθου (yg) που επικαλύπτουν τις κυψελίδες του φλοιού. Κλίμακα = 100 μm. D) Λεκιθικά ωοκύτταρα με σαφώς καθορισμένους και μετρήσιμους κόκκους λεκίθου (yg). Κλίμακα =100 μm (Charitonidou and Ganias 2021).

The size of the largest cortical alveoli (ca_{max}) and of the largest yolk granules (yg_{max}) were measured in OcGI and OcGII oocytes of the section, respectively. To achieve this measurement, the five to six largest cortical alveoli or yolk granules were visually detected, their diameters were measured, as the average major/minor axis, and the biggest value was corresponded to ca_{max} and yg_{max}, respectively. In both oocyte groups, the oocyte diameter (OD) was again measured as the average major/minor axis in cells with clearly visible nucleus. The intensity of cortical alveoli (ca_{int}) and of yolk granules (yg_{int}) was also considered. Both parameters were measured as the area fraction of cortical alveoli and of yolk granules in the cytoplasm of OcGI and OcGII oocytes, respectively. These measurements were performed using a semi-automated, image-analysis procedure - briefly described in **Fig. 4.2** similar to that described by Thorsen and Kjesbu (2001) to identify and count whole oocytes in ovarian samples of fishes using the ImageJ software (Rueden et al. 2017). This process can be performed automatically by preparing a proper Macro in ImageJ software. The above histological characteristics of the cytoplasmic structures (size and intensity) were used to group oocytes into different cohorts using the K-means clustering analysis (MacQueen 1967). The algorithm of Hartigan and Wong (1979) was used by default and 25 random starts were selected to distribute the data in order to set the initial centres for the clusters. To make use of as many data as possible, the analysis was carried out using oocytes with both visible and invisible nuclei. The optimal number of oocyte cohorts (k centroids) in each specimen was defined by 30 different indices using ca_{max} and ca_{int} for OcGI and yg_{max} and yg_{int} for OcGII. The K-means clustering results were evaluated by applying the Silhouette analysis (Kaufman and Rousseeuw 2005; Rousseeuw 1987). The Silhouette width metric indicated either the best (values close to 1) or the poorest (values close to -1) match between the data of the same and the neighbouring group (**Fig. 4.3**).

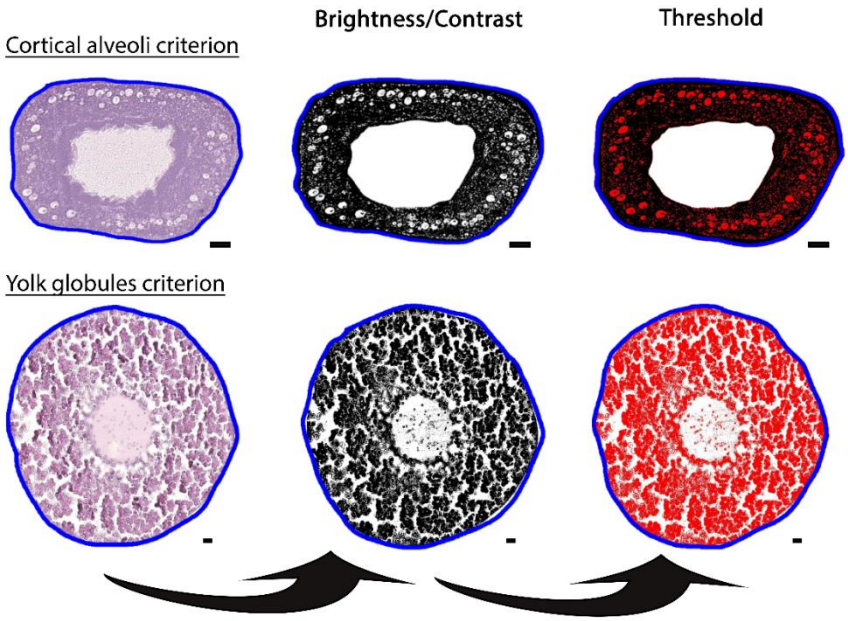

Figure 4.2. Measurement of cortical alveoli (ca; upper panel) and yolk granules (yg; lower panel) intensity in OcGI and OcGII oocytes, respectively, cropped from ovarian histomicrographs of sardine, *Sardina pilchardus*.

The important steps of the image analysis procedure for the identification of ca and yg, involving adjustments in brightness/contrast (middle panels) and threshold of 8-bit images (right panels), is presented. Scale bars= 20 μm (Charitonidou and Ganias 2021).

Εικόνα 4.2. Μέτρηση της πυκνότητας των κυψελίδων του φλοιού (ca, άνω πλαίσιο) και των κοκκίων λεκίθου (yg, κάτω πλαίσιο) στα ωοκύτταρα OcGI και OcGII, αντίστοιχα, που περικόπηκαν από φωτομικρογραφίες ωοθηκών σαρδέλας, *Sardina pilchardus*. Απεικονίζονται τα σημαντικά βήματα για τη διαδικασία ανάλυσης εικόνας για την αναγνώριση των ca και yg, που περιλαμβάνουν προσαρμογές στη φωτεινότητα/αντίθεση (μεσαίο πλαίσιο) και ορισμό του ορίου των εικόνων 8-bit (δεξί πλαίσιο). Κλίμακα= 20 μm (Charitonidou and Ganias 2021).

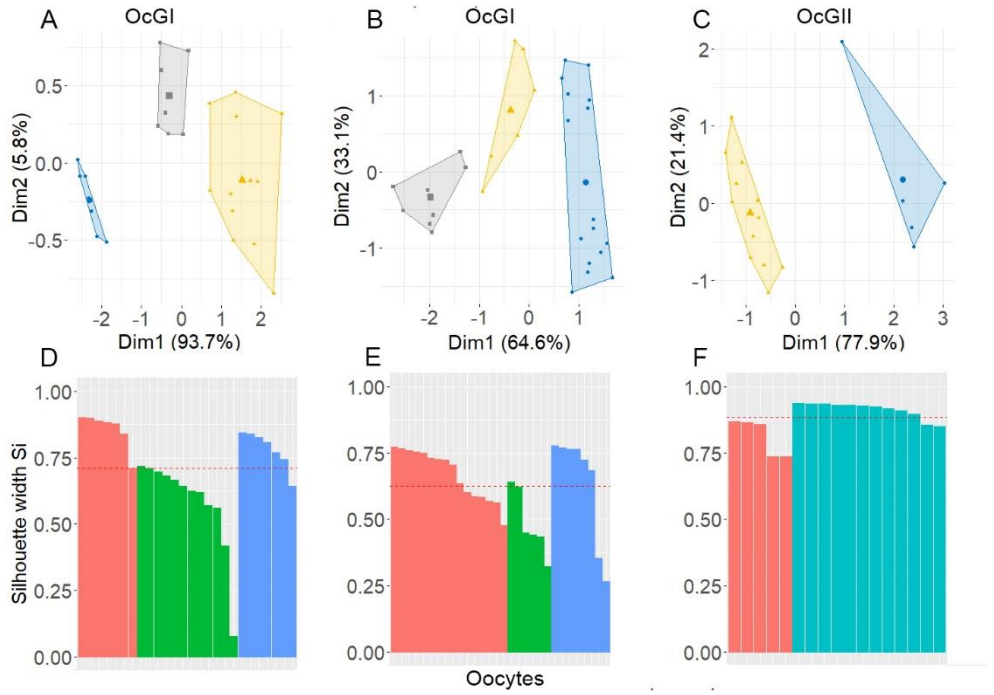

Figure 4.3. Results of the classification of oocytes in the ovaries of sardine, *Sardina pilchardus*, using the K means clustering analysis. A) Principal component analysis (PCA) in grouping results of a CA ovary. B-C) PCA in grouping results of a VTG3 ovary, of oocytes in group I (OcGI) (B) and oocytes in group II (OcGII) (C). D-F) evaluation of K means clustering analysis results through the average silhouette width, of OcGI oocytes of a CA ovary (D) and OcGI (E) and OcGII oocytes (F) of a VTG3 ovary. Red dotted line represents the average value of Silhouette width metric (Charitonidou and Ganias 2021).

Εικόνα 4.3. Αποτελέσματα της ταξινόμησης των ωοκυττάρων στις ωοθήκες της σαρδέλας, *Sardina pilchardus*, χρησιμοποιώντας την ανάλυση ομαδοποίησης K means. A) Ανάλυση κύριου συστατικού (PCA) στην ομαδοποίηση των αποτελεσμάτων μιας ωοθήκης στο στάδιο CA. B-C) PCA στην ομαδοποίηση των αποτελεσμάτων μιας ωοθήκης VTG3, των ωοκυττάρων στην ομάδα I (OcGI) (B) και των ωοκυττάρων στην ομάδα II (OcGII) (C). D-F) αξιολόγηση των αποτελεσμάτων της K means ανάλυσης ομαδοποίησης μέσω του μέσου πλάτους silhouette, των ωοκυττάρων OcGI μιας ωοθήκης CA (D) και των ωοκυττάρων OcGI (E) και OcGII (F) μιας

ωοθήκης VTG3. Η κόκκινη διακεκομμένη γραμμή αντιπροσωπεύει τη μέση τιμή της μέτρησης του πλάτους Silhouette (Charitonidou and Ganias 2021).

The main advantage of this method is that this classification is rather based on developmental processes than on oocyte growth trajectories, helping to circumvent traditional problems dealing with the cutting angle at histological sectioning and related bias issues on oocyte size. This bias is less prominent in small cytoplasmic structures such as cortical alveoli and yolk granules which are plenty in number and at different depths in the cytoplasm. Furthermore, two basic parameters were considered, both intensity and maximum size of the structures to minimize the cutting problem. So, combining this method with methods of stereological analysis, the volume fraction and oocyte number for each cohort can be assessed.

4.2.4 Examination of POFs dynamics

Given that POFs are the remnants of the follicular complex after ovulation, the number of POFs in a single daily cohort, i.e., POF fecundity (F_{POF}), should reflect batch fecundity (F_B), i.e., the number of eggs spawned in a single spawning event. Consequently, relative POF fecundity (number of POFs per gram eviscerated body weight; $RF_{POF} = F_{POF}/W_{EV}$) should equal relative batch fecundity (number of oocytes per gram eviscerated body weight; $RF_B=F_B/W_{EV}$), i.e., $RF_{POF}=RF_B$. In that respect, the ratio of the total number of POFs in the ovary (POF fecundity; F_{POF}) to batch fecundity (F_B) should be indicative of species-specific spawning dynamics. Ratio values close to unity denote the existence of a single POF cohort whilst higher values are expected based on the number of multiple POF cohorts. RF_{POF} was estimated using the Weibel method (see **Annex 2**) and specially designed packing density theory for POFs (POFPD) (see **Annex 3**).

The fact that sectioned POFs, in contrast to, for example, sectioned oocytes with a central nucleus, lack a proper orientation plane implied that the cutting angle was only indicative of the actual POF size. Consequently, critical POF diameter (POF_{DA}) was calculated through testing variability in RF_{POF} amongst the smallest (POF_{DAS}), the intermediate (POF_{DAI}) and the largest (POF_{DAL}) values within the stabilization range (see **Annex 3**).

Histological slides were examined for possible co-occurrence of distinct POF stages (see **Annex 8**). The determination of the number of POFs cohorts was particularly difficult due to overlapping characteristics between the smaller POFs of the younger daily cohort(s) and the bigger POFs of the next/older cohort(s), especially in mackerel ovaries. There existed a continuous range of POF sizes with no distinguishing modes, which meant that POF size could not be utilized to stage distinct cohorts as previously done (e.g., Ganias et al. 2007a). Furthermore, methodological factors such as the cutting angle and the varying quality of histological preparations influenced the fine cytomorphological aspects of individual POFs, such as follicle shape and the status of the granulosa layer (Ganias 2013).

As a result, our scorings only provided an estimate of the number of co-occurring POF cohorts, not a definitive assignment of all POFs from each specimen to various cohorts.

4.3 Results and Discussion

4.3.1 Dynamics of the secondary growth oocytes

In all three species, the oocyte size frequency distribution was continuous in the size range between 150 and 250 μm indicating continuous recruitment from primary growth to secondary growth oocytes during all reproductive stages (**Fig. 4.4**). This pattern is common in indeterminate spawners because oocyte recruitment is a continuous process throughout the spawning period (Hunter et al. 1985; Greer Walker et al. 1994; Murua and Saborido-Rey 2003; Armstrong and Witthames 2012). However, recent research shows that determinate spawners such as *Gadus morhua* can also have a continuous oocyte size frequency distribution (Anderson et al. 2020), while according to Ganias (2013), pure determinacy and indeterminacy are rather recognized as end- points along a continuum of intermediate patterns that is generally controlled by the time lag between oocyte recruitment period and spawning period. In that respect, the continuity between primary growth and secondary growth oocytes is not always indicative of the fecundity type and other aspects such as the characteristics of oocyte size frequency distribution should also be considered (Hunter et al. 1989, 1992; Kjesbu et al. 1990; Witthames and Greer Walker 1995; Ganias 2013). In addition, complexities in the seasonal spawning pattern such as the cessation of oocyte recruitment at the latter part of the spawning period also need to be considered (see **Section 4.2.3**; Brown-Peterson et al. 2017; Ganias et al. 2017; Mouchlianitis et al. 2020; Karlou- Riga et al. 2020).

However, the shape of the distributions differed, particularly between sardine (smooth pattern, **Fig. 4.4A**) and mackerel (highly skewed pattern, **Fig. 4.4C**), while the pattern in horse mackerel was intermediate (**Fig. 4.4B**). These differences lead to significant ($p < 0.05$) differences in the numerical ratio of early SG oocytes (200–250 μm) and late PG oocytes (150–200 μm), i.e., ESG:LPG, between the three species. In particular, the ESG:LPG ratio was significantly higher ($p < 0.05$) in sardine (0.48 ± 0.04) compared to horse mackerel (0.33 ± 0.04) and mackerel (0.19 ± 0.04). These findings apply to the peak of the spawning period; however, the situation may be different at the onset or end of the spawning period. As a result, it is suggested that the ESG:LPG ratio can serve as a proxy of secondary growth recruitment dynamics primarily indicating the annual fecundity type of a fish population/species. Sardine, for example, with continuous SG recruitment throughout the spawning period (Ganias et al. 2014a), tending to the indeterminate fecundity end- point, should display higher ESG:LPG ratios. On the other hand, horse mackerel was previously shown to cease recruiting secondary growth oocytes at the latter part of the spawning period (Ganias et al. 2017); this pattern is untypical for indeterminate spawners, consequently leading to a lower ESG:LPG ratio. In mackerel which displayed the lowest ESG:LPG ratio among the three species, the tapering of secondary growth recruitment should be even more pronounced. Indeed, Greer Walker et al. (1994) showed a sharp decrease in the proportion of small oocytes (120–144 μm) with ovarian development, suggesting a tapering in oocyte recruitment

with the progress of the reproductive period, this is also observed in the study of Mouchlianitis et al. (2021) for the blueback herring, *Alosa aestivalis*. Even if both mackerel and horse mackerel are now considered indeterminate spawners (Macer 1974; Karlou-Riga and Economidis 1997; Gordo et al., 2008; Ndjaula et al., 2009; ICES 2011, 2012, 2018; Ganias et al. 2017; Jansen et al. 2021; dos Santos Schmidt et al. 2021), their differences in ESG:LPG ratio indicates a tendency towards the 'determinate' end-point; this explains why the fecundity type of these two species has been so controversial during the last decades (see **Section 1.4**). We may thus conclude that even if oocyte growth rate and spawning interval affect the recruitment rate from LPG and ESG, the degree of overlap between the two oocyte groups is mostly regulated by the annual fecundity type, i.e., the time lag between the oocyte recruitment period and spawning period. Given that ambient temperature influences both spawning interval and oocyte development rate [see reviews by Ganias (2013) and Ganias et al. (2015)], we may assume that the ESG:LPG ratio is likewise temperature- dependent.

On the other hand, the ESG:LPG ratio did not differ significantly between the different ovarian stages in sardine ($p > 0.05$; **Fig. 4.5**). Nevertheless, in horse mackerel, the ESG:LPG ratio in GVBD was apparently lower compared to VTG and GVM, and in mackerel, a difference was noticed between the VTG and the other ovarian stages (**Fig. 4.5**). In both species, these GVBD and VTG values were close to the mean ratio of each ovarian stage, without high variances (**Fig. 4.5**).

The oocyte size frequency distribution of secondary growth oocytes in all three species was always continuous and polymodal (**Fig. 4.6**). The only clearly distinguishable mode was the advanced one (AM), which grew progressively and, at some point, was separated with a size hiatus from the intermediate secondary growth oocytes—i.e., those between the primary growth–secondary growth threshold and the AM hiatus—hereinafter referred to as the "SG pool". In sardine, the hiatus between the SG pool and the AM occurred at the early VTG stage (**Fig. 4.6A**), a similar pattern is also reported for two other clupeoids (*Etrumeus teres*: Plaza et al. 2007; *Etrumeus golanii*: Somarakis et al. 2021) in which the advanced batch grows rapidly after spawning and shortly separates from the smaller oocytes. Whereas in horse mackerel and mackerel it occurred later at the GVBD and GVBD-HYD stages, respectively (**Fig. 4.6B, C**). The maximum oocyte diameter of the SG pool reached 450–500 μm, but never exceeded 500 μm in sardine (**Fig. 4.6A**), 600–750 μm in horse mackerel (**Fig. 4.6B**), and 700–850 μm in mackerel (**Fig. 4.6C**). Most ovaries in sardine and mackerel were at the VTG and GVM stages, respectively, while horse mackerel again showed an intermediate pattern between the other two species (**Fig. 4.6**).

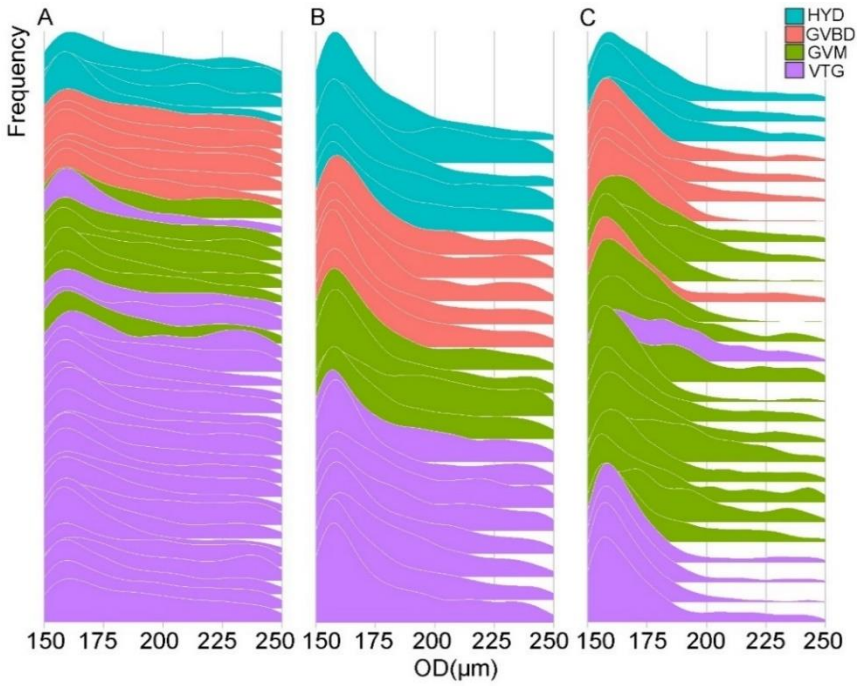

Figure 4.4. Frequency distributions of oocytes with diameters between 150 and 250 μm (OD, μm). Rows represent different individuals in ascending order of maximum oocyte size observed within the ovary: A) sardine (*Sardina pilchardus*), B) horse mackerel (*Trachurus trachurus*), and C) mackerel (*Scomber scombrus*). Colours indicate ovarian stages, vitellogenic stage (VTG, purple), germinal vesicle migration (GVM, green), germinal vesicle breakdown (GVBD, pink), and hydration stage (HYD, blue) (Charitonidou et al. 2022b).

Εικόνα 4.4. Κατανομές συχνοτήτων των ωοκυττάρων με διάμετρο μεταξύ 150 και 250 μm (OD, μm). Οι σειρές παρουσιάζουν διάφορα άτομα ιχθύων με αύξουσα σειρά μέγιστου μεγέθους ωοκυττάρου που παρατηρείται εντός της ωοθήκης: Α) σαρδέλα (*Sardina pilchardus*), Β) γκριζοσαύριδο (*Trachurus trachurus*) και C) σκουμπρί (*Scomber scombrus*). Τα χρώματα υποδεικνύουν στάδια των ωοθηκών, στάδιο λεκιθογένεσης (VTG, μωβ), μετανάστευση βλαστικού κυστιδίου (GVM, πράσινο), ρίξη βλαστικού κυστιδίου (GVBD, ροζ) και στάδιο ενυδάτωσης (HYD, μπλε) (Charitonidou et al. 2022b).

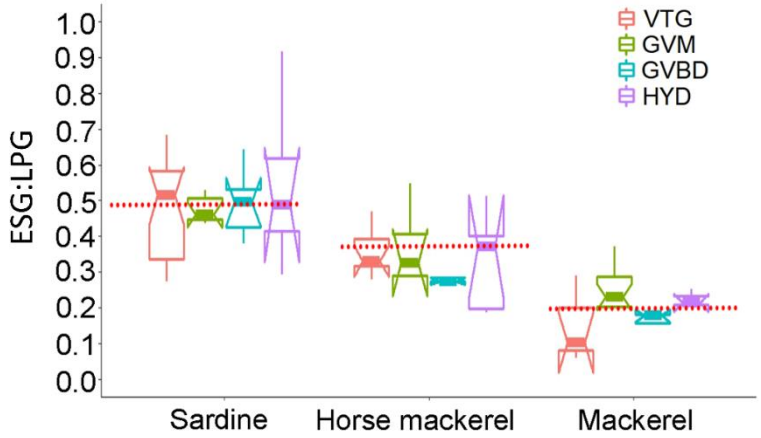

Figure 4.5. Box and whiskers plots of the numerical ratio of early secondary growth to late primary growth oocytes (ESG:LPG) per ovarian stage for sardine (*Sardina pilchardus*), horse mackerel (*Trachurus trachurus*), and

mackerel (*Scomber scombrus*). VTG vitellogenic stage, GVM germinal vesicle migration, GVBD germinal vesicle breakdown stage, HYD hydration stage. The median is marked by the thick line within each box and the mean ratio value of each species is indicated by the dashed line (Charitonidou et al 2022b).

Εικόνα 4.5. Διάγραμμα Box and whiskers του αριθμητικού κλάσματος των ωοκυττάρων πρώιμης δευτερογενούς ανάπτυξης προς όψιμης πρωτογενούς ανάπτυξης (ESG:LPG) ανά στάδιο ωοθήκης για τη σαρδέλα (*Sardina pilchardus*), το γκριζοσαύριδο (*Trachurus trachurus*) και το σκουμπρί (*Scomber scombrus*). VTG λεκιθικό στάδιο, GVM στάδιο μετανάστευσης βλαστικού κυστιδίου, GVBD στάδιο ρίξης βλαστκού κυστιδίου, HYD στάδιο ενυδάτωσης. Η διάμεσος σημειώνεται με τη γραμμή μέσα σε κάθε πλαίσιο και η μέση τιμή του κλάσματος κάθε είδους υποδεικνύεται από τη διακεκομμένη γραμμή (Charitonidou et al 2022b).

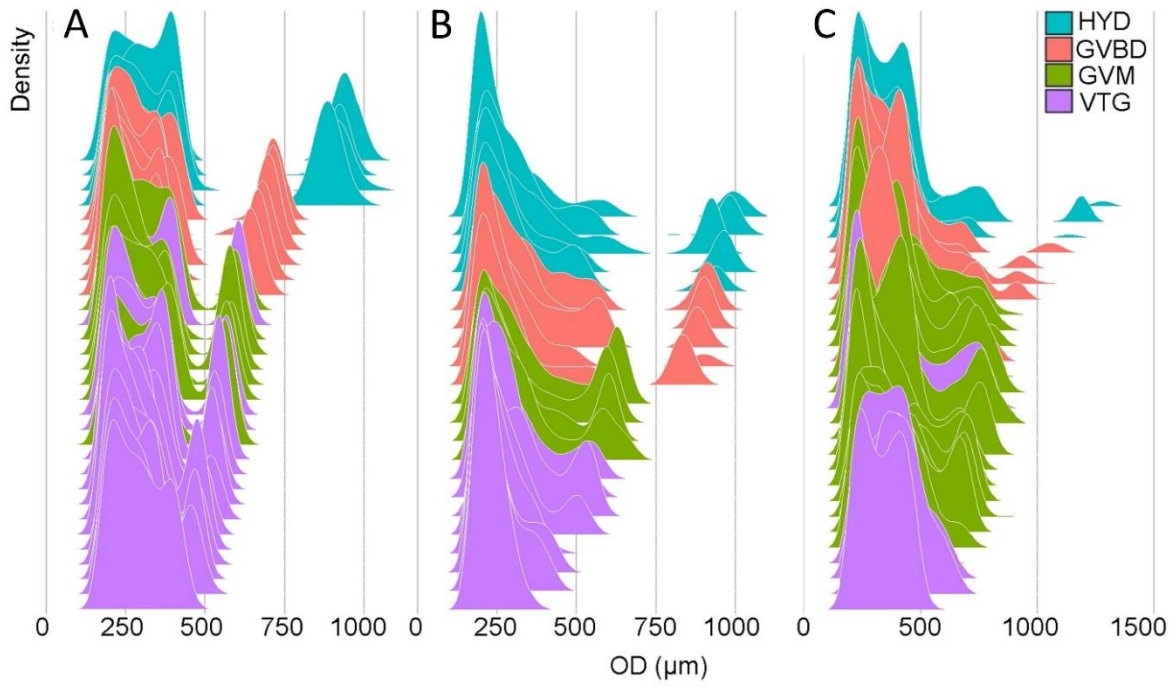

Figure 4.6. Oocyte size frequency distributions (diameter > 150 μm) per ovarian stage for the three assessed species: A) sardine (*Sardina pilchardus*), B) horse mackerel (*Trachurus trachurus*), and C) mackerel (*Scomber scombrus*). Rows represent different individuals of the three species in ascending order of maximum oocyte size. Vitellogenic stage (VTG), germinal vesicle migration (GVM), germinal vesicle breakdown stage (GVBD), hydration stage (HYD). Picking joint bandwidth was 15.3 for sardine, 7.15 for horse mackerel, and 9.44 for mackerel (Charitonidou et al 2022b).

Εικόνα 4.6. Κατανομές συχνοτήτων μεγεθών ωοκυττάρων (διάμετρος > 150 μm) ανά στάδιο ωοθήκης για τα τρία είδη που αξιολογήθηκαν: Α) σαρδέλα (*Sardina pilchardus*), Β) γκριζοσαύριδο (*Trachurus trachurus*) και C) σκουμπρί (*Scomber scombrus*). Οι σειρές αντιπροσωπεύουν διαφορετικά άτομα των τριών ειδών με αύξουσα σειρά μέγιστου μεγέθους ωοκυττάρου. Λεκιθικό στάδιο (VTG), μετανάστευση βλαστικού κυστιδίου (GVM), στάδιο ρίξης βλαστικού κυστιδίου (GVBD), στάδιο ενυδάτωσης (HYD). Το εύρος ζώνης επιλογής της ένωσης ήταν 15,3 για τη σαρδέλα, 7,15 για το γκριζοσαύριδο και 9,44 για το σκουμπρί (Charitonidou et al 2022b).

The mean RN_{PG} was 2474 (± 390) oocytes*g^{-1} for sardine, 2108 (± 459) oocytes*g^{-1} for horse mackerel, and 3409 (± 1335) oocytes*g^{-1} for mackerel (**Fig. 4.7**). The mean RN_{PG} of horse mackerel in the VTG stage was lower than for the two other species, but this difference was non-significant (ANOVA: $p > 0.05$) (**Fig. 4.7**). Also, the RN_{PG} values showed higher variances in the GVM stage in sardine, in the GVBD stage in horse mackerel, and in all stages in mackerel (**Fig. 4.7**).

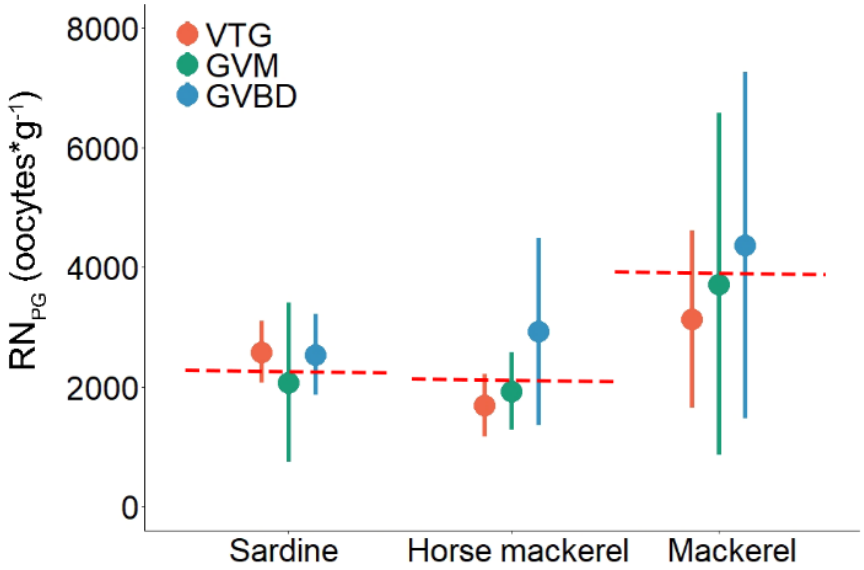

Figure 4.7. Relative number of primary growth oocytes (RN_{PG}, oocytes*g^{-1}) per ovarian stage (VTG: vitellogenesis; GVM: germinal vesicle migration; GVBD: germinal vesicle breakdown stage) for sardine (*Sardina pilchardus*), horse mackerel (*Trachurus trachurus*), and mackerel (*Scomber scombrus*). Filled circles: mean value of RN_{PG} at each ovarian stage; bar: 95% confidence intervals; horizontal dashed lines: mean RN_{PG} value of all ovarian stages in each species (Charitonidou et al 2022b).

Εικόνα 4.7. Σχετικός αριθμός ωοκυττάρων πρωτογενούς ανάπτυξης (RN_{PG}, oocytes*g^{-1}) ανά στάδιο ωοθήκης (VTG: λεκιθογένεση; GVM: μετανάστευση βλαστικού κυστιδίου; GVBD: στάδιο ρίξης του βλαστικού κυστιδίου) για τη σαρδέλα (*Sardina pilchardus*), το γκριζοσαύριδο (*Trachurus trachurus*) και το σκουμπρί (*Scomber scombrus*). Κύκλοι: μέση τιμή του RN_{PG} σε κάθε στάδιο της ωοθήκης; Κατακόρυφη γραμμή: 95% διαστήματα εμπιστοσύνης; οριζόντιες διακεκομμένες γραμμές: μέση τιμή RN_{PG} όλων των σταδίων των ωοθηκών σε κάθε είδος (Charitonidou et al 2022b).

The number of secondary growth oocyte cohorts estimated through the fecundity ratio in whole mounts and the clustering analysis in histological specimens did not differ significantly between the two methods, neither in sardine [5 (± 0.4) and 4.8 (± 0.3), respectively; $p > 0.05$], nor in horse mackerel [5.8 (± 0.8) and 6.4 (± 0.4), respectively; $p > 0.05$] (**Fig. 4.8A, B**). However, for mackerel, the results were significantly different between the two methods: 14.6 (± 2.5) modes were estimated through the fecundity ratio and 10.2 (± 2.2) through the clustering analysis ($p < 0.05$) (**Fig. 4.8C**).

In all three species, the fecundity ratio was not significantly different between ovarian stages ($p > 0.05$) (**Fig. 4.8**). Regarding the clustering analysis results, there was no statistical difference in the number of cohorts between the ovarian stages for sardine (**Fig. 4.8A**); however, for horse mackerel, the VTG stage was found to contain a significantly lower number of modes than the other two stages ($p < 0.05$) (**Fig. 4.8B**). Similarly, in mackerel, the number of modes was statistically lower between the VTG stage [8.8 (± 2.7)] and both the GVM (13) and GVB ovarian stages (13) ($p < 0.05$) (**Fig. 4.8C**).

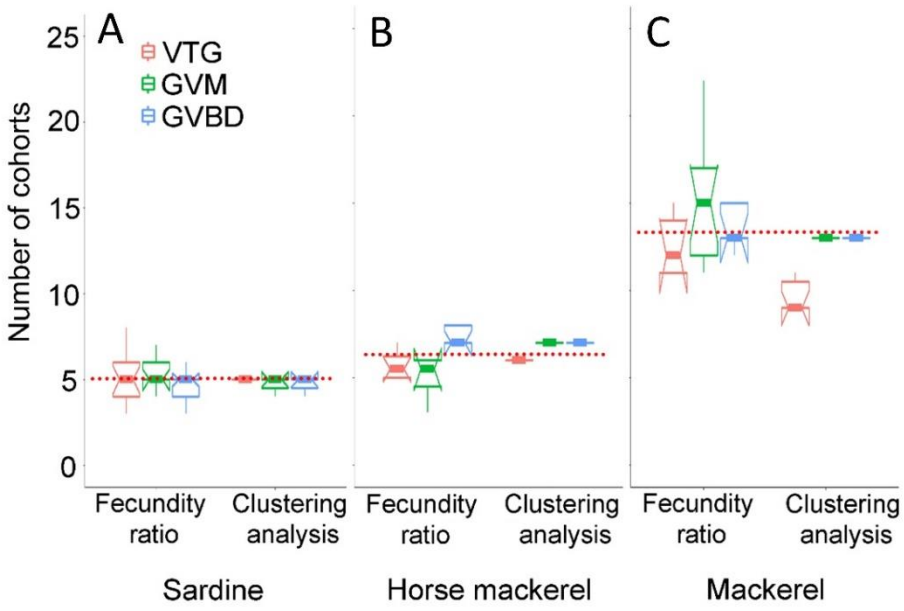

Figure 4.8. Box and whiskers plots of the number of oocyte cohorts estimated by the fecundity ratio and K-means clustering analysis at each ovarian stage, vitellogenic stage (VTG), germinal vesicle migration (GVM), and germinal vesicle breakdown (GVBD), for the three species: A) sardine (*Sardina pilchardus*), B) horse mackerel (*Trachurus trachurus*), and C) mackerel (*Scomber scombrus*). The median is marked by the thick line within each box and the general mean value (including all ovarian stages) of the number of modes estimated by the fecundity ratio of each species is indicated by the dashed horizontal line (Charitonidou et al 2022b).

Εικόνα 4.8. Διαγράμματα Box and whiskers του αριθμού των κοορτών των ωοκυττάρων που εκτιμήθηκαν από την αναλογία γονιμότητας και τη ανάλυση ομαδοποίησης K-means σε κάθε στάδιο ωοθηκών, λεκιθικό στάδιο (VTG), στάδιο μετανάστευσης βλαστικού κυστιδίου (GVM), και στάδιο ρίξης βλασικού κυστιδίου (GVBD), για τα τρία είδη: Α) σαρδέλα (*Sardina pilchardus*), Β) γκριζοσαύριδο (*Trachurus trachurus*) και C) σκουμπρί (*Scomber scombrus*). Η διάμεσος σημειώνεται από την παχιά γραμμή μέσα σε κάθε κουτί και η γενική μέση τιμή (συμπεριλαμβανομένων όλων των σταδίων των ωοθηκών) του αριθμού των ομάδων ωοκυττάρων που εκτιμάται από το κλάσμα γονιμότητας κάθε είδους υποδεικνύεται από τη διακεκομμένη οριζόντια γραμμή (Charitonidou et al 2022b).

Decomposition of overlapping oocyte modes provided an estimate of cohort specific fecundities (RF_{ci}) (**Fig. 4.9**). These estimates were contrasted with the mean values of advanced mode relative batch

fecundity values (RF_{AM}) for each species. For all three species, independently of ovarian stage, almost all oocyte cohorts showed stable mean RF_{ci} values that were very close to RF_{AM} values. Only cohorts of smaller oocytes, i.e., cohort #1 in sardine, cohorts #1 and #2 in horse mackerel, and cohorts #1 to #4 in mackerel, showed significantly higher ($p < 0.05$) mean RF_{ci} values compared to RF_{AM} and to the remaining cohorts (**Fig. 4.9**). Also, mean RF_{AM} between ovarian stages did not differ significantly ($p < 0.05$).

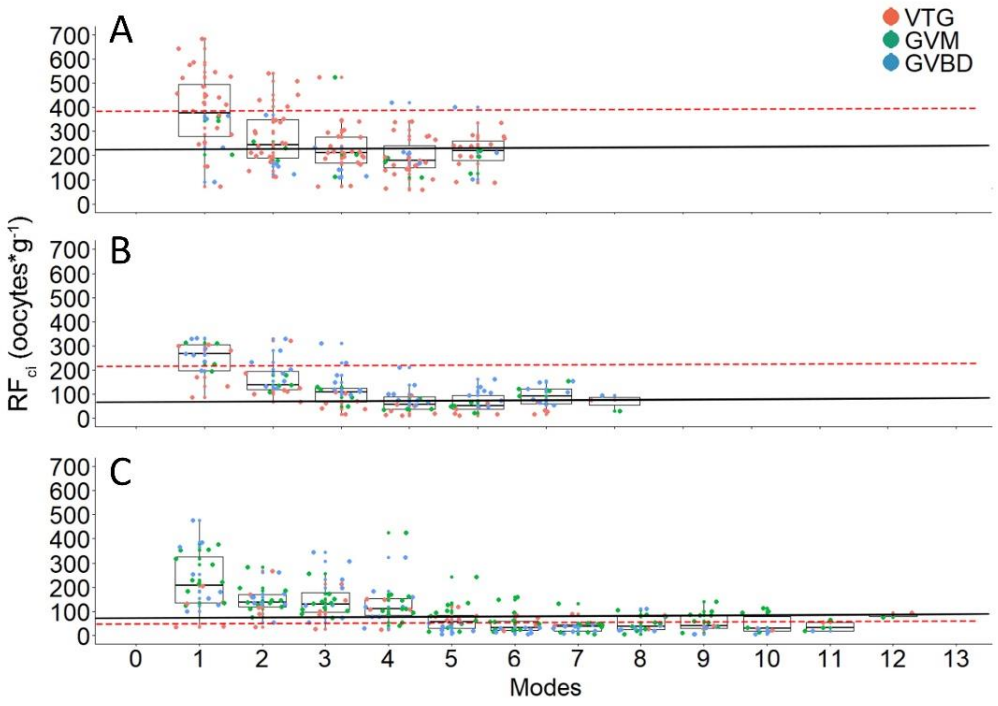

Figure 4.9. Box and whiskers plots of relative cohort fecundity values (RF_{ci}, oocytes*g^{-1}) as estimated for each mode from the decomposition of overlapping oocyte size distributions for each species: A) sardine (*Sardina pilchardus*), B) horse mackerel (*Trachurus trachurus*), and C) mackerel (*Scomber scombrus*). The median RF_{ci} value is indicated by the dashed horizontal lines. The solid horizontal lines indicate the mean values of advanced mode relative batch fecundity (RF_{AM}, oocytes*g^{-1}) for each species. The ovarian stages are indicated by different colours: vitellogenic stage (VTG), germinal vesicle migration (GVM), germinal vesicle breakdown stage (GVBD) (Charitonidou et al 2022b).

Εικόνα 4.9. Διαγράμματα Box and whiskers των σχετικών τιμών γονιμότητας κοόρτης (RF_{ci}, oocytes*g^{-1}) όπως υπολογίστηκε για κάθε ομάδα από την αποσύνθεση επικαλυπτόμενων κατανομών μεγέθους ωοκυττάρων για κάθε είδος: Α) σαρδέλα (*Sardina pilchardus*), Β) γκριζοσαύριδο (*Trachurus trachurus*) και C) σκουμπρί (*Scomber scombrus*). Η διάμεση τιμή RF_{ci} υποδεικνύεται από τις διακεκομμένες οριζόντιες γραμμές. Οι συμπαγείς οριζόντιες γραμμές υποδεικνύουν τις μέσες τιμές της σχετικής γονιμότητας της προηγμένης ομάδας ωοκυττάρων (RF_{AM}, ωοκύτταρα*g^{-1}) για κάθε είδος. Τα στάδια της ωοθήκης υποδεικνύονται με διαφορετικά χρώματα: λεκιθικό στάδιο (VTG), μετανάστευση βλαστικού κυστιδίου (GVM), στάδιο ρίξης βλαστικού κυστιδίου (GVBD) (Charitonidou et al 2022b).

The above results support the conceptual model of Ganias et al. (2015) and Ganias and Lowerre-Barbieri (2018), who simulated oocyte size frequency distribution in multiple spawners based on

oocyte growth, spawning interval, and the duration of the spawning period considering that both variables can be affected by water temperature and latitudinal distributions. Based on this modelling approach, sparse spawners, like the Atlantic sardine, with faster oocyte growth rates display polymodal oocyte size frequency distributions consisting of fewer and distinct oocyte cohorts, while frequent spawners, like the Atlantic mackerel, with slower oocyte growth rates tend to form a unimodal distribution consisting of numerous oocyte cohorts which are hardly distinguished from each other. Indeed, the number of estimated secondary growth cohorts for sardine and horse mackerel in Ganias and Lowerre-Barbieri (2018) matched the cohorts estimated in this study. However, mackerel exhibited a discrepancy between the present study (Fig. 4.9; n = 14.6 ± 2.5) and modelled estimates (n = 30) which is apparently due to deficiencies of the present methodology in distinguishing different cohorts amongst smaller oocyte classes due to the high degree of overlapping.

4.3.2 POF dynamics in sardine and mackerel

The mean estimate of relative POF fecundity (RF_{POF}) for sardine from the Weibel grid method was 337 (95% CI =±48) POFs g^{-1} (**Fig. 4.10**). Corresponding values from the packing density theory, modified and adopted for POFs (POFPD), were 586 (95% CI =±103), 346 (95% CI =±61) and 318 (95% CI =±67) POFs g^{-1} when setting POF_{DA} at POF_{DAS}=70, POF_{DAI}=125 and POF_{DAL}=180 µm, respectively (**Fig. 4.10 and Fig. A3.1A**). Only the first-mentioned RF_{POF} value was significantly different (higher) (**Table 4.1**). Thus, these POFPD-based outputs for sardine stabilized from 125 µm onwards (**Fig. A3.1A**). Consequently, RF_{POF} at POF_{DA}>125 µm was taken as an indication of a representative POFPD-based figure. Relative batch fecundity (RF_B) in sardine, as estimated gravimetrically in whole mounts, was 335 (95% CI =±50) oocytes g^{-1} (**Fig. 4.10**). For mackerel, application of the Weibel grid method resulted in RF_{POF}=170 (95% CI =±23) POFs*g^{-1} (**Fig. 4.10**). The alternative use of POFPD, setting POF_{DA} at POF_{DAS}=125, POF_{DAI}=150 and POF_{DAL}=175 µm, led to RF_{POF} equal to 131 (95% CI =±26), 114 (95% CI =±26) and 110 (95% CI =±29) POFs g^{-1}, respectively (**Fig. 4.10**). No significant differences were observed amongst these values (**Table 4.1**); RF_{POF} at>125 µm was hence adopted. Contrary to sardine, RF_{POF} values from the Weibel method and POFPD differed significantly (**Table 4.1**). Also, RF_{POF} differed significantly from RF_B outputs: mean 34 (95% CI =±12) oocytes*g^{-1} (**Fig. A3.1A**; **Table 4.1**).

The histological assessment for the co-occurrence of POF stages using fine cytomorphological criteria confirmed that sardines only displayed one single daily cohort of POFs in an ovary. For mackerel, this analysis showed the existence of one to up to four POF cohorts in an ovary (**Fig. 4.11 and 4.12**). There was a pattern of increase in RF_{POF}, as estimated using the Weibel method, with the number of POF cohorts (**Fig. 4.12**). Specifically, RF_{POF} in mackerel females with a single daily cohort was 73.4 (95% CI =±34.7) POFs*g^{-1} which compared with the gravimetric RF_B estimation, despite the statistically significant difference between the two values (Welch's t-test, $p < 0.05$), values of RF_{POF} were shown to significantly increase in females with more cohorts (Kruskal–Wallis test, $p < 0.05$, followed by Wilcoxon-Mann-Whitney test applying Benjamini- Hochberg post hoc adjustment, $p < 0.05$) ending-up with an almost fourfold increase from one to four POF cohorts. The existence of one single daily POF cohort in sardines should be related to its much lower spawning frequency, as there is a wider

time window for the resorption of POFs before new ones appear. In mackerel, the spawning interval is markedly shorter than in sardine, POFs are not anticipated to have completed the resorption process between successive egg releases, leading to the accumulation of multiple POF cohorts. A link between high spawning frequency (i.e., short spawning interval) values and multiple POF cohorts has been suggested for other fish species such as Spanish mackerel, *Scomberomorus commerson* (Mackie et al. 2005) and the tautog, *Tautoga Onitis* (White et al. 2003). Anderson et al. (2020) suggested for the Atlantic cod, *Gadus morhua*, a species with very low resorption rates (Witthames et al. 2009) a gradual accumulation of recent as well as older POFs in the ovary during the spawning period. Mouchlianitis et al. (2020) postulated that there are multiple POF cohorts present whenever the POF degeneration progress is longer than the ovulatory cycle.

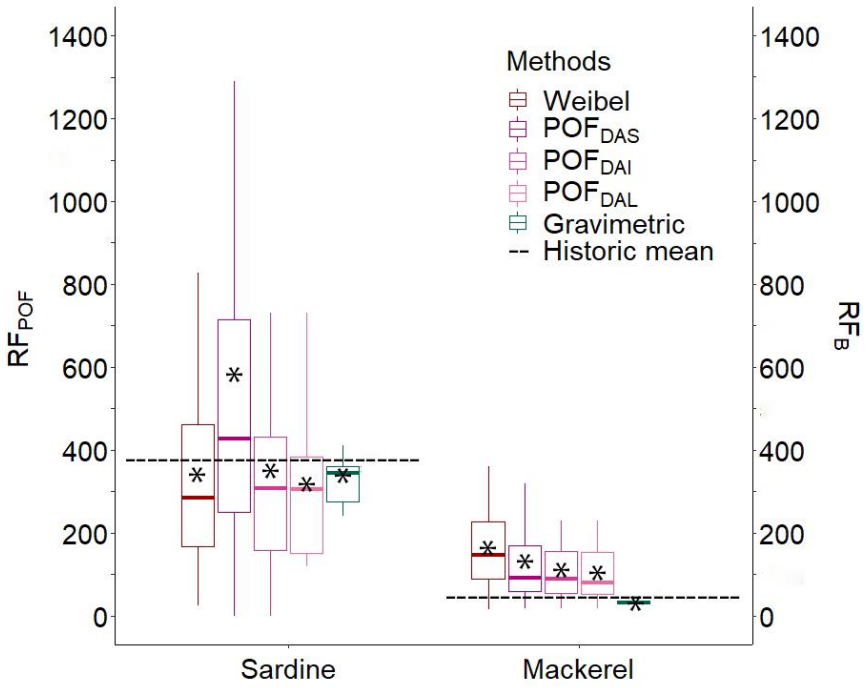

Figure 4.10. Box and whiskers plots (Tukey style) of relative POF fecundity (RF_{POF}: POFs*g^{-1}) and respective estimates of relative batch fecundity (RF_B: advanced oocytes*g^{-1}) for the Atlantic sardine (left plot) and the Atlantic mackerel (right plot), using different laboratory methods: the Weibel method, the POFPD method at different POF diameter threshold values (POF_{DAS}, POF_{DAI} and POF_{DAL}) and the gravimetric method. Horizontal dashed lines refer to historic mean RFB values for the two species. Asterisks correspond to arithmetic means (Charitonidou et al. 2020).

Εικόνα 4.10. Διαγράμματα Box and whiskers (στυλ Tukey) της σχετικής γονιμότητας των κενών ωοθυλακίων (POF) (RF_{POF}: POFs*g^{-1}) και αντίστοιχες εκτιμήσεις της σχετικής γονιμότητας ομάδας (RF_B: ανεπτυγμένα ωοκύτταρα*g^{1}) για τη σαρδέλα του Ατλαντικού, *Sardina pilchardus* (αριστερό διάγραμμα), και το σκουμπρί του Ατλαντικού, *Scomber scombrus* (δεξί διάγραμμα), χρησιμοποιώντας διαφορετικές εργαστηριακές μεθόδους: τη μέθοδο Weibel, τη μέθοδο POFPD σε διαφορετικά όρια τιμών της διαμέτρου POF (POF_{DAS}, POF_{DAI} and POF_{DAL}) και τη βαρυμετρική μέθοδο. Οι οριζόντιες διακεκομμένες γραμμές αναφέρονται σε ιστορικές μέσες τιμές RF_B για τα δύο είδη. Οι αστερίσκοι αντιστοιχούν σε αριθμητικά μέσα (Charitonidou et al. 2020).

Table 4.1. Statistical comparison (Wilcoxon-Mann-Whitney test applying Benjamini- Hochberg post-hoc adjustment) of estimated values of relative POF fecundity (RF_{POF}, POFs*g^{-1}) estimated by POFPD and Weibel methods, and relative batch fecundity (RF_B, advanced oocytes*g^{-1}) estimated by the gravimetric method in Atlantic sardine and in Atlantic mackerel. Specifically, for the POFPD method POF_{DAS}, POF_{DAI}, and POF_{DAL} correspond to the smallest, intermediate and largest values respectively within the stabilization range of RF_{POF}. ns: not significant difference; *: P < 0.05; **P < 0.01 (Charitonidou et al. 2020).

Πίνακας 4.1. Στατιστική σύγκριση (Wilcoxon-Mann-Whitney test με εφαρμογή Benjamini- Hochberg post-hoc adjustment) των εκτιμώμενων τιμών της σχετικής γονιμότητας POF (RF_{POF}, POFs*g^{-1}), εκτιμώμενος με τις μεθόδους POFPD και Weibel, και της σχετικής γονιμότητας ομάδας (RF_B, αναπτυγμένα ωοκύτταρα*g^{-1}) με τη βαρυμετρική μέθοδο στη σαρδέλα, *Sardina pilchardus,* και στο σκουμπρί του Ατλαντικού, *Scomber scombrus.* Ειδικότερα, για τη μέθοδο POFPD τα POF_{DAS}, POF_{DAI} και POF_{DAL} αντιστοιχούν στις μικρότερες, ενδιάμεσες και μεγαλύτερες τιμές αντίστοιχα εντός του εύρους σταθεροποίησης του RFPOF. ns: όχι σημαντική διαφορά. *: P < 0.05; **P <0.01 (Charitonidou et al. 2020).

Species	Method	POF_{DAS}	POF_{DAI}	POF_{DAL}	Weibel
Sardine	POF_{DAI}	*			
	POF_{DAL}	*	ns		
	Weibel	**	ns	ns	
	Gravimetric	ns	ns	ns	ns
Mackerel	POF_{DAI}	ns			
	POF_{DAL}	ns	ns		
	Weibel	**	**	**	
	Gravimetric	*	*	*	**

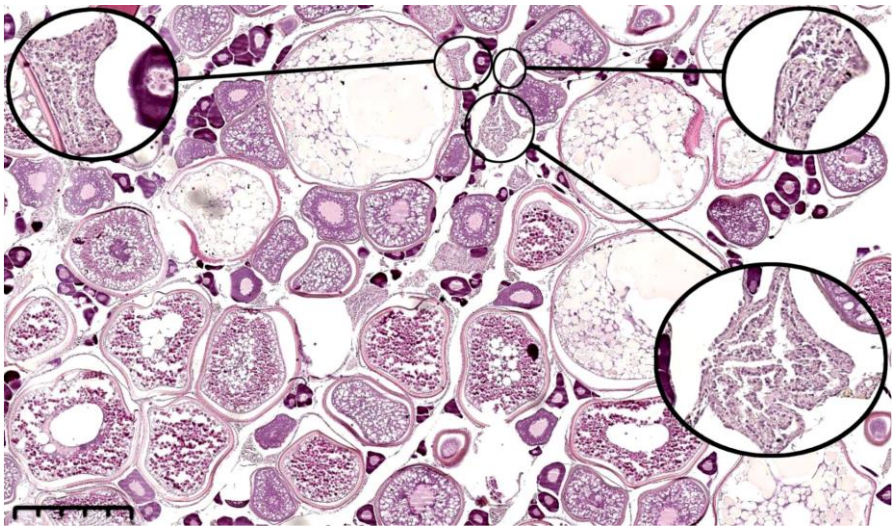

Figure 4.11. Focusing on POF production in the Atlantic mackerel, *Scomber scombrus*. Photomicrograph of an imminent spawner with hydrated oocytes and POFs assigned to three different daily cohorts. Indicative POFs from each cohort are magnified. Scale bar: 500 μm (Charitonidou et al. 2020).

Εικόνα 4.11. Κενά ωοθυλάκια (POF) στο σκουμπρί του Ατλαντικού, *Scomber scombrus*. Φωτομικρογραφία μιας τομής από ωοθήκη σε φάση αναπαραγωγής με ενυδατωμένα ωοκύτταρα και POF από τρεις διαφορετικές ημερήσιες κοόρτες. Τα ενδεικτικά POFs της κάθε κοόρτης είναι σε μεγέθυνση. Κλίμακα: 500 μm (Charitonidou et al. 2020).

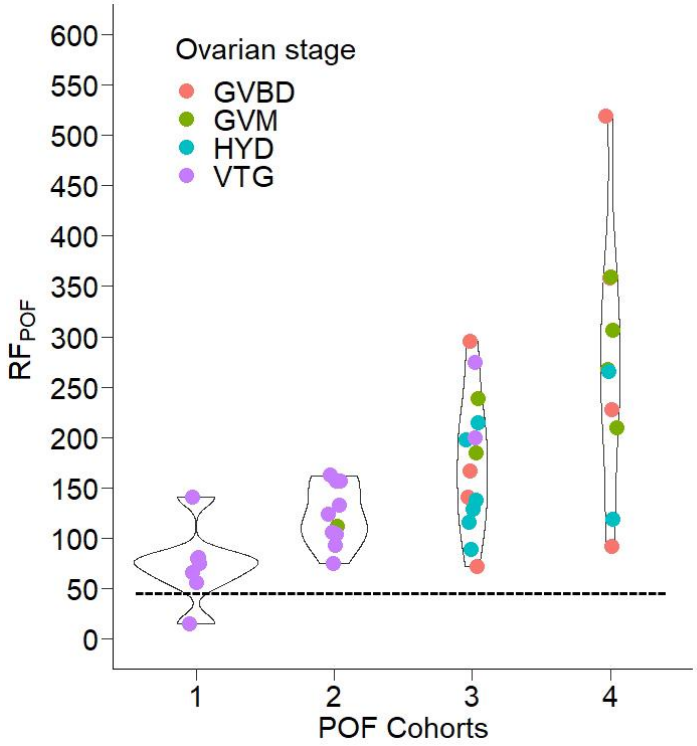

Figure 4.12. Atlantic mackerel, *Scomber scombrus*, violin plot of POF fecundity as estimated from the Weibel method (RF_{POF}) for females of different developmental stages across different number of POF cohorts. VTG= all vitellogenic stages (i.e., from VTG1 to VTG3), GVM=germinal vesicle migration stage, GVBD: germinal vesicle breakdown, HYD=hydration stage. Horizontal dashed line refers to historic mean RF_B values (Charitonidou et al. 2020).

Εικόνα 4.12. Σκουμπρί Ατλαντικού, *Scomber scombrus*, διάγραμμα violin της γονιμότητας POF όπως εκτιμήθηκε από τη μέθοδο Weibel (RF_{POF}) για θηλυκά διαφορετικών αναπτυξιακών σταδίων σε διαφορετικό αριθμό κοορτών POF. VTG= όλα τα λεκιθικά στάδια (δηλαδή, από το VTG1 έως το VTG3), GVM=στάδιο μετανάστευσης βλαστικών κυστιδίων, GVBD: διάσπαση βλαστικών κυστιδίων, HYD=στάδιο ενυδάτωσης. Η οριζόντια διακεκομμένη γραμμή αναφέρεται σε ιστορικές μέσες τιμές RF_B (Charitonidou et al. 2020).

The effect of spawning dynamics on the number of POF cohorts was also shown through different patterns of POF resorption across ovarian stages between the two species. Specifically, POF diameter in sardine gradually decreased from the onset of vitellogenesis, when newly formed POFs occur just after spawning (Ganias et al. 2007a), to pre-ovulatory stages, when the POFs are either very old or absent (**Fig. 4.13A**), suggesting the occurrence of one cohort. In mackerel, there was no such apparent

trend, ascribed to the co-occurrence of multiple daily cohorts (**Fig. 4.13B**). Specifically, 16 out of the 17 (94%) females with one or two cohorts were at VTG stages, respectively. In contrast, 22 out of the 24 (94%) of females with three or four POF cohorts were from GVM stage onwards (**Fig. 4.12**). Also, there was a clear pattern of increase in RF_{POF}, as estimated from the Weibel method, with the number of co-occurring POF stages reflecting the gradual accumulation of multiple cohorts (**Fig. 4.12**). Thus, the existence of a low or high number of POF cohorts reflects not only inter- but also intra-specific differences in the spawning dynamics. In common with sardines, mackerel with longer spawning intervals should exhibit one (or a maximum of two) POF cohort(s) and are thus less likely to be captured in imminent spawning stages. In contrast, females with short spawning intervals should accumulate multiple POF cohorts at a rate that is proportional to the duration of full POF resorption. Given their high spawning rate, these individuals should always have their leading mode of oocytes at imminent spawning stages, i.e., from the GVM stage onwards.

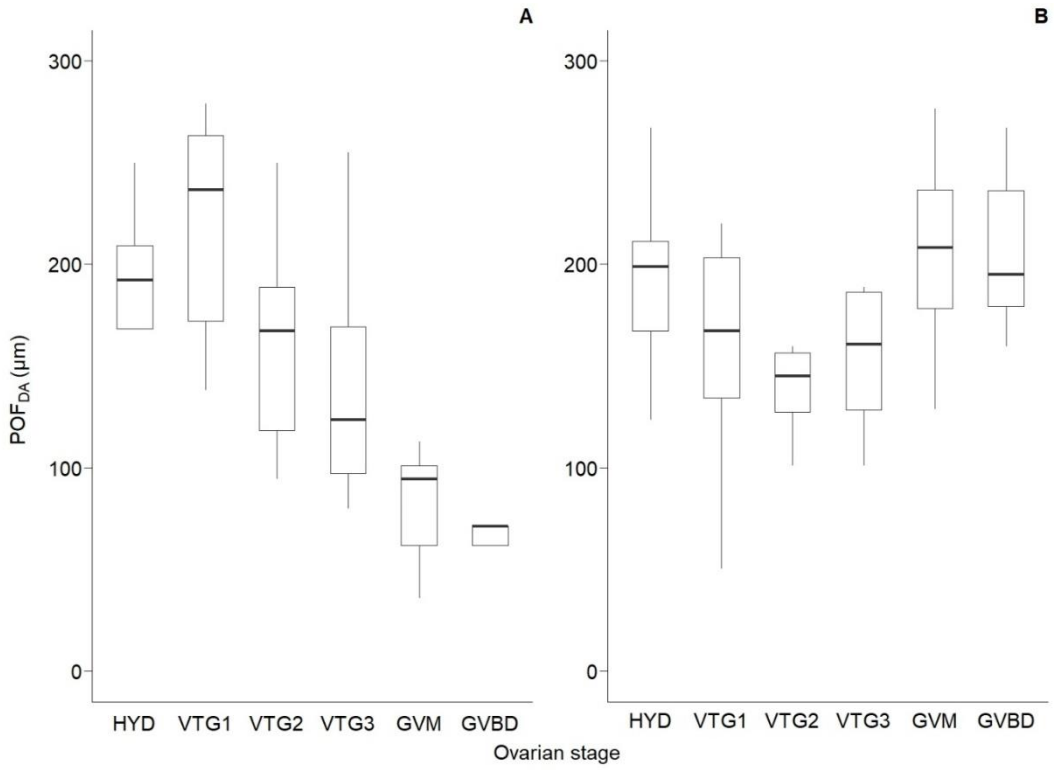

Figure 4.13. Box and whiskers plots (Tukey style) of POF diameter (POF_{DA}, µm) per developmental stage for Atlantic sardine (A) and Atlantic mackerel (B). HYD: oocyte hydration; VTG1, VTG2 and VTG3: progressing vitellogenic stages; GVM: germinal migration; GVBD: germinal vesicle breakdown (Charitonidou et al. 2020).

Εικόνα 4.13. Διαγράμματα Box and whiskers (στυλ Tukey) της διαμέτρου των POF (POF_{DA}, µm) ανά στάδιο ανάπτυξης για τη σαρδέλα του Ατλαντικού (A) και το σκουμπρί του Ατλαντικού (B). HYD: ενυδατωμένα ωοκύτταρα. VTG1, VTG2 και VTG3: προοδευτικά λεκιθικά στάδια. GVM: στάδιο μετανάστευσης βλαστικού κυστιδίου. GVBD: ρίξη βλαστικού κυστιδίου (Charitonidou et al. 2020).

Given that POF size can serve as an accurate proxy for the elapsed time since egg release, we assumed that larger POFs were to be younger (i.e., new POFs) and thus closer to a previous spawning event. According to Ganias et al. (2007a), sardines that spawned in less than 24 hrs before capture should exhibit POF_{DA} values larger than 150 μm (for specimens embedded in paraffin). In the present study, and in order to target females that came from a very recent spawning event we used a range of threshold POF_{DA} values above 185 μm. The fraction of females with POF_{DA} above these threshold values was much higher for mackerel than for sardine. Specifically, this difference ranged from 14% for POF_{DA} =220 μm to 34% for POF_{DA} =195 μm (**Fig. 4.14**).

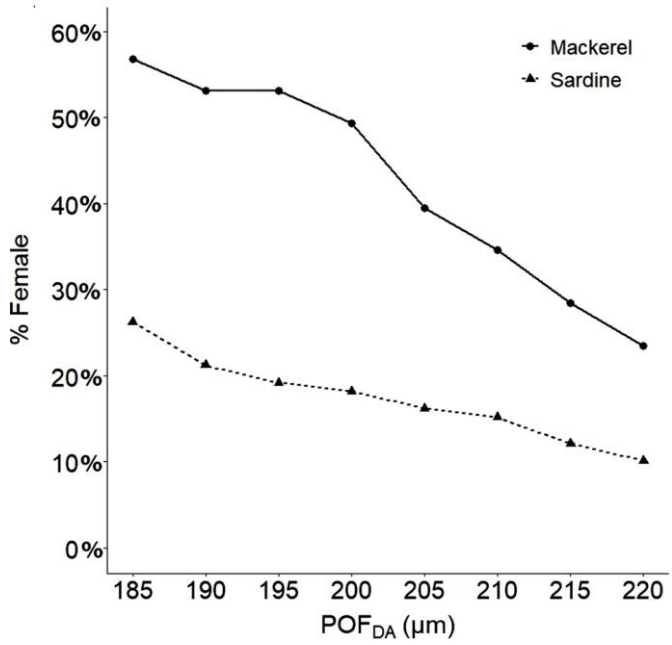

Figure 4.14. Variation of the fraction of females with POFs above a certain threshold of POF diameter (POF_{DA}) for the two species (Charitonidou et al. 2020).

Εικόνα 4.14. Διακύμανση του κλάσματος των θηλυκών ατόμων με POFs πάνω από ένα ορισμένο όριο διαμέτρου (POF_{DA}) για τα δύο είδη (Charitonidou et al. 2020).

Comparing the two methods implied for the estimation of the POFs cohorts number, the sardine example shows that application of either POFPD or Weibel methods proved equally valid for species with a single daily POF cohort. RF_{POF} in mackerel, was close to RF_B only in a small number of individuals that seemed to display a single POF cohort. In addition, for mackerel clear statistical differences existed between the outputs of the two methods. One apparent reason might be that the Weibel method considers all POFs included in the histological section, whereas the POFPD is based on the largest POFs only. Therefore, in case of multiple POF cohorts this latter method excludes the older POF cohorts. Consequently, RF_{POF} from the POFPD method should in theory be closer to RF_B, as

observed for mackerel. Furthermore, the typical morphometric characteristics of POFs (see **Annex 8**; Grier et al. 2017) can only be considered in the larger and newer POFs in each histological section. Another reason for the overestimation of RF_{POF} estimates in POFPD is probably that the volume occupied by POFs, in the presence of multiple daily POF cohorts, would be exaggerated in terms of the representative youngest/smallest daily POF cohort volume. When multiple cohorts of POFs coexist, it is virtually impossible in 2D (cf. histological slides) to discriminate the seemingly smallest POFs of recent cohorts from the seemingly largest POFs of older cohorts. Regarding POFPD, mathematically speaking a given measurement error (e.g., 10 µm) in POF size becomes less and less important as the true POF size increases (e.g., the volume at 110 µm is 33% greater than at 100 µm, while only 16% greater at 210 µm compared to 200 µm). This principle probably contributes to the observation that RF_{POF} flattened out (reaches as stabilization plateau) with increasing POF size.

4.4 Conclusion

This chapter investigates the ovarian dynamics during the secondary growth phase, at the interspecies level, in three pelagic fish species with indeterminate fecundity but with very distinct spawning dynamics. Both recruitment and dynamics of the secondary growth oocytes and POFs dynamics varied significantly between the species studied, linking with their differences in oocyte recruitment, spawning interval, and oocyte growth rate. Based on the seasonal pattern of oocyte recruitment, it was demonstrated that ongoing recruitment from primary growth to secondary growth oocytes occur in indeterminate spawners, however, they exhibit changing proportions of oocytes at the size range between the late primary and early secondary growth phases. It was also revealed that fishes with long spawning intervals and fast oocyte growth rates, such as the Atlantic sardine, *Sardina pilchardus*, exhibit relatively few, clearly separated oocyte cohorts, while fishes with shorter spawning intervals provide an increased number of coexisting cohorts. Furthermore, the hypothesis that one single daily POF cohort contained in the ovaries of sardine was confirmed, and both Weibel and POFPD methods led to similar results. However, several daily POF cohorts cooccurred in the mackerel ovary, a species with a higher spawning interval, which is an obstacle in the application of the daily egg production method (DEPM) (see **Chapter 5**). Our working hypothesis was confirmed as interspecies differences were found in ovarian dynamics among the three species studied.

Chapter 5: General Discussion and Conclusions

Many aspects of the phases of oogenesis, particularly the early phase, are unknown in highly commercial fish species. Current egg production methods for fish population assessment require confirmation in light of the ovarian dynamics of each fish species. Considering this, the primary goal of this study was to describe ovarian dynamics in the early and secondary phases of oogenesis and to investigate how the link between ovarian and spawning dynamics shapes fecundity type as well as other aspects such as total fecundity and the number of co-occurring oocyte cohorts. This work presented many innovative ways for assessing ovarian dynamics throughout oogenesis, including approaches for evaluating POFs, differentiating various oocyte cohorts, and examining oogonia and early oocytes in 3D rather than typical 2D histology slides.

Due to their different spawning dynamics, the Atlantic and Mediterranean sardine, the European anchovy, the Atlantic horse mackerel, and the Atlantic mackerel were the species studied in this study. The early phase of oogenesis in the Mediterranean sardine and the European anchovy, two species with different spawning frequency and energy allocation to reproduction strategies, was specifically studied throughout the reproductive cycle. The secondary phase of oogenesis was investigated at the interspecies level using Atlantic sardine, horse mackerel, and mackerel with different spawning intervals and oocyte growth rates.

The aim of the present study was to provide broad results for each of the three main scientific questions (Q1–Q3). Firstly, the pattern of oogonial proliferation and early oocyte dynamics differ throughout the reproductive cycle among indeterminate spawners (Q2). In particular, in sardines, oogonial proliferation persisted throughout the entire reproductive cycle, whereas in anchovy, it was more pronounced in the developing and resting reproductive phases. Anchovy exhibited a higher rate of meiotic activity in the developing reproductive phase, whereas sardine exhibited a higher rate in the resting phase. Also, the cytoplasmic development of primary and early secondary growth oocytes differs among close phylogenetical fish species indicating differences in the developmental functions of their oocytes (Q1). In addition, the intensity of oocyte recruitment from the primary to secondary growth phase and the secondary growth oocyte dynamics varied among indeterminate species with distinct spawning dynamics (Q3), showing that the fecundity type is flexible from determinacy to indeterminacy along a continuum. The secondary growth oocyte dynamics differ reflecting the spawning dynamics of the species (Q3). Moreover, POF dynamics varied among species with distinct spawning intervals, showing that sardine, with long spawning interval, has only a single daily POF cohort, whereas mackerel, with shorter spawning interval, exhibit co-occurrence of multiple daily POF cohorts (Q3), which is an obstacle in the proper assessment of parameters, such as spawning fraction, used in the application of daily egg production method (DEPM).

5.1 Answers to the main scientific questions

Q1. Are there differences in the fine structure of oocytes during the primary and early secondary growth phases in closely related phylogenetic fish species?

In **chapter 3**, the cytoplasmic development of oocytes was examined in two fish species, the Mediterranean sardine, and the European anchovy. Despite the close phylogenetical relationship of these two species, both similarities and differences exist in the cytoplasmic development of their primary and secondary growth phase oocytes. In both species, the cytoplasm of their primary growth oocytes contained an identical spherical Balbiani body and a perinuclear ring that consisted of different organelles in the two species. After Bb was dissembled, cytoplasmic zonation developed differently in the two species in secondary growth oocytes. Based on recent evidence, the morphology of the Balbiani body is not a phylogenetic feature of species and it differs not only among species of different families but also between species within the same family (Dymek et al. 2021a; Dymek et al. 2021b). These oocyte cytoplasmic characteristics could be utilized as markers for estimating significant parameters for the applied reproductive biology of fisheries, such as the spawning fraction (Ganias et al. 2014a). Also, the structure (mitochondria size, shape, and cristae density) and abundance of mitochondria were similar in chromatin nucleolus and primary growth oocytes in the two species, however, they differed in their secondary growth oocytes. Modifications in cristae development were also observed in different oocyte growth phases in sardine and anchovy. Therefore, the distinct cytoplasmic zonation formed by differences in organelles organization in early secondary growth oocytes of sardine and anchovy, together with the existence of modified mitochondria in different oocyte stages between both studied species, indicate differences in the developmental functions of their oocytes. These modifications in the structure of mitochondria and their cristae were also observed in the oocytes of other fish species in different oocyte growth phases suggesting their participation in different developmental pathways (e.g., Droller and Roth 1966; Pfannestiel and Grünig 1982; Grier 2000; Kunz 2004; Chung et al. 2009; Zelazowska and Kilarski 2009; Jun et al. 2018; Zelazowska and Fopp-Bayat 2019; Yang et al. 2021).

Q2. Are the dynamics of oogonial proliferation and early oocytes throughout the reproductive cycle identical in fish species with the same fecundity type?

In **chapter 3**, the oogonial proliferation and early (chromatin nucleolus) oocytes dynamics were examined in the Mediterranean sardine and European anchovy throughout the reproductive cycle. These two species have indeterminate fecundity type, but different energy allocation to reproduction strategies. Specifically, sardine is mainly a capital breeder, feeding before the spawning period, whereas anchovy feeds opportunistically based on food availability (income breeder). Observations of ovaries in 3D dimensions with confocal laser scanning microscopy (CLSM) revealed extensive information on markers of oogonial proliferation (mitotic divisions, oogonia nests) and meiotic prophase I divisions of oocytes in nests. The working hypothesis was confirmed since the continuous

recruitment from oogonia to early oocytes occurred throughout the reproductive cycle in both iteroparous species with indeterminate fecundity type. However, the intensity of mitotic and meiotic divisions varied throughout the reproductive cycle. In particular, the oogonial proliferation was higher before and after the spawning period in anchovy, while it was consistent throughout the reproductive cycle in sardine. In several species, most oogonial divisions occur after the spawning period, but some species undergo most oogonial proliferation during spawning or even throughout the reproductive cycle (Tokarz 1978). So far, no evidence occurs for a link between oogonial dynamics and reproductive modes (e.g., oviparity, viviparity), species taxonomy, or fecundity type. In general, the higher rate of oogonial proliferation occurred after the spawning period, regardless of the reproductive strategy, ensuring the availability of eggs for the spawning event (Wildner et al. 2013; de Jesus-Silva et al. 2018). During the reproductive cycle, anchovy ovaries had a higher rate of prophase I meiotic activity before the spawning period, whereas sardine ovaries had a higher rate after the spawning period. However, there is not a specific pattern of meiotic activity of oocytes in nests during the reproductive cycle. In some fish species, they are plenty during or after the peak of oogonial proliferation throughout the reproductive cycle (Eggert 1931; Yamazaki 1965) or after ovulation (Barr 1963). The observed differences between the two species can potentially be attributed to different seasonal patterns of energy allocation to reproduction and the synchronization between the feeding and the spawning period (McBride et al. 2015). Understanding the oogonia and early oocyte patterns of species is important because recent research (Higashino et al. 2002; dos Santos Schmidt et al. 2017; Thome et al. 2012) revealed that both regulate the configuration of fecundity during oogenesis, which is a crucial parameter in applied fisheries.

Q3. What is the relationship between spawning and ovarian dynamics (secondary growth oocytes and postovulatory follicles (POFs) cohorts dynamics), and how do they affect fecundity type and other fecundity parameters in fish species with distinct spawning dynamics?

In **chapter 4**, the ovarian dynamics were investigated in three fish species with indeterminate fecundity type and different spawning dynamics. The Atlantic mackerel, *Scomber scombrus*, with short spawning interval, exhibited a higher number of oocyte cohorts, whereas the Atlantic sardine, *Sardina pilchardus* with longer spawning interval and fast oocyte growth rate, had comparatively few oocyte modes with clearly separated cohorts. This remarkable difference in spawning intervals was also reflected in the dynamics of daily POF cohorts between sardine and mackerel. One single daily POF cohort was found in sardine, whereas co-occurrence of multiple POFs cohorts existed in mackerel. Among the three species, only sardine may safely be characterized with regards to its fecundity type matching all the traditional criteria of indeterminate spawners (see **Section 1.4**). On the other hand, the Atlantic horse mackerel, *Trachurus trachurus,* and especially mackerel show mixed characteristics. Based on the traditional criteria for the distinction between determinate and indeterminate fecundity types, the continuous recruitment from primary growth to secondary growth oocytes is a common pattern observed in indeterminate spawners throughout the spawning period. However, it was shown that indeterminate spawners can display varying proportions of oocytes at the range between primary

and secondary growth phase based on the seasonal dynamics of oocyte recruitment intensity. This finding indicates that determinacy and indeterminacy should rather be recognized as endpoints along a continuum that is shaped by the time lag between oocyte recruitment and spawning (Ganias 2013). Although both mackerel and horse mackerel are now considered indeterminate spawners (Macer 1974; Karlou-Riga and Economidis 1997; Gordo et al. 2008; Ndjaula et al. 2009; ICES 2011, 2012, 2018; Ganias et al. 2017; Jansen et al. 2021; dos Santos Schmidt et al. 2021), this evidence indicates a tendency towards the 'determinate' end- point, explaining the controversial fecundity type of these two species during the last decades. Even though intra-seasonal reproductive traits like oocyte growth rate and spawning interval can also influence the dynamics between late primary growth and early secondary growth oocytes, it was found that the degree of overlap and the ratio between the two oocyte groups are mainly affected by the annual fecundity type of a fish population or species, as well as the timing within the reproductive period. Both the spawning interval and the oocyte growth rate shape the size frequency distribution of secondary growth oocytes. The current study demonstrated that the ovarian stage, where the size hiatus between the advanced oocyte mode and the SG pool was established, varied between the three species.

5.2 Main findings

In this study, the ovarian dynamics were examined in highly commercial fish species with distinct spawning dynamics in different aspects of early and secondary oogenesis. Also, the relationship of spawning with ovarian dynamics was investigated to reveal their impact on the fecundity type, an important parameter in the implementation of egg production methods. Despite their close phylogeny, differences in the distribution of organelles in the cytoplasm during the development of the early oocyte were identified in two indeterminate spawners, the Mediterranean sardine and the European anchovy (**Chapter 3**). Variations in cytoplasmic asymmetry were observed in other fish species, suggesting that it is not a phylogenetic feature (Dymek et al. 2021a, 2021b). These species-specific features could be used as markers for the distinction of the maturity stage and for the imminent reproduction and spawning periods (Kjesbu et al. 2011; McPherson and Kjesbu 2012). Based on the chromosomic divisions (mitosis and meiosis prophase I), the dynamics of oogonial proliferation and early oocytes were studied throughout the reproductive cycle in sardine and anchovy (**Chapter 3**). It was shown that the activity of cell divisions varied between the reproductive phases, as well as between the two fish species (**Chapter 3**). These differences were also noticed in other fish species with indeterminate fecundity type (Tokarz 1978; Wildner et al. 2013). Understanding these early dynamics is critical since evidence suggests that they are influenced by environmental factors and also regulate fecundity (dos Santos Schmidt et al. 2017; Higashino et al. 2002; Thome et al. 2012). Both species exhibit continuous recruitment from oogonia to early oocytes within the spawning period (**Chapter 3**), which is a general characteristic of indeterminate spawners (see **Section 1.4**). Also, the ongoing oocyte recruitment was observed from primary to secondary growth oocytes in all three indeterminate spawners, sardine, horse mackerel, and mackerel (**Chapter 4**). However, they displayed varying proportions of oocytes at the size range between the primary and secondary growth phases based on the seasonal pattern of oocyte recruitment (**Chapter 4**) indicating that the degree of overlap between the oocyte recruitment period and the spawning period controls the identification of

determinate and indeterminate fecundity type as end- points along a continuum (Ganias et al. 2013). This explains the controversial fecundity type considered in both horse mackerel and mackerel (see **Section 1.4**). The secondary growth oocytes dynamics showed that sardine, with long spawning intervals and fast oocyte growth, had relatively few, clearly distinct secondary growth oocyte cohorts, whereas mackerel with shorter spawning intervals, had an increase in coexisting cohorts, an intermediate situation was observed in horse mackerel (**Chapter 4**) (Ganias et al. 2015; Ganias and Lowerre-Barbieri 2018). This was further supported by investigating the POFs dynamics within the spawning period (**Chapter 4**). Sardines only had one single daily POF cohort, but mackerel exhibited a co-occurrence of multiple daily POF cohorts (**Chapter 4**), which leads to inaccurate estimates of spawning fraction applying the current methods. Therefore, the assessment of the spawning fraction for the appropriate application of the POF method requires validation based on the spawning dynamics of the assessed species (e.g., Ganias 2012; ICES 2016).

5.3 New knowledge acquired

Investigating spawning dynamics in fish species requires new approaches, especially in batch spawning fish, where the secondary growth oocytes (SG) are recruited and spawned in successive cohorts, resulting in the co-occurrence of multiple cohorts in spawning-capable females. So far, histological features such as the prevalence of cortical alveoli or yolk granules are conservatively used to distinguish oocytes in different developmental stages which do not necessarily correspond to different cohorts. In this way, valuable information about spawning dynamics remains unseen and consequently misleading conclusions might be drawn, especially for species with high spawning frequencies and increased overlapping among oocyte cohorts. A new clustering method was introduced in this study (**Section 4.2.3**) for grouping oocytes into different cohorts based on the application of the K-means clustering algorithm on the characteristics of cytoplasmic structures, such as the varying size and intensity of cortical alveoli and yolk granules in oocytes of different development. The method allowed the grouping of oocytes without the need of using oocyte diameter, and thus, a crucial histological bias dealing with the cutting angle and the orientation of reference points (e.g., nucleus) has been overcome. This method represents an improved tool to study species with complex ovarian dynamics. In addition, the examination of various attributes of ovarian dynamics such as the oocyte size frequency distribution, the ratio of total to batch fecundity, the number of oocyte cohorts, and the recruitment of early secondary growth oocytes related to historic estimates of spawning interval and oocyte growth rate may provide a proxy of spawning interval and thereby of the spawning frequency (**Chapter 4**). So far, applied fisheries biology assesses spawning activity over space and time mostly based on static indicators of reproductive state, typically a measurement of gonadal development with histological analysis (Kjesbu 2009; Lowerre-Barbieri et al. 2011), however, the ovarian dynamics are shaped by long-term processes such as the synergistic effect of oocyte recruitment and oocyte growth rate (Greer Walker et al. 1994; Ganias et al. 2015). Sampling the phenotypic expression of individuals at one point in time - a snapshot - can be useful for classifying individuals as mature or immature, and for assessing their spawning season and spawning frequency.

In addition, examining the oogenesis process is challenging since it is influenced by environmental factors such as ambient temperature, dissolved oxygen, and food availability (e.g., Tveiten et al. 2001; Zucchetta et al. 2012; Bobe 2015). Under favorable environmental conditions, oogonial proliferation and early oocyte recruitment increase during early oogenesis (Kjesbu et al. 2010; Thome et al. 2012). Although elevated temperatures accelerated this increase, fish responses to prolonged exposure to this condition resulted in high rates of atresia (see Alix et al. 2020). Poor environmental conditions reduce oogonial proliferation, resulting in low rates of early oocyte recruitment, and increase the rate of atresia (Thome et al. 2012). Studies have shown that fecundity is already regulated by early oogenesis (dos Santos Schmidt et al. 2017), emphasizing the importance of understanding the dynamics of oogonia, early oocytes (chromatin nucleolus), and primary growth oocytes, particularly in the context of climate change. Secondary oogenesis and the final stages of oocyte maturation are also temperature-sensitive, influencing egg quality and the production of viable offspring (see Alix et al. 2020). In terms of fish stock fecundity types, little is known about the process that drives the two fecundity types (determinacy and indeterminacy) and whether they are genetically controlled or an ecophenotypic response to a variable environment (Kjesbu and Witthames 2007) (see **Section 1.4**). The most general pattern for fecundity type is the one that connects it to thermal habitat and fish stock latitudinal distribution (Ganias 2013; Hunter et al. 1985; Lowerre-Barbieri et al. 2011). Coldwater species with boreal geographic distributions, in particular, have determinate fecundity, whereas temperate and tropical species are mostly indeterminate spawners (Hunter et al. 1985). Hunter et al. (1985) also linked determinate fecundity to species with total (isochronal) spawning and short spawning periods, whereas indeterminate fecundity was associated with multiple spawning and long spawning periods. In particular, batch spawners with indeterminate fecundity are common in warm-water environments, where they continue to recruit batches to be spawned throughout the spawning season (Korta et al. 2010). In cold climates, on the other hand, there are usually batch spawners with determinate fecundity because the short spawning periods and long OGP make the development of additional oocyte batches during the spawning season impossible (Kjesbu et al. 2010). As a result, studying ovarian dynamics and reproductive traits of fish species is critical for understanding fish responses and adaptations in the context of changing environmental conditions caused by global warming.

The proper recognition of the fecundity type (determinate, indeterminate) of fish species is critical as it determines the selection of the appropriate egg production method (daily egg production method, *DEPM*, annual egg production method, *AEPM*) for the assessment of the SSB. A number of traditional criteria occur for the determination of fecundity type (see **Section 1.4**). In this study, we showed that despite the continuity between primary and secondary growth oocytes, the ratio of early secondary to late primary growth oocytes (ESG:LPG ratio) varies between indeterminate fish species, indicating that determinacy and indeterminacy are end points along a continuum which is controlled by the degree of overlap between oocyte recruitment period and spawning period (Ganias et al. 2013). In this regard, traditional criteria are not always indicative of the fecundity type and other aspects such as the characteristics of oocyte size frequency distribution should also be considered (Hunter et al. 1989, 1992; Kjesbu et al. 1990; Witthames and Greer Walker 1995; Ganias 2013). Also, complexities

in the seasonal spawning pattern such as the cessation of oocyte recruitment at the latter part of the spawning period also need to be considered (see **Section 1.4**; Brown-Peterson et al. 2017; Ganias et al. 2017; Mouchlianitis et al. 2020; Karlou- Riga et al. 2020).

5.4 Implications in DEPM application

The application of DEPM faces obstacles when using current methods, such as the POF method, for estimating the spawning fraction, particularly in fish species with complex ovarian dynamics without prior validation and when sampling schemes are not carefully designed (Stratoudakis et al. 2006; Ganias 2012). Specifically, POF method has a number of biases related to POFs staging and ageing, to sampling, and in consequence to the estimates of spawning fraction (Ganias 2012). The present study showed that whilst the POF method works well on species such as Atlantic sardine with a single daily POF cohort, limitations are detected when applied to species such as Atlantic mackerel with several, co-occurring daily POF cohorts due to overlapping histomorphological characteristics preventing the decisive identification of distinct daily cohorts. Hence, the eligibility of the POF method in applications of the DEPM should be judged based on the spawning dynamics of the assessed species, especially whether single or multiple daily POF cohorts coexist within the ovary either because the high spawning frequency or the slow degeneration of POFs.

New insights were suggested in this study to address biases in the application of POF method, especially in fish species with complex ovarian dynamics. First of all, species-specific spawning dynamics could be investigated through the ratio of the total number of POFs in the ovary (POF fecundity; F_{POF}) to batch fecundity (F_B), where values close to unity indicate the existence of a single POF cohort whilst higher values are expected based on the number of multiple POF cohorts. Also, differences in the spawning frequency of species could be explored through the pattern of POF size, given that POF size can serve as an accurate proxy for elapsed time since egg release (Ganias et al. 2007a; Witthames et al. 2010) it is assumed that larger POFs were to be younger (i.e., new POFs) and thus closer to a previous spawning event. Therefore, species with multiple daily POFs cohorts exhibit higher fractions of females with large POFs than species with single POF cohorts, as also shown in the results of the present study.

In addition, the range of POF size (e.g., **Fig. 4.14**) where the historical means of spawning frequency observed, may provide population estimates of spawning fraction focusing on the largest, thus newest, POFs and can be particularly helpful for species such as mackerel with multiple POF cohorts. Alternatively, in such species, spawning frequency might be estimated at an individual level based on the assumption that the number of POF cohorts reflects differences in the spawning interval of different females. This alternative has the advantage that it requires smaller sample numbers, but it needs first to be calibrated with population estimates of spawning frequency.

Furthermore, given that POFs correspond to oocytes that are ovulated and then spawned (i.e., spawning batch) their quantification may also lead to estimation of batch fecundity, F_B (e.g., Aragón et al. 2010). This is important when whole tissue samples are missing or discarded and (re-)

calculations of fecundity can only be based on histological samples. In such cases, (re-)calculations of batch fecundity could be based on histological screening using methods described in this study (**Chapter 4**). However, an important requirement for utilizing POFs when estimating batch fecundity is the existence of a single daily POF cohort.

Aside from all of potential causes of bias, the procedure of current application of POF method is highly expensive and labour-intensive because it requires a significant number of adult samples and extensive histology. Even if POFs – mainly of an earlier age and larger size - may be detected in whole mounts of ovarian tissue by means of specific staining protocols (Witthames et al. 2010), histology still constitutes the most reliable way to identify and consequently quantify the various stages of POFs (Ganias 2013). In this regard, it appears worthwhile to explore alternate methodologies for estimating spawning frequency. Other methods such as the GSI method (e.g., Pacific sardine, Claramunt and Roa 2001), the co-occurrence of different spawning stages (e.g., Bay of Biscay anchovy, Uriarte et al. 2012), and the oocyte growth method (e.g., Atlantic sardine, Ganias et al. 2011) have been proposed on a few occasions based on the specificities of the assessed stocks. In this study, using confocal laser scanning microscopy, specific cytoplasmic characteristics of oocytes were identified during their development. These characteristics, such as the perinuclear ring in primary growth oocytes in sardine and the mitochondria-rich ring of early secondary growth oocytes in anchovy (**Chapter 3**), which are also discernible in histological sections by standard procedures could thus be used as markers of maturity or imminent spawning period (Kjesbu et al. 2011; McPherson and Kjesbu 2012). Furthermore, these markers provide information on the onset of secondary growth and, thus, of the forthcoming reproductive period, with this information, the oocyte growth period for each species, as well as the spawning interval can be estimated (Ganias et al. 2014a). This is an alternative method to estimate the spawning frequency through spawning interval rather than the spawning fraction estimates from the conventional POF method.

5.5 Conclusions and future recommendations

In summary, this study explored different aspects of early and secondary oogenesis in highly commercial pelagic fish species and related the ovarian with spawning dynamics to investigate their impact on fecundity type and the application of egg production methods. Initially, the early oogenesis was examined through novel techniques, using observations of the confocal laser scanning microscopy, which can reconstruct in 3D the oogonia and early oocytes, providing an improved representation of these tiny cells compared to conventional 2D histological observations. Both the development of early oocytes and the oogonial proliferation and early oocyte dynamics showed interspecies differences in two close phylogenetical fish species. The understanding of early oogenesis dynamics, which has received little attention so far, is critical as recent studies showed that the dynamics of oogonia and early oocytes are affected by environmental and other conditions and consequently it has an impact on the fecundity of species which is an important parameter in applied fisheries (dos Santos Schmidt et al. 2017; Thome et al. 2012; Higashino et al. 2022). Another significant contribution of this study was the investigation of the oocyte recruitment from the primary to secondary growth phase and the secondary growth oocyte dynamics in three indeterminate spawners

with distinct spawning dynamics. Different methods were applied as well as new methods were introduced, such as a clustering analysis for the identification of the secondary growth oocyte cohorts and the ratio of the early secondary to late primary growth oocyte cohorts. It was shown that indeterminate spawners can display varying proportions of oocytes at the size range between primary and secondary growth based on the seasonal pattern of oocyte recruitment. Also, the study of secondary growth oocytes dynamics showed that sparse spawners, like sardine, with faster oocyte growth rates, display polymodal oocyte size frequency distributions consisting of fewer and distinct oocyte cohorts, while frequent spawners, like mackerel, with slower oocyte growth rate, tend to form a unimodal distribution consisting of numerous oocyte cohorts which are hardly distinguished from each other, these results support previous assumptions, such as the conceptual model of Ganias et al. (2015) and Ganias and Lowerre-Barbieri (2018), who simulated oocyte size frequency distribution in multiple spawners based on oocyte growth rate, spawning interval, and the duration of the spawning period. Studying the POFs dynamics with two stereological methods, the Weibel method and the POFPD following adaptations to procedures used previously on oocytes (Kjesbu et al. 2011), showed that sardines with short spawning interval exhibit one daily POFs cohort, whereas mackerel had co-occurrence of multiple daily POFs cohorts, indicating the obstacles faced by the implementation of POF method, especially in fish species with complex ovarian dynamics. This study also suggested improvements in the application of the POFs method and alternative approaches for the spawning fraction assessment as well as indicators of a proxy of spawning interval.

Knowledge of early and secondary oogenesis, as well as how ovarian and spawning dynamics determine the fecundity type of fish species, is critical in applied fisheries. This study introduced new approaches and methods for studying ovarian dynamics at all levels, from oogonia to secondary growth oocytes. Initially, this study contributes to our understanding of early oogenesis by demonstrating that the development of early oocytes, as well as their seasonal dynamics and oogonial proliferation, differs even among fish species with the same fecundity type and that other parameters, such as feeding strategy and environmental conditions influence this early phase. It was also demonstrated that indeterminate spawners can exhibit the varying intensity of oocyte recruitment from primary to secondary growth based on their seasonal pattern, which contributes to a better understanding of the controversial fecundity type of species with complex ovarian dynamics, as well as the need for new criteria in the fecundity type definition, taking determinacy and indeterminacy as endpoints along a continuum. In addition, it showed how the spawning dynamics are reflected in ovarian dynamics of indeterminate spawners, investigating both secondary growth oocytes and POFs, indicating the impact on the fecundity type and the obstacles faced in the universal use of the current methods for the assessment of egg production when it comes in species with complex ovarian dynamics. Also, suggestions and new approaches for the assessment of critical parameters, such as spawning fraction, for the application of DEPM were provided. These results could be generalized in other fish species for revealing valuable information about their species-specific reproductive traits important for their application in egg production methods. It is the author's impression that this study has hopefully unravelled different aspects of early and secondary oogenesis in highly commercial fish

species and provided new tools and details about the species-specific reproductive traits which could be essential for improving their application in applied fisheries.

5.5 Main conclusions in bullets

- The cytoplasmic development of primary and early secondary growth oocytes differed between phylogenetically closely related fish species, indicating differences in the functional path of their oocytes during development.

- The Balbiani body occured as a spherical structure in both sardine and anchovy primary growth oocytes; however, a thick perinuclear zone of mitochondria, nuage and tiny vesicles was also observed in sardine, whilst nuage and mitochondria complexes were unevenly distributed around the nucleus in anchovy.

- Both Balbiani body and cytoplasmic zonation could be used as markers to distinguish immature from mature fishes, as well as to indicate the onset of the reproductive phase, providing a valuable tool for applied fisheries biology.

- The pattern of oogonial proliferation and early oocyte dynamics was different throughout the reproductive cycle among indeterminate spawners. In anchovies, oogonial proliferation was higher, both before (developing ovaries) and after (resting ovaries) spawning, whereas, in sardine it was stable throughout the reproductive period. Anchovy ovaries had a higher rate of prophase I meiotic activity before the spawning period (developing phase), whereas sardine ovaries had a higher rate after the spawning period (resting phase).

- The intensity of oocyte recruitment from the primary to secondary growth phase differed between indeterminate species with different spawning dynamics, indicating that fecundity type is flexible from determinacy to indeterminacy along a continuum, explaining the controversial fecundity type considered in both horse mackerel and mackerel.

- A new clustering method was introduced, allowing the grouping of oocytes in different cohorts without using oocyte diameter and thus a crucial histological bias dealing with the cutting angle and the orientation of reference points (e.g., nucleus) has been overcome. This method represents an improved tool to study species with complex ovarian dynamics.

- The secondary growth oocyte dynamics differed among fish species, reflecting their spawning dynamics. Sardine, which shows long spawning intervals and fast oocyte growth, had relatively few, clearly distinct secondary growth oocyte cohorts, whereas mackerel with shorter spawning intervals, had an increase in coexisting cohorts, an intermediate situation was observed in horse mackerel.

- POF dynamics varied among species with distinct spawning intervals, showing that sardine, with long spawning interval, had only a single daily POF cohort in the ovaries, whereas mackerel, with shorter spawning interval, showed co-occurrence of multiple daily POF cohorts. The coexistence of multiple daily POF cohorts in ovaries is an obstacle in the proper application of the daily egg production method (DEPM).

Literature cited

Abou-Seedo F, Dadzie S, Al-Kanaan K (2003). Histology of ovarian development and maturity stages in the yellowfin seabream, *Acanthopagrus latus* (Teleostei: Sparidae) (Hottuyn, 1782) reared in cages. Kuwait Journal of Science and Engineering 30: 121–13

Alheit J (1993). Use of the daily egg production method for estimating biomass of clupeoid fishes: a review and evaluation. Bulletin of Marine Science 53:750-67

Alix M, Kjesbu OS, Anderson KC (2020). From gametogenesis to spawning: How climate-driven warming affects teleost reproductive biology. Journal of Fish Biology 97:607-32

Alonso-Fernandez A, Vallejo AC, Saborido-Rey F, Murua H, Trippel EA (2009). Fecundity estimation of Atlantic cod (*Gadus morhua*) and haddock (*Melanogrammus aeglefinus*) of Georges Bank: application of the autodiametric method. Fisheries Research 99:47–54

Anderson E (1968). Cortical alveoli formation and Vitellogenesis during oocyte differentiation in the pipefish, *Syngnathus fuscus*, and the killifish, *Fundufus heteroclitus*. Journal of Morphology 125: 23–60

Anderson KC, Alix M, Charitonidou K, Thorsen A, Thorsheim G, Ganias K, Kjesbu OS (2020). Development of a new 'ultrametric' method for assessing spawning progression in female teleost serial spawners. Scientific Reports 10:9677

Armstrong MJ, Witthames PR (2012). Developments in understanding of fecundity of fish stocks in relation to egg production methods for estimating spawning stock biomass. Fisheries Research 117–118:35–47

Bandarra NM, Marçalo A, Cordeiro AR, Pousão-Ferreira P (2018). Sardine (*Sardina pilchardus*) lipid composition: Does it change after one year in captivity? Food Chemistry 244:408-13

Barr WA (1963). The endocrine control of the sexual cycle in the plaice, *Pleuronectes platessa* (L.). I. Cyclical changes in the normal ovary. General and Comparative Endocrinology 3: 197- 204

Beams HW, Kessel RG (1973). Oocyte structure and early vitellogenesis in the trout, *Salmo gairdneri*. American Journal of Anatomy 136: 105–122

Begovac PC, Wallace RA (1988). Stages of oocyte growth in the pipefish, *Syngnathus scouelli*. Journal of Morphology 197: 353-369

Benjamini Y, Hochberg Y (1995). Controlling the false discovery rate: a practical and powerful approach to multiple testing. Journal of the Royal Statistical Society Series B 57:289–300

Bhattacharya CG (1967). A simple method of resolution of a distribution into Gaussian components. Biometrics 23:115–135

Bilinski SM, Jaglarz MK, Szymanska B, Etkin LD, Kloc M (2004). Sm proteins, the constituents of the spliceosome, are components of nuage and mitochondrial cement in Xenopus oocytes. Experimental Cell Research 299: 171–178

Bilinski SM, Kloc M, Tworzydlo W (2017). Selection of mitochondria in female germline cells: is Balbiani body implicated in this process? Journal of Assisted Reproduction and Genetics 34: 1405- 1412

Bobe J (2015). Egg quality in fish: Present and future challenges. Animal Frontiers 5: 66–72

Borges MF, Gordo LS (1991) Spatial distribution by season and some biological parameters of horse mackerel (*Trachurus trachurus* L.) in the Portuguese continental waters (Division IXa). ICES C.M., pp 16

Braekevelt CR, McMillan DB (1967). Cyclic changes in the ovary of the brook stickleback *Eucalia inconstans* (Kirtland). Journal of Morphology 123: 373- 396

Brown-Peterson NJ, Wyanski DM, Saborido-Rey F, Macewicz BJ, Lowerre-Barbieri SK (2011). A standardized terminology for describing reproductive development in fishes. Marine and Coastal Fisheries 3: 52-70

Brown-Peterson NJ, Leaf RT, Scueller AM, Andres MJ (2017) Reproductive dynamics of Gulf Menhaden (*Brevoortia patronus*) in the Northern Gulf of Mexico: effects on stock assessments. Fishery Bulletin 115:284–299

Bullough WS (1942). Gametogenesis and some endocrine factors affecting it in the adult minnow (*Phoxinus laevis* L.). Journal of Endocrinology 3: 211-219

Charrad M, Ghazzali N, Boiteau V, Niknafs A (2014). NbClust: An R package for determining the relevant number of clusters in a data Set. Journal of Statistical Software, 61: 1-36. URL http://www.jstatsoft.org/v61/i06/.

Chan DC (2006). Dissecting mitochondrial fusion. Developmental Cell 11:592-4

Chung EY, Choi KH, Jun JC, Choi MS, Lee KY (2009). Ultrastructural studies on oocyte development and vitellogenesis during oogenesis in female *Boleophthalmus pectinirostris*. Animal Cells & Systems 13: 49–57

Claramunt G, Roa R (2001). An indirect approach to estimate spawning fraction as applied to *Sardinops sagax* from northern Chile. Scientia Marina 65: 87–94

Colozza G, De Robertis EM (2014). Maternal syntabulin is required for dorsal axis formation and is a germ plasm component in Xenopus. Differentiation 88: 17-26

Costa AM (2009). Macroscopic vs. microscopic identification of the maturity stages of female horse mackerel. ICES Journal of Marine Science 66: 509–516

Coward K, Bromage NR (1998). Histological classification of ovarian growth and the dynamics of ovarian recrudescence in Tilapia zillii (Gervais). Journal of Fish Biology 53: 285–302

Craig-Bennett A (1931). The reproductive cycle of the three-spined stickleback, *Gasterosteus aculeatus*. Philosophical Transactions of the Royal Society B 219: 197-279

de Jesus-Silva LM, Oliveira PV, Ribeiro CO, Ninhaus-Silveira A, Veríssimo-Silveira R (2018). Ovarian cycle in *Devario aequipinnatus* with emphasis on oogenesis. Zygote 26: 168–176

De Vlaming VL (1972). Environmental control of teleost reproductive cycles: a brief review. Journal of Fish Biology 4: 131–140

Domínguez-Castanedo O, Uribe MC (2019). Ovarian structure, folliculogenesis and oogenesis of the annual killifish *Millerichthys robustus* (Cyprinodontiformes: Cynolebiidae). Journal of Morphology 280: 316–328

dos Santos Schmidt TC, Slotte A, Kennedy J, et al. (2017). Oogenesis and reproductive investment of Atlantic herring are functions of not only present but long-ago environmental influences as well. Proceedings of the National Academy of Sciences of the United States of America 114: 2634–2639

dos Santos Schmidt TC, Thorsen A, Slotte A, Nottestad L, Kjesbu OS (2021). First thorough assessment of de novo oocyte recruitment in a teleost serial spawner, the Northeast Atlantic mackerel (*Scomber scombrus*) case. Scientific Reports 11:21795

Droller MJ, Roth TF (1966). An electron microscope study of yolk formation during oogenesis in *Mebistes reticulatus* guppyi. Journal of Cell Biology 28: 209–232

Dunn OJ (1961). Multiple Comparisons among Means. Journal of the American Statistical Association 56:52-64

Dymek AM, Pecio A, Piprek RP (2021a). Diversity of Balbiani body formation in internally and externally fertilizing representatives of Osteoglossiformes (Teleostei: Osteoglossomorpha). Journal of Morphology 282: 1313-1329

Dymek AM, Piprek RP, Boron A, Kirschbaum F, Pecio A (2021b). Ovary structure and oogenesis in internally and externally fertilizing Osteoglossiformes (Teleostei: Osteoglossomorpha). Acta Zoologica azo.12378

Eggert B (1931). Die Geschlechtsorgane der Gobiiformes und Blenniformes. *Z Wiss Zool Abt A* 139: 249- 558

Elkouby YM, Jamieson-Lucy A, Mullins MC (2016). Oocyte polarization is coupled to the chromosomal bouquet, a conserved polarized nuclear configuration in meiosis. PLoS Biology 14: e1002335

Elkouby YM, Mullins MC (2017). Coordination of cellular differentiation, polarity, mitosis and meiosis – New findings from early vertebrate oogenesis. Developmental Biology 430: 275–287

Elkouby YM (2017). All in one – Integrating cell polarity, meiosis, mitosis and mechanical forces in early oocyte differentiation in vertebrates. International Journal of Developmental Biology 61: 179–193

Emerson LS, Walker MG, Witthames PR (1990). A stereological method for estimating fish fecundity. Journal of Fish Biology 36: 721–730

FAO (Food And Agriculture Organization of the United Nations). http://www.fao.org/fishery/topic/16072/en

Fitzhugh RG, Hettler FW (1995). Temperature influence on postovulatory follicle degeneration in Atlantic menhaden, *Brevoortia tyrannus*. Fishery Bulletin 93: 568-572

Forberg KG (1982). A histological study of development of oocytes in capelin, *Mallotus villosus* villosus (Muller). Journal of Fish Biology 143e54

Fusco S, Filosa M, Iacoviello P, Indolfi S, Tammaro S, Motta CM (2000). New site of temporary storage of rRNA in *O. mykiss* previtellogenic oocytes. Molecular Reproduction and Development 56: 198–206

Ganias K, Somarakis S, Machias A, Theodorou A (2004). Pattern of oocyte development and batch fecundity in the Mediterranean sardine. Fisheries Research 67:13-23

Ganias K, Nunes C, Stratoudakis Y (2007a). Degeneration of postovulatory follicles in the Iberian sardine *Sardina pilchardus*: Structural changes and factors affecting resorption. Fishery Bulletin 105: 131–139

Ganias K, Somarakis S, Koutsikopoulos C, Machias A (2007b). Factors affecting the spawning period of sardine in two highly oligotrophic Seas. Marine Biology 151:1559-69

Ganias K (2009). Linking sardine spawning dynamics to environmental variability. Estuarine, Coastal and Shelf Science 84:402-8

Ganias K, Rakka M, Vavalidis T, Nunes C (2010). Measuring batch fecundity using automated particle counting. Fisheries Research 106: 570-574

Ganias K, Nunes C, Vavalidis T, Rakka M, Stratoudakis Y (2011). Estimating oocyte growth rate and its potential relationship to spawning frequency in teleosts with indeterminate fecundity. Marine and Coastal Fisheries 3:119-26

Ganias K (2012). Thirty years of using the postovulatory follicles method: overview, problems and alternatives. Fisheries Research 117-118: 63-74

Ganias K (2013). Determining the indeterminate: Evolving concepts and methods on the assessment of the fecundity pattern of fishes. Fisheries Research 138: 23–30

Ganias K, Somarakis S, Nunes C (2014a). Reproductive potential. In: Ganias K (ed) Biology and ecology of sardines and anchovies, Boca Raton, FL: CRC Press, pp 79–121

Ganias K, Murua H, Claramunt G, Dominguez-Petit R, Gonçalves P, Juanes Fet al. (2014b). Chapter 4: Egg production. In: Domínguez-Petit R, Murua H, Saborido-Rey F and Trippel E (Eds), Handbook of applied fisheries reproductive biology for stock assessment and management. Vigo, Spain. Digital CSIC. http://hdl. handle.net/10261/87768.

Ganias K, Lowerre-Barbieri SK, Cooper W (2015). Understanding the determinate indeterminate fecundity dichotomy in fish populations using a temperature dependent oocyte growth model. Journal of Sea Research 96:1e10

Ganias K, Mouchlianitis FA, Nunes C, Costa AM, Angelico MM (2017). A reassessment of the fecundity type of Atlantic horse mackerel (*Trachurus trachurus*) in Atlantic Iberian waters (ICES division IXa) shows that indeterminate spawners can cease recruiting oocytes during their spawning season. ICES Journal of Marine Science 74:31–40

Ganias K, Lowerre-Barbieri S (2018). Oocyte recruitment and fecundity type in fishes: Refining terms to reflect underlying processes and drivers. Fish and Fisheries 19:562-72

Ganias K, Marmara D, Solla A, Garabana D, Dominguez-Petit R (2018). Atlantic mackerel daily spawning dynamics and implications for batch fecundity estimations. ICES Journal of Marine Science 75:1647-54

Garrido S, Ben-Hmadou R, Oliveira P, Cunha M, Chıcharo M, van der Lingen C (2008). Spatial and temporal variation in dietary composition and feeding intensity of sardine *Sardina pilchardus* off Portugal and relationships with satellite-derived chlorophyll data. Marine Ecology Progress Series 354: 235–244

Gayanillo FCJr, Sparre P, Pauly D (1996). FAO-ICLARM Fish Stock Assessment (FiSAT) user's guide. FAO Computerized Information Series (Fisheries) 7. FAO of the United Nations, Rome, Italy
Girden ER (1992). ANOVA: Repeated measures. Sage

Goncalves P, Costa AM, Murta AG (2009). Estimates of batch fecundity and spawning fraction for the southern stock of horse mackerel (*Trachurus trachurus*) in ICES Division IXa. ICES Journal of Marine Science 66: 617–622

Gordo LS, Costa A, Abaunza P, Lucio P, Eltink ATGW, Figueiredo I (2008). Determinate versus indeterminate fecundity in horse mackerel. Fisheries Research 89:181–185

Greer Walker M, Witthames PR, De Los B, Santos JI (1994). Is the fecundity of the Atlantic mackerel (*Scomber scombrus*: scombridae) determinate? Sarsia 79:13–26

Grier H (2000). Ovarian germinal epithelium and folliculogenesis in the Common snook, *Centropomus undecimalis* (Teleostei: Centropomidae). Journal of Morphology 243: 265-281

Grier H, Uribe MC, Parenti LR (2007). Germinal epithelium, folliculogenesis, and postovulatory follicles in ovaries of rainbow trout, Oncorhynchus mykiss (Walbaum, 1792) (Teleostei, *Protacanthopterygii, Salmoniformes*). Journal of Morphology 268: 293–310

Grier HJ, Uribe MC, Patiño R (2009). The ovary, folliculogenesis and oogenesis in teleosts. In: Jamieson BGM (Ed), Reproductive biology and phylogeny of fishes (agnathans and bony fishes), Vol. 8A. Enfield, NH: Science Publishers, pp. 25-84

Grier H (2012). Development of the follicle complex and oocyte staging in Red Drum, *Sciaenops ocellatus* Linnaeus, 1776 (Perciformes, Sciaenidae). Journal of Morphology 273: 801–829

Grier HJ, Neidig CL, Quagio-Grassiotto I (2017). Development and fate of the postovulatory follicle complex, postovulatory follicle, and observations on folliculogenesis and oocyte atresia in ovulated common snook, *Centropomus undecimalis* (Bloch, 1792). Journal of morphology 278:547-62

Grier HJ, Porak WF, Carroll J, Parenti LR (2018). Oocyte development and staging in the Florida bass, *Micropterus floridanus* (Lesueur, 1822), with comments on the evolution of pelagic and demersal eggs in bony fishes. Copeia, 106: 329-345

Hann HW (1927). The history of the germ cells of *Cottus bairdii* Girard. Journal of Morphology 43: 427-498

Hartigan JA, Wong MA (1979). Algorithm AS 136: A K-means clustering algorithm. Journal of the Royal Statistical Society 28:100e8

Haslob H, Kraus G, Saborido-Rey F (2012). The dynamics of postovulatory follicle degeneration and oocyte growth in Baltic sprat. Journal of Sea research 67:27-33

Higashino T, Miura T, Miura C, Yamauchi K (2002). Histological studies on early oogenesis in barfin flounder (*Verasper moseri*). Zoological science 19:557-63

Hughes LC, Ortí G, Huang Y, Sun Y, Baldwin CC, Thompson AW, Arcila D, Betancur RR, Li C, Becker L, et al. (2018). Comprehensive phylogeny of ray-finned fishes (Actinopterygii) based on transcriptomic and genomic data. Proceedings of the National Academy of Sciences of the United States of America 115: 6249-6254

Hunter JR, Goldberg SR (1980). Spawning incidence and batch fecundity in Northern anchovy, *Engraulis mordax*. Fishery Bulletin 77: 641-652

Hunter JR, Macewicz BJ (1985). Measurement of spawning frequency in multiple spawning fishes. In: Lasker R (Ed), An egg production method for estimating spawning biomass of pelagic fish: application to the Northern anchovy, *Engraulis mordax*. NOAA Technical Report NMFS 36, pp. 79-94

Hunter JR, Lo NCH, Leong RJH (1985). Batch fecundity in multiple spawning fishes. In: Lasker R (Ed), An egg production method for estimating spawning biomass of pelagic fish: application to the Northern anchovy, *Engraulis mordax*. NOAA Technical Report NMFS 36, pp. 67-77

Hunter JR, Macewicz BJ, Sibert HR (1986). The spawning frequency of Skipjack tuna, *Katsuwonus pelamis*, from the South Pacific. Fishery Bulletin 84: 895-903

Hunter JR, Macewicz BJ, Kimbrell CA (1989). Fecundity and other aspects of the reproduction of sablefish *Anoplopoma fimbria* in central Californian waters. California Cooperative Ocean Fish Investigations Report 30:61–72

Hunter JR, Macewicz BJ, Lo NC, Kimbrell C (1992). Fecundity, spawning, and maturity of female Dover sole *Microstomus pacificus*, with an evaluation of assumptions and precision. Fishery Bulletin 90:101–128

Hunter JR, Lo NCH (1993). Ichthyoplankton methods for estimating fish biomass: introduction and terminology. Bulletin of Marine Science 53: 723–727

ICES (1993). Report of the mackerel/horse mackerel egg production workshop, Aberdeen, 8–12 March 1993. ICES Document CM 1993/H: 4. 142 pp.

ICES (1994). Report of the mackerel/horse mackerel egg production workshop, Vigo, 31 January – 4 February 1994. ICES Document CM 1994/H: 4. 58 pp.

ICES (2002). Working group on mackerel and horse mackerel egg surveys. ICES Expert Group reports (until 2018). Report.

ICES (2003). Report of the working group on mackerel and horse mackerel egg survey (WGMEGS). ICES Expert Group reports (until 2018). Report.

ICES (2011). Report of the working group on mackerel and horse mackerel egg surveys (WGMEGS). San Sebastian, Spain, p 109

ICES (2012). Report of the working group on mackerel and horse mackerel egg surveys (WGMEGS), 18–21 April 2012, Galway, Ireland. ICES Document CM 2012/SSGESST: 04: 135.

ICES (2017). Report of the report of the working group on widely distributed stocks (WGWIDE). ICES Headquarters, Copenhagen, Denmark, 994 pp.

ICES (2018). Report of the working group on mackerel and horse mackerel egg surveys (WGMEGS). Marine Institute, Dublin, Ireland, pp 135

ICES (2019). Working group on widely distributed stocks (WGWIDE). ICES Scientific Reports. Report.

Iwamatsu T, Nakashima S (1996). Dynamic growth of oocytes of the Medaka, *Oryzias latipes* I. A relationship between establishment of the animal-vegetal axis of the oocyte and its surrounding granulosa cells. Zoological Science 13: 873-882

Jansen T, Slotte A, dos Santos Schmidt TC, Sparrevohn CR, Jacobsen JA, Kjesbu OS (2021). Bioenergetics of egg production in Notheast Atlantic mackerel changes the perception of fecundity type and annual trends in spawning stock biomass. Progress in Oceanography 198: 102658

Jun JC, Gang WH, Lee KY (2018). Ultrastructural studies on oocyte differentiation and vitellogenesis in the oocytes of female *Kareius bicoloratus* in Western Korea. Development & Reproduction 22: 213–223

Karlou-Riga C, Economidis PS (1996). Ovarian atretic rates of European horse mackerel, *Trachurus trachurus* (L.), in the Saronikos Gulf (Greece). Fishery Bulletin 94:66–76

Karlou-Riga C, Economidis PS (1997). Spawning frequency and batch fecundity of horse mackerel, *Trachurus trachurus* (L.), in the Saronikos Gulf (Greece). Journal of Applied Ichthyology 13: 97–104

Karlou-Riga C, Petza D, Charitonidou K, Anastopoulos P, Koulmpaloglou DS, Ganias K (2020). Ovarian dynamics in picarel (*Spicara smaris*, L., Sparidae) and implications for batch fecundity and spawning interval estimation. Journal of Sea Research 160–161: 101894

Kassambara A (2019). Ggpubr: 'ggplot2' Based Publication Ready Plots. R package version 0.2.3. https://CRAN.R-project.org/package=ggpubr

Kassambara A, Mundt F (2020). Factoextra: Extract and visualize the results of multivariate data analyses, R package v. 1.0. 7.

Kaufman L, Rousseeuw PJ (2005). Finding groups in data. An introduction to cluster analysis. Wiley-Interscience: A John Wiley & Sons, INC., Publication.

Kjesbu OS, Kryvi H (1989). Oogenesis in cod, *Gadus morhua* L., studied by light and electron microscopy. Journal of Fish Biology 34: 735-746

Kjesbu OS, Witthames PR, Solemdal P, Greer Walker M (1990). Ovulatory rhythm and a method to determinate the stage of spawning in Atlantic cod (*Gadus morhua*). Canadian Journal of Fisheries and Aquatic Science 47:1185–1193

Kjesbu OS, Kryvi H, Norberg B (1996). Oocyte size and structure in relation to blood plasma steroid hormones in individually monitored, spawning Atlantic cod. Journal of Fish Biology 49: 1197–1215

Kjesbu OS, Witthames PR (2007). Evolutionary pressure on reproductive strategies in Flatfish and Groundfish: relevant concepts and methodological advancements. Journal of Sea Research 58: 23-34

Kjesbu OS (2009). Applied fish reproductive biology: contribution of individual reproductive potential to recruitment and fisheries management. In: Jakobsen T, Fogarty MJ, Megrey BA, Moksness E (Eds), Fish reproductive biology: implications for assessment and management. Hoboken, New Jersey: John Wiley and Sons, pp. 293-332

Kjesbu OS, Fonn M, Gonzales BD, Nilsen T (2010). Stereological calibration of the profile method to quickly estimate atresia levels in fish. Fisheries Research 104:8–18

Kjesbu OS, Thorsen A, Fonn M (2011). Quantification of primary and secondary oocyte production in Atlantic cod by simple oocyte packing density theory. Marine and Coastal Fisheries 3: 92-105

Klibansky N, Juanes F (2008). Procedures for efficiently producing high-quality fecundity data on a small budget. Fisheries Research 89: 84–89

Kloc, M, Bilinski S, Chan AP, Allen LH, Zearfoss NR, Etkin LD (2001). RNA localization and germ cell determination in Xenopus. International Review of Cytology 203: 63–91

Kloc M, Bilinski SM, Dougherty MT, Brey EM, Etkin LD (2004). Formation, architecture and polarity of female germline cyst in Xenopus. Developmental Biology 266: 43–61

Kloc M, Etkin LD (2005). RNA localization mechanisms in oocytes. Journal of Cell Science 118: 269– 282

Kloc M, Bilinski SM, Dougherty MT (2007). Organization of cytokeratin cytoskeleton and germ plasm in the vegetal cortex of *Xenopus laevis* oocytes depends on coding and non-coding RNAs: Three dimensional and ultrastructural analysis. Experimental Cell Research 313: 1693-1651

Kloc M, Jaglarz M, Dougherty M, Stewart MD, Nel-Themaat L, Bilinski S (2008). Mouse early oocytes are transiently polar: Three-dimensional and ultrastructural analysis. Experimental Cell Research 314: 3245–3254

Kloc M, Jedrzejowska I, Tworzydlo W, Bilinski SM (2014). Balbiani body, nuage and sponge bodies-term plasm pathway players. Arthropod Structure & Development 43: 341-348

Kobayashi W (1985). Communications of oocyte-granulosa cells in the chum salmon ovary detected by transmission electron microscopy. Development, Growth & Differentiation 27: 553–561

Kobayashi H, Iwamatsu T (2000). Development and fine structure of the yolk nucleus of previtellogenic oocytes in the medaka *Oryzias latipes*. Development, Growth and Differentiation 42: 623-631

Korta M, Murua H, Kurita Y, Kjesbu OS (2010). How are the oocytes recruited in an indeterminate fish? Applications of stereological techniques along with advanced packing density theory on European hake (*Merluccius merluccius* L.). Fisheries Research 104:56–63

Kruskal WH, Wallis WA (1952). Use of Ranks in One-Criterion Variance Analysis. Journal of the American Statistical Association 47: 583-621

Kunz YW (2004). Development biology of teleost fishes. Springer.

Kurita Y, Kjesbu OS (2009). Fecundity estimation by oocyte packing density formulae in determinate and indeterminate spawners: Theoretical considerations and applications. Journal of Sea Research 61:188–196

Langdon YG, Mullins MC (2011). Maternal and Zygotic Control of Zebrafish Dorsoventral Axial Patterning. Annual Review of Genetics 45: 357–77

Le S, Josse J, Husson F (2008). FactoMineR: A package for multivariate analysis. Journal of Statistical Software 25: 1–18

Lo NCH, Hunter JR, Moser HG, Smith PE, Methot RD (1992). The daily fecundity reduction method: a new procedure for estimating adult fish biomass. ICES Journal of Marine Science 49: 209–215

Lo NH, Hunter JR, Moser HG, Smith PE (1993). A daily fecundity reduction method of biomass estimation with application to Dover sole *Microstomus pacificus*. Bulletin of marine science 53:842-63

Lowerre-Barbieri SK, Brown-Peterson NJ, Murua H, Tomkiewicz J, Wyanski DM, Saborido-Rey F (2011). Emerging issues and methodological advances in fisheries reproductive biology, Marine and Coastal Fisheries: Dynamics, Management, and Ecosystem Science 3: 32-51

Lubzens E, Young G, Bobe J, Cerdà J (2010). Oogenesis in teleosts: How fish eggs are formed. General and Comparative Endocrinology 165: 367–389

Lubzens E, Bode J, Young G, Sullivan C (2017). Maternal investment in fish oocytes and eggs: The molecular cargo and its contributions to fertility and early development. Aquaculture 472: 107–143

Luckenbach JA, Iliev DB, Goetz FW, Swanson P (2008). Identification of differentially expressed ovarian genes during primary and early secondary oocyte growth in coho salmon, *Oncorhynchus kisutch*. Reproductive biology and endocrinology 6:1-5

Lyman-Gingerich J, Pelegri F (2007). Maternal factors in fish oogenesis and embryonic development. In: Babin PJ, Cerdà J, Lubzens L (Eds), The fish oocyte from basic studies to biotechnological applications, The Netherlands: Springer, pp. 141–174

Macer CT (1974). The reproductive biology of the horse mackerel *Trachurus trachurs* (L.) in the North Sea and English Channel. Journal of Fish Biology 6:415-38

Mackie MC, Lewis PD, Gaughan DJ, Newman SJ (2005). Variability in spawning frequency and reproductive development of the narrow-barred Spanish mackerel (*Scomberomorus commerson*) along the west coast of Australia. Fishery Bulletin 103: 344–354

MacQueen J (1967). Some methods for classification and analysis of multivariate observations. Proc Fifth Berkeley Symp Math Stat Probab 1:281e97

Marlow FL, Mullins MC (2008). Bucky ball functions in Balbiani body assembly and animal-vegetal polarity in the oocyte and follicle cell layer in zebrafish. Developmental Biology 321: 40

Marshall CT, Yaragina NA, Lambert Y, Kjesbu OS (1999). Total lipid energy as a proxy for total egg production by fish stocks. Nature 402: 288–290

Matthews SA (1938). The seasonal cycle in the gonads of Fundulus. Biology Bulletin 75: 66-74

Mayer I, Shackley SE, Ryland JS (1988). Aspects of the reproductive biology of the bass, *Dicentrarchus labrax* L.I. An histological and histochemical study of oocyte development. Journal of Fish Biology 33: 609–622

McBride RS, Somarakis S, Fitzhugh GR, Albert A, et al. (2015). Energy acquisition and allocation to egg production in relation to fish reproductive strategies. Fish and Fisheries 16: 23−57

McBride RS, Ferreri R, Towle EK, Boucher JM, Basilone G (2016). Yolked oocyte dynamics support agreement between determinate- and indeterminate-method estimates of annual fecundity for a Northeastern United States population of American shad. PLoS ONE 11: e0164203

McPherson LR, Kjesbu OS (2012). Emergence of an oocytic circumnuclear ring in response to increasing day length in Atlantic herring (*Clupea harengus*). Marine Biology 159: 341–353

Mendoza G (1943). The reproductive cycle of the viviparous teleost, *Neotoca bilineata*, a member of the family Goodeidae. IV. The germinal tissue. Biology Bulletin 84: 87- 97

Mooseker MS (1985). Organisation, chemistry and assembly of the cytoskeletal apparatus of the brush border. Annual Review of Cell Biology 1: 209–241

Morrison CM (1990). Histology of cod reproductive tract. Canada Special Publication of Fisheries and Aquatic Sciences 110

Moser HG (1967). Seasonal histological changes in the gonads of *Sebastodes paucispinis* Ayres, an ovoviparous teleost (family Scorpaenidae). Journal of Morphology 123: 329- 354

Mouchlianitis FA, Belo AF, Vieira AR, Quintella BR, Almeida PR, Ganias K (2019) Primary and secondary oocyte growth dynamics in anadromous semelparous Allis shad *Alosa alosa*. Journal of Fish Biology 95:1447–1456

Mouchlianitis FA, Minos G, Ganias K (2020). Timing of oocyte recruitment within the ovulatory cycle of Macedonian shad, *Alosa macedonica*, a batch spawning fish with indeterminate fecundity. Theriogenology 146:31–38

Mouchlianitis FA, Schultz ET, dos Santos Schmidt TC, Davis JP, Ganias K (2021). Ovarian dynamics and fecundity regulation in blueback herring, Alosa aestivalis, from the Connecticut River, US. Journal of Applied Ichthyology 37:64–72

Murua H, Saborido-Rey F (2003). Female reproductive strategies of marine fish species of the North Atlantic. Journal of Northwest Atlantic Fishery Science 33:23–31

Murua H, Motos L (2006). Reproductive strategy and spawning activity of the European hake *Merluccius merluccius* (L.) in the Bay of Biscay. Journal of Fish Biology 69:1288-303

Mustac B, Sinovcic G (2009). Comparison of mesenteric and tissue fat content in relation to sexual cycle of the sardine, *Sardina pilchardus* (Walb. 1792), in the eastern Middle Adriatic fishery grounds (Croatia). Journal of Applied Ichthyology 25: 595–599

Nakamura S, Kobayashi K, Nishimura T, Higashijima SI, Tanaka M (2010). Identification of germline stem cells in the ovary of the teleost Medaka. Science 328: 1561-1563

Nakamura S, Kobayashi K, Nishimura T, Tanaka M (2011). Ovarian Germline Stem Cells in the Teleost Fish, Medaka (*Oryzias latipes*). International Journal of Biological Sciences 7: 403-409

Ndjaula HON, Hansen T, Kruger-Johnsen M, Kjesbu OS (2009). Oocyte development in captive Atlantic horse mackerel *Trachurus trachurus*. ICES Journal of Marine Science 66:623–630

Nejedli S, Petrinec Z, Kužir S, Srebočan E (2004). Annual oscillation of ovarian morphology in European pilchard (*Sardina pilchardus* Walbaum) in the Northern Adriatic Sea. Veterinarski arhiv. 74:97-106

Nunes C, Silva A, Soares E, Ganias K (2011). The use of hepatic and somatic indices and histological information to characterize the reproductive dynamics of Atlantic Sardine *Sardina pilchardus* from the Portuguese coast. Marine and Coastal Fisheries 3: 127–144

Olafsdottir AH, Utne KR, Jacobsen JA, Jansen T, Óskarsson GJ, Nøttestad L, Elvarsson BÞ, Broms C, Slotte A (2019). Geographical expansion of Northeast Atlantic mackerel (*Scomber scombrus*) in the Nordic Seas from 2007 to 2016 was primarily driven by stock size and constrained by low temperatures. Deep Sea Research Part II: Topical Studies in Oceanography 159:152-68

Panteris E, Apostolakos P, Quader H, Galatis B (2004). A cortical cytoplasmic ring predicts the division plane in vacuolated cells of *Coleus*: the role of actomyosin and microtubules in the establishment and function of the division site. New Phytologist 163: 271-286

Pappas D, Gkelis S, Panteris E (2020). The effects of microcystin-LR in *Oryza sativa* root cells: F-actin as a new target of cyanobacterial toxicity. Plant Biology 22: 839-849

Parker K (1980). A direct method for estimating northern anchovy, *Engraulis mordax*, spawning biomass. Fishery Bulletin 78: 541–544

Patzner RA (2008). Reproductive strategies of fish. In: Rocha MJ, Arukwe A, Kapoor BG (Eds), Fish reproduction. Science Publishers, Enfield, New Hampshire, pp. 311–350

Pavlov, DA, Emelyanova NG, Novikov GG (2009). Reproductive dynamics. In: Jakobsen T, Fogarty MJ, Megrey BA, Moksness E (Eds), Fish reproductive biology. Wiley-Blackwell Scientific Publications, Chichester, UK., pp 48–90

Pfannestiel HD, Grünig C (1982). Yolk formation in an annelid (Ophryotrocha puerilis, polychaeta). Tissue and Cell 14: 669–680

Priede IG, Watson JJ (1993). An evaluation of the daily egg production method for estimating biomass of Atlantic mackerel (*Scomber scombrus*). Bulletin of Marine Science 53:891–911

Quagio-Grassiotto I, Grier H, Mazzoni TS, Nobrega RH, de Arruda Amorim JP (2011). Activity of the ovarian germinal epithelium in the freshwater catfish, *Pimelodus maculatus* (Teleostei: Ostariophysi: Siluriformes): Germline cysts, follicle formation and oocyte development. Journal of Morphology 272: 1290–1306

Quagio-Grassiotto I, Dantas D, Cristina A, Guimaraes-bassoli D (2014). A cytochemical approach to describe oocyte development in the freshwater ostariophysan, *Serrasalmus maculatus* (Characiformes). Micron 60:18e28

R Core Team (2020) R language and environment for statistical computing R Foundation for statistical computing, Vienna, Austria. URL https://www.R-project.org/

Raikova EV (1976). Evolution of the nucleolar apparatus during oogenesis in Acipenseridae. Journal of Embryology and Experimental Morphology 35: 667- 687

Rasband WS, ImageJ US (1997-2018). National Institutes of Health, Bethesda, Maryland, USA. https://imagej.nih.gov/ij/

Rideout RM, Rose GA, Burton MP (2005). Skipped spawning in female iteroparous fishes. Fish and Fisheries 6:50-72

Rijnsdorp AD, Witthames PR (2005). Ecology of reproduction. In: Gibson RN (Ed), Flatfishes: biology and exploitation. Fish and Aquatic Resources Series 9. Oxford: Blackwell Science, pp 68-93

Rousseeuw PJ (1987). Silhouettes: a graphical aid to the interpretation and validation of cluster analysis. Computational and Applied Mathematics 20:53e65

Rueden CT, Scgindelin J, Hiner MC, DeZonia BE, Walter AE, Arena ET, et al. (2017). ImageJ2: ImageJ for the next generation of scientific image data. BMC Bioinformatics 18:529

Saber S, Macías D, Ortiz de Urbina J, Kjesbu OS (2015). Stereological comparison of oocyte recruitment and batch fecundity estimates from paraffin and resin sections using spawning albacore (*Thunnus alalunga*) ovaries as a case study. Journal of Sea Research 95: 226–238

Saborido-Rey F, Junquera S (1998). Histological assessment of variations in sexual maturity of Cod (*Gadus morhua* L.) at the Flemish Cap (North-west Atlantic). ICES Journal of Marine Science 55: 515-521

Saito K, Sakai C, Kawasaki T, Sakai N (2014). Telomere distribution pattern and synapsis initiation during spermatogenesis in zebrafish. Developmental Dynamics 243: 1448-1456

Santos B, Rizzo E, Bazzoli N, Sato Y, Moro L (2005). Ovarian regression and apoptosis in the South American teleost *Leporinus taeniatus* Lütken (Characiformes, Anostomidae) from the Sao Francisco Basin. Journal of Fish Biology 67: 1446-1459

Schismenou E, Somarakis S, Thorsen A, Kjesbu OS (2012). Dynamics of de novo vitellogenesis in fish with indeterminate fecundity: an application of oocyte packing density theory to European anchovy, *Engraulis Encrasicolus.* Marine Biology 159:757–768

Selman, K, Wallace RA (1986). Gametogenesis in *Fundulus heteroclitus*. American Zoologist, 26: 173–192

Selman K, Wallace AR (1989). Cellular aspects of oocyte growth in Teleosts. Zoological Science 6: 211-231

Selman K, Wallace RA, Sarka A, Qi X (1993). Stages of oocyte development in the zebrafish, *Brachydanio rerio*. Journal of morphology 218:203-24

Serrat A, Saborido-Rey F, Garcia-Fernandez C, Munoz M, Lloret J, Thorse A, Kjesbu OS (2019). New insights in oocyte dynamics shed light on the complexities associated with fish reproductive strategies. Scientific Reports 9: 18411

Shapiro SS, Wilk MB (1965). An analysis of variance test for normality (complete samples). Biometrika 52: 591–611

Shirokova MY (1977). Peculiarities of the sexual maturation of females of the Baltic cod, *Gadus morhua* callarias. Journal of lchthyology 17: 574-581

Škugor A, Tveiten H, Johnsen H et al. (2016). Multiplicity of Buc copies in Atlantic salmon contrasts with loss of the germ cell determinant in primates, rodents and axolotl. BMC Evolutionary Biology 16: 232

Smith P, Wilhelm D, Rodgers RJ (2014). Development of mammalian ovary. Journal of Endocrinology 221: R145–R161

Somarakis S, Palomera I, Garcia A, Quintanilla L, Koutsikopoulos C, Uriarte A, Motos L (2004). Daily egg production of anchovy in European waters. ICES Journal of Marine Science 61: 944– 958

Somarakis S (2005). Marked interannual differences in reproductive parameters and daily egg production of anchovy in the northern Aegean Sea. Belgian Journal of Zoology 135: 247–252

Somarakis S, Schismenou E, Siapatis A, Giannoulaki M, Kallianiotis A, Machias A (2012). High variability in the daily egg production method parameters of an eastern Mediterranean anchovy stock: influence of environmental factors, fish condition and population density. Fisheries Research 117: 12–21

Somarakis S, Giannoulaki M, Markakis K, Tsiaras K, Schismenou E, Peristeraki P (2021). Ovarian dynamics, batch fecundity and spawning phenology of the lessepsian migrant *Etrumeus golanii* DiBattista, Randall & Bowen, 2012 (Clupeidae: Dussumieriinae). Mediterranean Marine Science 22:466–479

Sorokin VP (1957). The oogenesis and reproductive cycle of the cod (*Gadus morhua* Linn.). Trudy Pinro. 10: 125-144. (In Russian; English translation No. 72F49 Ministry Agric. Fish. Food, U.K. 1961).

Stratoudakis Y, Bernal M, Ganias K, Uriarte A (2006). The daily egg production method: recent advances, current applications and future challenges. Fish and Fisheries 7:35-57

Stratoudakis Y, Coombs S, de Lanzós AL, Halliday N, Costas G, Caneco B, Franco C, Conway D, Santos MB, Silva A, Bernal M (2007). Sardine (*Sardina pilchardus*) spawning seasonality in European waters of the northeast Atlantic. Marine Biology 152:201-12

Takita T, Iwamoto T, Kai S, Sogabe I (1983). Maturation and spawning of the Dragonet, *Callionymus enneactis*, in an aquarium. Japanese Journal of Ichthyology 30: 221-226

Thomé RG, Domingos FFT, Santos HB, Martinelli PM, Sato Y, Rizzo E, Bazzoli N (2012). Apoptosis, cell proliferation and vitellogenesis during the folliculogenesis and follicular growth in teleost fish. Tissue Cell 44: 54–62

Thompson BR, Lobo S, Bernlohr DA (2010). Fatty acid flux in adipocytes: The in's and out's of fat cell lipid trafficking. Molecular and Cellular Endocrinology 318: 24–33

Thorsen A, Kjesbu OS (2001). A rapid method for estimation of oocyte size and potential fecundity in Atlantic cod using a computer-aided particle analysis system. Journal of Sea Research 46: 295-308

Tokarz RR (1978). Oogonial proliferation, oogenesis and folliculogenesis in nonmammalian vertebrates. In Jones RE (ed) The Vertebrate Ovary (pp. 145-179). Plenum Press

Tukey J (1949). Comparing Individual Means in the Analysis of Variance. Biometrics 5: 99–114

Tveiten H, Solevag SE, Johnsen HK (2001). Holding temperature during the breeding season influences final maturation and egg quality in common wolffish. Journal of Fish Biology 58: 374–385

Tworzydlo W, Kisiel E, Jankowska W, Bilinski SM (2014). Morphology and ultrastructure of the germarium in panoistic ovarioles of a basal “apterygotous” insect, *Thermobia domestica*. Zoology 117: 200–206

Tworzydlo W, Kisiel E, Jankowska W, Witwicka A, Bilinski SM (2016). Exclusion of dysfunctional mitochondria from Balbiani body during early oogenesis of Thermobia. Cell and Tissue Research 366: 191–201

Uriarte A, Alday A, Santos M, Motos L (2012). A re-evaluation of the spawning fraction estimation procedures for Bay of Biscay anchovy, a species with short interspawning intervals. Fisheries Research 117:96-111

Uribe MC, Grier H (2011). Oogenesis of microlecithal oocytes in the viviparous teleost *Heterandria formosa* (Poeciliidae). Journal of Morphology 272: 241–257

van Damme CJG, Thorsen A, Fonn M, Alvarez P, Garabana D, O'Hea B, Dickey-Collas M (2014). Fecundity regulation in horse mackerel. ICES Journal of Marine Science 71:546–558

Wallace RA, Selman K (1981). Cellular and dynamic aspects of oocyte growth in teleosts. American zoologist 21:325-43

Wallace RA, Selman K (1990). Ultrastructural aspects of oogenesis and oocyte growth in fish and amphibians. Journal of electron microscopy technique 16:175-201

Weibel ER, Kistler GS, Scherle WF (1966). Practical stereological methods for morphometric cytology. Journal of Cell Biology 30: 23-38
Welch BL (1947). The generalization of "Student's" problem when several different population variances are involved. Biometrika 34: 28–35

White GG, Munroe TA, Austin HM (2003). Reproductive seasonality, fecundity, and spawning frequency of tautog (*Tautoga onitis*) in the lower Chesapeake Bay and coastal waters of Virginia. Fishery Bulletin 101: 424–442

Wickham H (2016). Ggplot2: Elegant graphics for data analysis. Springer-Verlag, New York

Wickham H, François R, Henry L, Müller K, Vaughan D (2023). *dplyr: A Grammar of Data Manipulation*. https://dplyr.tidyverse.org, https://github.com/tidyverse/dplyr.

Wiegand MD (1996). Composition, accumulation, and utilization of yolk lipids in teleost fish. Review in Fish Biology and Fisheries 6: 259–286

Wilcoxon F (1945). Individual comparisons by ranking methods. Biometrics 1:80–83

Wildner DD, Grier H, Quagio-Grassiotto I (2013). Female germ cell renewal during the annual reproductive cycle in Ostariophysians fish. Theriogenology 79: 709–724

Wilke CO (2018). Ggridges: Ridgeline plots in "ggplot2". R package version 0.5.1. https://CRAN.R-project.org/package=ggridges

Witthames PR, Greer-Walker M (1995). Determinacy of fecundity and oocyte atresia in Sole (*Solea solea*) from the channel, the North-Sea and the Irish Sea. Aquatic Living Resources 8: 91-109

Witthames PR, Greenwood LN, Dominguez R, Korta M, Kjesbu OS, Thorsen A, Murua H, Saborido-Rey F (2009). Advances in methods for determining fecundity: Application of the new methods to some marine fishes. Fishery Bulletin 107: 148–16

Witthames PR, Thorsen A, Kjesbu OS (2010). The fate of vitellogenic follicles in experimentally monitored Atlantic cod *Gadus morhua* (L.): application to stock assessment. Fisheries Research 104:27-37

Wootton RJ (1974). The inter-spawning interval of the female three-spined stickleback, *Gasterosteus aculeatus*. Journal of Zoology, 172: 331–342

Wootton RJ (1984). Tactics and strategies in fish reproduction. Fish reproduction: strategies and tactics, 1-12

Wootton RJ (1990). Ecology of teleost fishes. Chapman and Hall, London, pp. 386

Wootton RJ (1994). Life histories as sampling devices: optimum egg size in pelagic fishes. Journal of fish biology, 45: 1067-1077

Wuenschel MJ, McBride RS, Fitzhugh GR (2013). Relations between total gonad energy and physiological measures of condition in the period leading up to spawning: results of a laboratory experiment on black sea bass (*Centropristis striata*). Fisheries Research 138:110-9

Yamamoto K (1962). Origin of the yearly crop of eggs in the medaka, *Oryzias latipes*. Annotationes Zoologicae Japonenses 35: 156- 161

Yamamoto K, Shirai K (1962). Origin of the yearly crop of eggs in the bitterling *Rhodeus ocellatus*. Annotationes Zoologicae Japonenses 35: 218- 222

Yamamoto K, Yamazaki F (1961). Rhythm of development in the oocyte of the gold-fish, *Carassius auratus*. Bulletin of the Faculty of Fisheries Hokkaido University, 12: 93–110

Yamazaki F (1965). Endocrinological studies on the reproduction of the female goldfish, *Carassius auratus* L., with special reference to the function of the pituitary gland. Memoirs of the Faculty of Fisheries Hokkaido University 13: 1-64

Yang Y, Ning C, Li Y, Wang Y, Hu J, Liu Y, Zhang M, Sun Y, Gu W, Zhang Y, Sun J, Xu S (2021). Dynamic changes in mitochondrial DNA, morphology, and fission during oogenesis of a seasonal-breeding teleost. *Pampus argenteus*. Tissue and Cell 72: 101558

Ye H, Li CJ, Yue HM, Yang XG, Wei QW (2015). Differential expression of fertility genes boule and dazl in Chinese sturgeon (*Acipenser sinensis*), a basal fish. Cell and Tissue Research 360: 413–425

Ye H, Yue H, Yang X, Li C, Wei Q (2018). Molecular characterization, tissue distribution, localization and mRNA expression of the bucky ball gene in the Dabry's sturgeon (*Acipenser dabryanus*) during oogenesis. Gene Expression Patterns 28: 62–71

Yue, H.M., Cao, H., Chen, X.H., Ye, H., Li, C.J., & Du, H. (2014). Molecular characterization of the cDNAs of two zona pellucida genes in the Chinese sturgeon, *Acipenser sinensis* gray, 1835. Journal of Applied Ichthyology, 30, 273–1281.

Zamarro J, Cervino S, González M (1993). Identification of female Cod (*Gadus morhua*) from Flemish Cap (Northwest Atlantic) at the beginning of ripening. Northwest Atlantic Fisheries Organization, Scientific Council Research Document 93/25

Zelazowska M, Kilarski W, Bilinski SM, Podder DD, Kloc M (2007). Balbiani cytoplasm in oocytes of a primitive fish, the sturgeon *Acipenser gueldenstaedtii*, and its potential homology to the Balbiani body (mitochondrial cloud) of *Xenopus laevis* oocytes. Cell and Tissue Research 329: 137–145

Zelazowska M, Kilarski W (2009). Possibile participation of mitochondria in lipid yolk formation in oocytes of paddlefish and sturgeon. Cell and Tissue Research 335: 585–591

Żelazowska M, Jankowska W, Plewniak E, Rajek U (2015). Ovarian nests in cultured Russian sturgeon *Acipenser gueldenstaedtii* and North American paddlefish *Polyodon spathula* comprised of previtellogenic oocytes. Journal of Fish Biology 86: 1669–1679

Żelazowska M, Fopp-Bayat D (2017a). Previtellogenic and vitellogenic oocytes in ovarian follicles of cultured Siberian sturgeon *Acipenser baerii* (Chondrostei, Acipenseriformes). Journal of Morphology 278: 50–61

Żelazowska M, Fopp-Bayat D (2017b). Ovarian nests in cultured females of the Siberian sturgeon *Acipenser baerii* (Chondrostei, Acipenseriformes). Journal of Morphology 278: 1438–1449

Zelazowska M, Fopp-Bayat D (2019). Germline cysts and asymmetry in early previtellogenic ovarian follicles in cultured albino females of sterlet *Acipenser ruthenus* L. 1758 (Chondrostei, Acipenseriformes). Protoplasma 256: 1229–1244

Zelazowska M, Halajian A (2019). Previtellogenic oocytes of south African largemouth bass *Micropterus salmoides* Lacépède 1802 (Actinopterygii, Perciformes) – The Balbiani body, cortical alveoli and developing eggshell. Journal of Morphology 280: 360–369

Zelazowska M, Kilarski W (2009). Possibile participation of mitochondria in lipid yolk formation in oocytes of paddlefish and sturgeon. Cell and Tissue Research 335: 585–591

Zhang YZ, Ouyang YC, Hou Y, Schatten H, Chen DY, Sun QY (2008). Mitochondrial behaviour during oogenesis in zebrafish: A confocal microscopy analysis. Development Growth and Differentiation 50: 189– 201

Zhong X, Cui P, Cai Y, Wang L, He X, Long P, Lu K, Yan R, Zhang Y, Pan X, Zhao X, Li W, Zhang H, Zhou Q, Gao P (2019). Mitochondrial dynamics is critical for the full pluripotency and embryonic developmental potential of pluripotent stem cells. Cell Metabolism 29: 1–14

Zou K, Yuan Z, Yang Z, Luo H, Sun K, Zhou L, Xiang J, Shi L, Yu Q, Zhang Y, Hou R, Wu J (2009). Production of offspring from a germline stem cell line derived from neonatal ovaries. Nature Cell Biology 11: 631–636

Zucchetta M, Cipolato G, Pranovi F, Antonetti P, Torricelli P, Franzoi P, Malavasi S (2012). The relationships between temperature changes and reproductive investment in a Mediterranean goby: Insights for the assessment of climate change effects. Estuarine, Coastal and Shelf Science 101: 15–23

Zwolinski J, Stratoudakis Y, Soares E (2001). Intra-annual variation in the batch fecundity of sardine off Portugal. Journal of Fish Biology 58:1633-45

Cover picture

The fish on the cover image were illustrated by **Jessica Eggers Illustration** (https://www.jessieggers.com/?fbclid=IwAR09_CJeeMyFPeFeGa36OO7wtfnG1h5Jpo8zaP0Dkh6YQ74PGstWB4-xU)

Annexes

Annex 1: Reproductive phases of ovary

The ovaries were classified into three reproductive phases based on the study of Brown-Peterson et al. (2011): developing (DEV), indicated by the entry of oocytes into the secondary growth phase, spawning-capable (SPC), with signs of oocyte maturation and postovulatory follicles (POFs), and resting (REST) (**Fig. A1.1**). The latter phase included the regressing (early resting) ovaries, which indicates the end of the spawning period and includes atresia, POFs and few (if any) healthy vitellogenic oocyte in VTG2 OR VTG3 stage, and regenerating (late resting) ovaries, contained oocytes in primary growth phase preparing the ovary for the next reproductive cycle (**Fig. A1.1**). Due to the ephemeral occurrence of the regressing phase at the end of the spawning period, only a small number of individuals belonged to this reproductive phase. In addition, no immature individuals were included in the present study. Generally, the absence of vitellogenic atresia and POFs are the most important differences that distinguish immature from both regressing and regenerating ovaries in both anchovies, *Engraulis encrasicolus,* and sardines, *Sardina pilchardus* (Morrison 1990; Brown-Peterson et al. 2011).

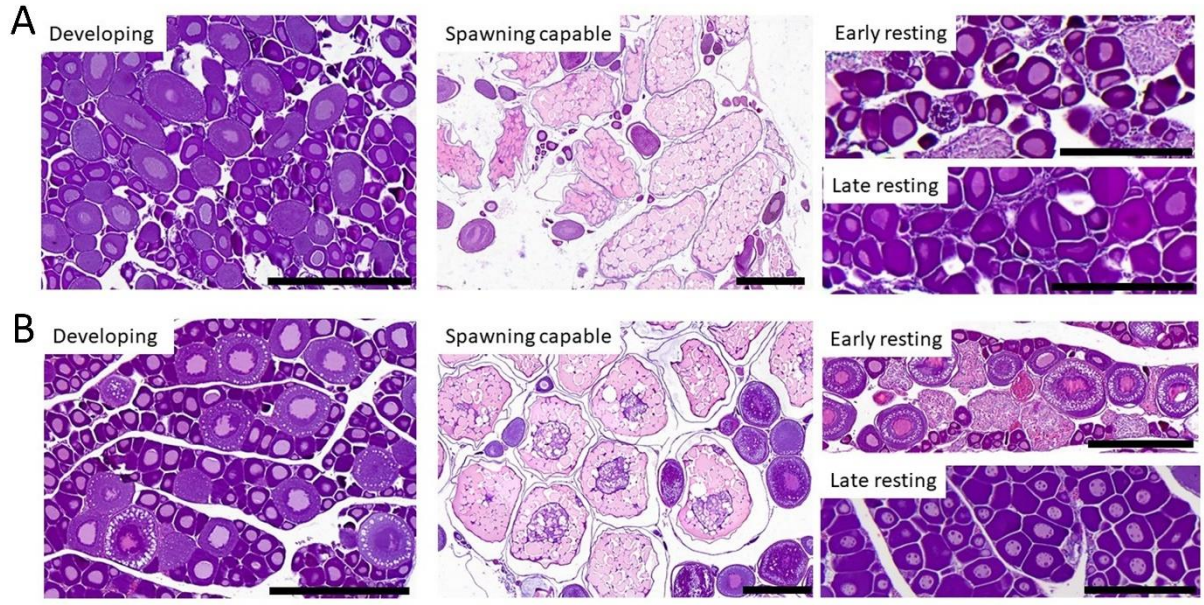

Figure A1.1. Haematoxylin/eosin-stained sections of anchovy and sardine ovaries in various reproductive phases (developing, spawning-capable, and early/ late resting phases). A) anchovy, *Engraulis encrasicolus,* B) sardine, *Sardina pilchardus.* Scale bars= 500μm (Charitonidou et al. 2022d).

Εικόνα A1.1. Τομές ωοθηκών γαύρου και σαρδέλας με χρώση αιματοξυλίνης/ηωσίνης σε διάφορες αναπαραγωγικές φάσεις (αναπτυσσόμενες, αναπαραγωγικά ικανές, και πρώιμες/όψιμες φάσεις απενεργοποίησης). Α) γαύρος, *Engraulis encrasicolus,* Β) σαρδέλα, *Sardina pilchardus*. Κλίμακα= 500μm (Charitonidou et al. 2022d)

Annex 2: Stereological method

The stereological method or Weibel method is based on the Delesse Principle stating that the fractional area of a particle (or group of particles) measured in a random section of a structure (e.g., tissue) equals the fractional volume (V_i) that the particle occupies in the same structure (Weibel et al. 1966). A high-resolution photomosaic picture of the entire histological ovarian transverse section was reconstructed. The V_i of POFs was estimated using a standard grid of 256 points within 4 counting fields of 5mm^2 each (**Fig. A2.1**) following a pilot study similar to Saber et al. (2015). In particular, a standard grid is placed over the photomicrograph, and the number of points that hit any POFs is counted and then divided by the total number of points inside 4 counting fields of specified area (Emerson et al. 1990) (**Fig. A2.1**). The number of POFs in V_i (N_{vi}) was given as:

$$N_{vi} = \frac{K}{\beta} * \frac{N\alpha^{\frac{3}{2}}}{Vi^{\frac{1}{2}}}$$

where N_a is the number of POFs sectioned per unit of area, and β and K are coefficients reflecting POF shape and size distribution, respectively (Emerson et al. 1990). N_a is estimated from the same counting fields used for calculating V_i. Values of β and K were based on POF diameter (POF_{DA}) given from POF_{xsa}. It was assumed that the shape of POFs reflected a sphere according to POF reconstructions in Korta et al. (2010) because our purpose was not to describe the exact 3-D structure of individual POFs. Mean β equalled 1.25 for both species, whereas mean K was 1.41 for sardine and 1.25 for mackerel. F_{POF} was given as N_{vi} times ovary volume (OV). OV was estimated by dividing OW by the assumed ovarian specific gravity, set to 1.026 for both species (Ganias et al. 2015). RF_{POF} was thereafter calculated as described below.

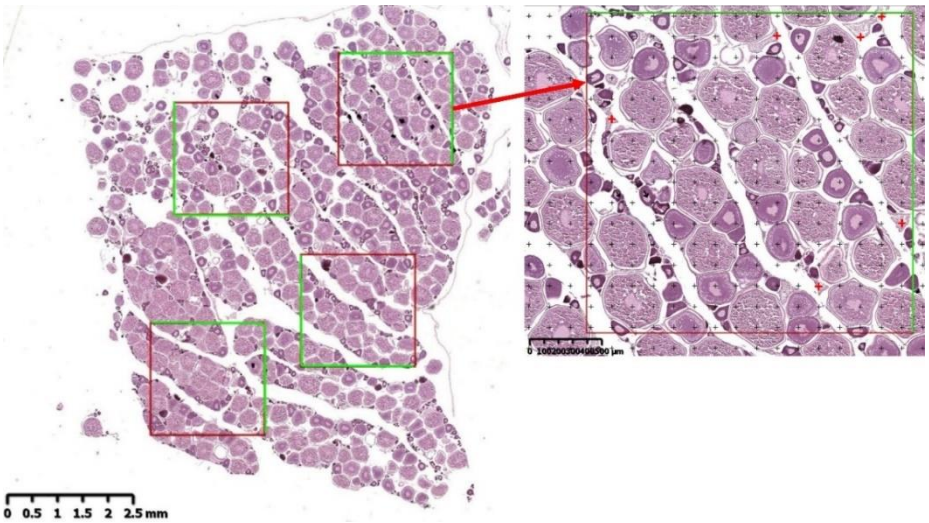

Figure A2.1. Weibel method procedure: the fields are placed over an ovarian photomicrograph and the positive (green) and negative (red) sides of each field are determined (left panel). The crosses of the grid laid on postovulatory follicles (POFs) are indicated with red in the right panel.

Εικόνα Α2.1. Διαδικασία της μεθόδου Weibel: τα πεδία τοποθετούνται πάνω από μια φωτομικρογραφία ωοθηκών και προσδιορίζονται η θετική (πράσινο) και η αρνητική (κόκκινη) πλευρά κάθε πεδίου (αριστερό πλαίσιο). Οι σταυροί του πλέγματος που τέμνονται με κενά ωοθυλάκια (POFs) υποδεικνύονται με κόκκινο στο δεξί πλαίσιο.

Given that POFs are the remnants of the follicular complex after ovulation, the number of POFs in a single daily cohort, i.e., POF fecundity (F_{POF}), should reflect batch fecundity (F_B), i.e., the number of eggs spawned in a single spawning event. Consequently, relative POF fecundity (number of POFs per gram eviscerated body weight; $RF_{POF} = F_{POF}/W_{EV}$) should equal relative batch fecundity (number of oocytes per gram eviscerated body weight; $RF_B=F_B/W_{EV}$), i.e., $RF_{POF}=RF_B$.

Annex 3: Oocyte packing density theory

A quantitative "grid method" based on simple oocyte packing density (OPD) theory (Thorsen and Kjesbu 2001; Klibansky and Juanes 2008; Alonso-Fernandez et al. 2009), combining information from both histology and image analysis (Kurita and Kjesbu 2009; Korta et al. 2010) was applied. The number of POFs was also calculated using the packing density theory (POFPD) following adaptations to procedures used previously on oocytes (Kjesbu et al. 2011). Specifically, the number of POFs (F_{POF}) in the whole ovary of an individual was estimated by dividing the total volume occupied by POFs ($V_{TOT\text{-}POFs}$) by the corresponding, representative POF size ($V_{SIZE\text{-}POF}$). $V_{TOT\text{-}POFs}$ was given by multiplying the ovary volume (OV) with the volume fraction of POFs (V_i) (analogous to **Annex 2**). The largest, sectioned POF was considered as the most appropriate representative of the youngest daily POF cohort (Ganias et al. 2007a). Consequently, $V_{SIZE\text{-}POF}$ was based on POF_{DA} (area-based POF diameter) of the largest POF, correcting for shrinkage during histological processing. In the $V_{SIZE\text{-}POF}$ formula, mackerel was set to show the same level of ovarian tissue shrinkage as sardine, i.e., 51.4% (Ganias et al. 2007a):

$$V_{SIZE-POF} = \left[\left(\frac{4}{3}\right) * \pi * (\frac{POF_{DA}}{2})^3\right] / (1 - 0.514)$$

Theoretically, underestimated POF_{DA} values would be expected to lead to inflated RF_{POF} values given this methodology. To examine this potential bias, sensitivity tests were run by plotting RF_{POF} for both sardine and mackerel as a function of POF_{DA} (**Fig. A3.1**). RF_{POF} values first dropped but then stabilized as a function of POF_{DA}; thus, above a critical value of POF_{DA}, POFs are likely sectioned through the equatorial plane representing correct size measurements. Critical POF_{DA} was estimated by using the best fitted RF_{POF} vs. POF_{DA} functions to calculate the percent reduction in RF_{POF} by successive 5 µm bins. For both species, the percent reduction spanned from>45% at small POF_{DA} values to less than 5% at large POF_{DA} values while the stabilization range for RF_{POF} was found to occur for percent reduction values between 10% and 5%.

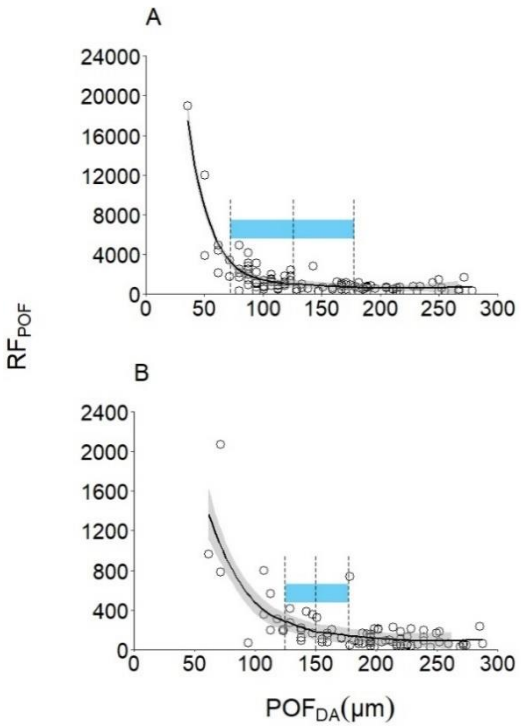

Figure A3.1. Relationship between POF size, represented by POF_{DA} (area-based POF diameter), and relative POF fecundity (RF_{POF}, POFs per gram eviscerated weight) for Atlantic sardine (A) and mackerel (B) using the packing density theory method. The 95% confidence interval (predicted lines with shaded area), the tested stabilization range (shaded blue area) of RF_{POF}, with the corresponding mathematically defined smallest, intermediate and largest values of POF_{DA} inserted (vertical dotted lines) are also provided (Charitonidou et al. 2020).

Εικόνα Α3.1. Σχέση μεταξύ του μεγέθους POF, που αντιπροσωπεύεται από την POF_{DA} (διάμετρος POF βάσει επιφάνειας) και τη σχετική γονιμότητα POF (RF_{POF}, POFs ανά γραμμάριο εκσπλαχνισμένου βάρους) για τη σαρδέλα Ατλαντικού (A) και το σκουμπρί του Ατλαντικού (B) χρησιμοποιώντας τη Θεωρία βασιμένη στον όγκο. Παρέχονται επίσης το διάστημα εμπιστοσύνης 95% (προβλεπόμενες γραμμές με σκιασμένη περιοχή), το δοκιμασμένο εύρος σταθεροποίησης (σκιασμένη μπλε περιοχή) του RF_{POF}, με τις αντίστοιχες μαθηματικά καθορισμένες μικρότερες, ενδιάμεσες και μεγαλύτερες τιμές POF_{DA} (κάθετες διακεκομμένες γραμμές) (Charitonidou et al. 2020).

Annex 4: Estimates of threshold between primary and secondary growth oocytes

In the oocyte size frequency distributions (OSFD), primary growth (PG) oocytes highly overlapped with secondary growth (SG) oocytes. Therefore, to estimate the diameter threshold value between PG and SG oocytes, the Shazam package in R software (R core team 2020) was used (see also Mouchlianitis et al. 2020; dos Santos Schmidt et al. 2021). The threshold values were assessed in all ovaries and the mean values of each species were set as the species-specific threshold value. The threshold values between primary and secondary growth oocytes were quite close among the three species: 174.6 (± 3.5) μm for sardine (**Fig. A4.1A**), 176.8 (± 6.6) μm for horse mackerel (**Fig. A4.1B**), and 197.4 (± 7.4) μm) for mackerel (**Fig. A4.1C**), even though the threshold in mackerel was significantly higher (ANOVA: $p < 0.05$). These statistically given thresholds based on OSFDs of PG oocytes were incorporated in the further estimation of the relative number of PG oocytes (RN_{PG}), the relative total number of SG oocytes (RN_{SG}), and to construct the OSFDs of SG oocytes for each species.

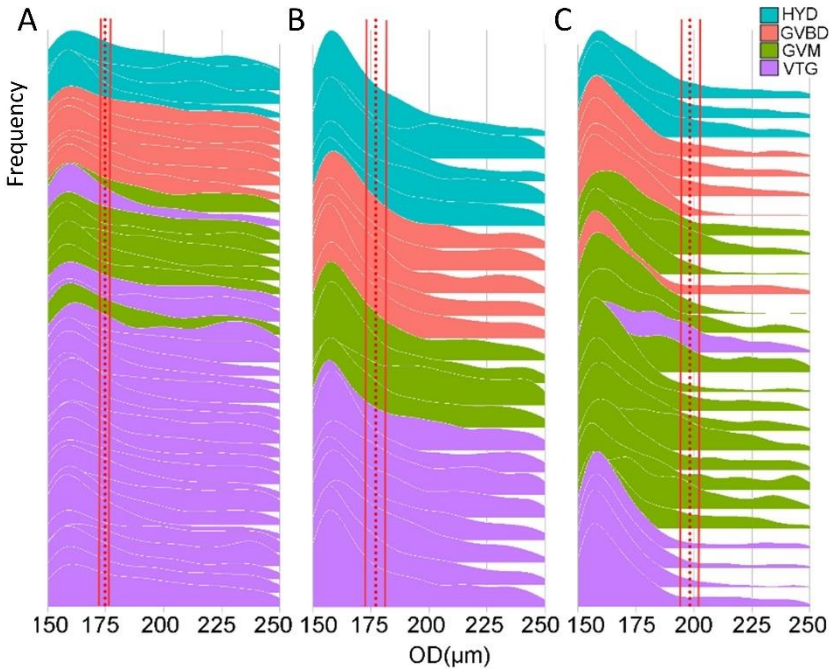

Figure A4.1. Frequency distributions of oocytes with diameters between 150 and 250 μm (OD, μm). Rows represent different individuals in ascending order of maximum oocyte size observed within the ovary: A) Atlantic sardine (*Sardina pilchardus*), B) Atlantic horse mackerel (*Trachurus trachurus*), and C) Atlantic mackerel (*Scomber scombrus*). Colours indicate ovarian stages, vitellogenic stage (VTG, purple), germinal vesicle migration (GVM, green), germinal vesicle breakdown (GVBD, pink), and hydration stage (HYD, blue). Mean threshold diameter values between primary growth and secondary growth oocytes are indicated by the vertical red dashed lines. Solid lines: 95% confidence intervals (Charitonidou et al. 2022b).

Εικόνα Α4.1. Κατανομές συχνοτήτων ωοκυττάρων με διάμετρο μεταξύ 150 και 250 μm (OD, μm). Οι σειρές αντιπροσωπεύουν διαφορετικά άτομα με αύξουσα σειρά μέγιστου μεγέθους ωοκυττάρου που παρατηρείται εντός της ωοθήκης: Α) σαρδέλα του Ατλαντικού (*Sardina pilchardus*), Β) γκριζοσαύριδο του Ατλαντικού (*Trachurus trachurus*) και C) σκουμπρί του Ατλαντικού (*Scomber scombrus*). Τα χρώματα υποδεικνύουν τα στάδια των ωοθηκών, λεκιθικό στάδιο (VTG, μωβ), μετανάστευση βλαστικού κυστιδίου (GVM, πράσινο), ρίξη

βλαστικού κυστιδίου (GVBD, ροζ) και στάδιο ενυδάτωσης (HYD, μπλε). Οι μέσες τιμές του ορίου διαμέτρου μεταξύ της πρωτογενούς ανάπτυξης και των ωοκυττάρων δευτερογενούς ανάπτυξης υποδεικνύονται από τις κάθετες κόκκινες διακεκομμένες γραμμές. Συμπαγείς γραμμές: 95% διαστήματα εμπιστοσύνης (Charitonidou et al. 2022b).

Annex 5: Estimates of relative number of primary, and secondary growth oocytes and relative batch fecundity

The relative number of primary growth oocytes (RN_{PG}, oocytes*g^{-1}) was calculated gravimetrically using the following equation:

$$RN_{PG} = \frac{n_{PG} * \frac{OW}{OWs}}{W_v}$$

Where, n_{PG} is the total number of oocytes with diameters between 50 µm and species-specific threshold value for each species (see **Annex 4**). OW is the ovarian weight, OWs is the subsample weight, and Wv is the viscerated weight.

Relative total number of secondary growth oocytes (RN_{SG}, oocytes*g^{-1}) was also estimated gravimetrically based on the following equation:

$$RN_{SG} = \frac{n_{SG} * \frac{OW}{OWs}}{W_v}$$

where n_{SG} is the total number of oocytes with diameters between species-specific threshold value and larger. OW is the ovarian weight, OWs is the subsample weight, and W_v is the viscerated weight.

The advanced mode (AM) of each oocyte size frequency distribution corresponded to the spawning batch and was considered equivalent to batch fecundity, i.e., the number of oocytes released per spawning event. Identification of the spawning batch was straightforward in oocyte size frequency distributions that exhibited a clear hiatus between the AM and the following oocytes, i.e., most sardine individuals, as well as GVBD and HYD individuals in horse mackerel and mackerel (see **Section 4.3.1**). The relative batch fecundity (RF_B, oocytes*g^{-1}) was estimated gravimetrically with the following equation:

$$RF_B = \frac{n_{AM} * \frac{OW}{OWs}}{W_v}$$

where n_{AM} is the number of oocytes in the AM. OW is the ovarian weight, OWs is the subsample weight, and Wv is the viscerated weight.

Annex 6: Morphological measurements in mitochondria

TEM micrographs were analysed using the ImageJ software (Rasband and ImageJ 1997-2018) to perform specific morphological measurements of mitochondria in oocytes at various phases of development. The volume fraction of mitochondria in oocyte cytoplasm at various phases of development was estimated using the percentage of mitochondrial area in cytoplasmic area (**Fig. A6.1**). A representative micrograph from each oocyte developmental phase was used in the mitochondria volume fraction calculations. Also, the volume fraction of cristae in mitochondria of oocytes was counted using the percentage of cristae area in mitochondrial area. Measurements of 5–7 mitochondria were utilized to determine the cristae volume fraction. To assess mitochondria size, the diameter of four optimally sectioned mitochondria in each oocyte was measured (nearest to 0.1 μm). The average values of each mitochondrion's major and minor diameters were considered, and the average mitochondrial sizes at each oocyte development phase were calculated. Both Kruskal-Wallis test and Pairwise Wilcoxon Rank Sum Test were used in conjunction with Benjamini-Hochberg post-hoc adjustment to perform non-parametric statistical analysis on diameter measurements.

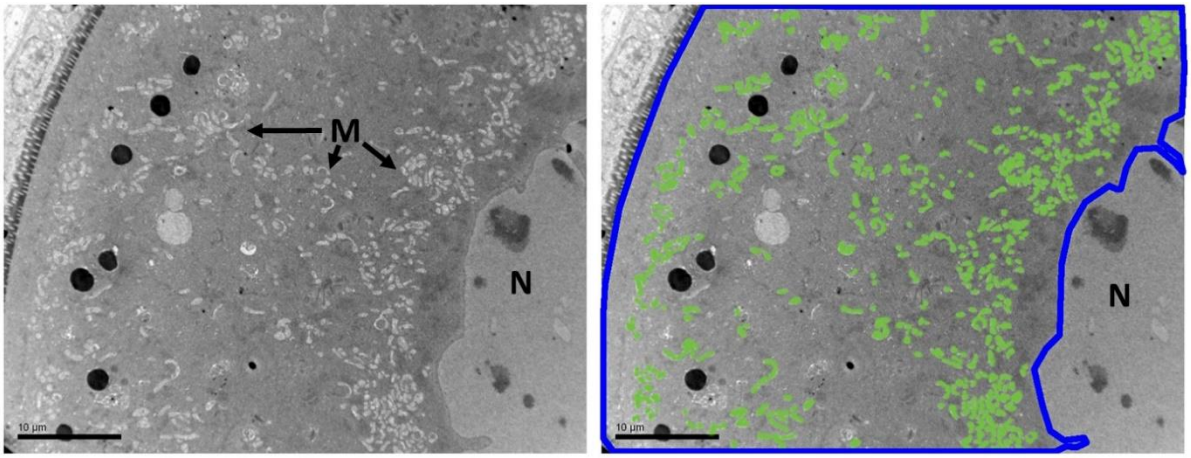

Figure A6.1. The volume fraction (%) of mitochondria (M) in the cytoplasm was estimated by the sum area of mitochondria (green) in an area of the cytoplasm (blue) using the ImageJ software. The nucleus (N) was excluded from the measurements. Scale bar= 10μm (Charitonidou et al. 2022a).

Εικόνα Α6.1. Το κλάσμα όγκου (%) των μιτοχονδρίων (Μ) στο κυτταρόπλασμα υπολογίστηκε από το άθροισμα της περιοχής των μιτοχονδρίων (πράσινο) σε μια περιοχή του κυτταροπλάσματος (οριοθετημένη σε μπλε πλαίσιο) χρησιμοποιώντας το λογισμικό ImageJ. Ο πυρήνας (Ν) εξαιρέθηκε από τις μετρήσεις. Κλίμακα= 10μm (Charitonidou et al. 2022a).

Annex 7: Bhattacharya method

The Bhattacharya (1967) method is a modal progression analysis that is utilized within the FiSAT II software (http://www.fao.org/) to detect different modes or means in a time series of length-frequency samples (Gayanillo et al. 1996). In particular, it recognizes discrete normally distributed groups in mixed multimodal frequency distributions. In applied fisheries reproductive biology, this method is used for the identification of recognizable modes, different oocyte batches, or groups of batches, in oocyte size frequency distributions (OSFDs) (**Fig. A7.1**). Initially, oocytes are classified into fine-size classes (e.g., 15 mm). The discernible modes are then separated semiautomatically, and the oocyte number and mean oocyte diameter in each mode are estimated.

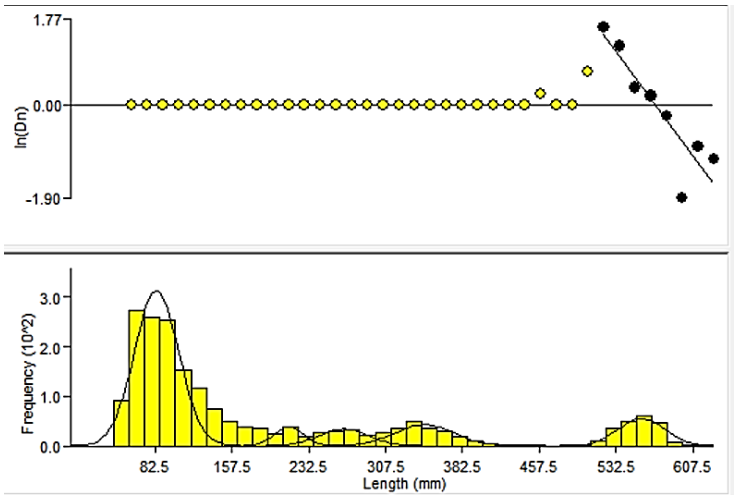

Figure A7.1. The distinction of different modes within a multimodal oocyte size frequency distribution with a semiautomated manner using the Bhattacharya method through the FiSAT II software. Fine-size class= 15mm.

Εικόνα Α7.1. Διαχωρισμός των διαφορετικών ομάδων ωοκυττάρων εντός μίας πολυπαραγοντικής κατανομής συχνοτήτων μεγεθών ωοκυττάρων με έναν ημι-αυτοματοποιημένο τρόπο χρησιμοποιώντας τη μέθοδο Bhattacharya μέσω του λογισμικού FiSAT II. Τάξη μεγέθους= 15mm.

The estimations of oocyte number of each mode applying the Bhattacharya method used for the assessment of the relative fecundity of each cohort of secondary growth oocytes (cohort specific fecundity, $RF_{ci;}$oocytes*g^{-1}) was gravimetrically assessed as indicated below.

$$RF_{ci} = \frac{n_{ci} * \frac{OW}{OWs}}{W_v}$$

where n_{ci} is the number of oocytes in each cohort. OW is the ovarian weight, OWs is the subsample weight, and Wv is the viscerated weight.

Annex 8: Postovulatory follicles (POFs)

Postovulatory follicles (POFs) are the remnants of the released eggs in the ovaries and indicate recent spawning activity. They are consisted of the follicular layers that remain in the ovary after the release of the ovum during spawning. POFs degrade progressively until they are completely absorbed (**Fig. A8.1**) and their degeneration rate is influenced by the ambient water temperature (Hunter and Macewicz 1985; Fitzhugh and Hettler 1995; Ganias et al. 2007a; Ganias 2012). They can be ephemeral and last a few hours (Takita et al. 1983; Hunter et al. 1986) to a few days (Santos et al. 2005; Ganias et al. 2007a) or months (Zamarro et al. 1993; Saborido-Rey and Junquera 1998) in the ovaries. For example, species with high spawning frequency and/or slow POF resorption rates are reported to exhibit multiple POF cohorts (e.g., Haslob et al. 2003; White et al. 2003; Mackie et al. 2005; Lang et al. 2012; Mouchlianitis et al. 2020). Specifically, Mackie et al. (2005) noticed the existence of old and new POF cohorts in the ovaries of the Spanish mackerel, *Scomberomorus commerson*, as a result of the high spawning frequency. Additionally, Mouchlianitis et al. (2020) showed that two different POF cohorts due to two sequential daily spawning events exist in the ovaries of the Macedonian shad, *Alosa macedonica*. The authors postulated that POF degeneration was longer than the ovulatory cycle, leading to the coexistence of two POF cohorts. Because the degeneration of POFs is a continuous process, the existence of multiple cohorts with overlapping histomorphological characteristics hinders the decisive identification of distinct daily cohorts. The latter might have severe consequences for the assignment of females to the correct daily spawning class and for the correct enumeration of the spawning batch. The following characteristics are common in new POFs (Hunter and Goldberg 1980; Hunter and Macewicz 1985; Ganias et al. 2007a) (**Fig. A8.1**): (1) convoluted irregular shape with folds or loops, (2) granular or particulate material in the lumen, (3) a definite granulosa epithelial cell layer lining the lumen, (4) linearly arranged granulosa cells of cuboidal or columnar shape with a prominent nucleus, (5) a definite thecal connective tissue layer with blood capillaries, and (6) no signs of follicle degeneration. Older POFs have shrunk greatly, forming a semi-rectangular shape, and the granulosa layer has lost its convoluted appearance, forming a single layer. As POF degeneration progresses, their shape becomes triangular, and the granulosa layer thins until only remnants as residual vacuoles remain.

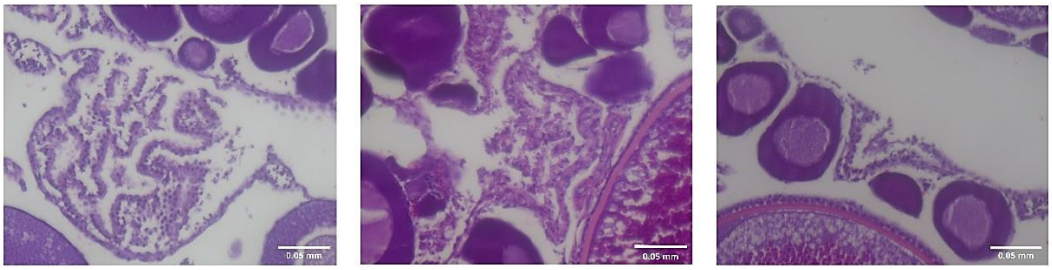

Figure A8.1. Sequential phases of postovulatory follicle (POFs) degeneration in sardine, *Sardina pilchardus*. Scale bars= 50 μm.

Εικόνα Α8.1. Διαδοχικές φάσεις εκφυλισμού των κενών ωοθυλακίων (POFs) στη σαρδέλα, *Sardina pilchardus*. Κλίμακα = 50 μm.

Publications

Publications from PhD thesis

Charitonidou K, Kjesbu OS, Dominguez-Petit R, Garabana D, Korta MA, Santos M, van Damme CJG, Thorsen A, Ganias K (2020). Contrasting post-ovulatory follicle production in fishes with different spawning dynamics. Fisheries Research 231: 105710

Charitonidou K, Ganias K (2021). Using clustering algorithms for identification of fish oocyte cohorts based on the characteristics of cytoplasmic structures. Theriogenology 170: 46-53

Charitonidou K, Panteris E, Ganias K (2022a). Ultrastructural changes in mitochondria during oogenesis in two phylogenetically close fish species. Journal of Morphology 283: 502-509

Charitonidou K, Kjesbu OS, Nunes C, Angélico MM, Dominguez-Petit R, Garabana D, Ganias K (2022b). Linking the dynamic organization of the ovary with spawning dynamics in pelagic fishes. Marine Biology 169: 47

Charitonidou K, Panteris E, Ganias K (2022c). Balbiani body formation and cytoplasmic zonation during early oocyte development in two Clupeiform fishes. Journal of Fish Biology 100: 1223-1232

Charitonidou K, Panteris E, Ganias K. (2022d). Oogonial proliferation and early oocyte dynamics during the reproductive cycle of two Clupeiform fish species. Journal of Fish Biology, 102: 44-52

Publications during PhD

Malea P, Charitonidou K, Sperdouli I, Mylona Z, Moustakas M (2019). Zinc uptake, photosynthetic efficiency and oxidative stress in the seagrass *Cymodocea nodosa* exposed to ZnO nanoparticles. Materials, 12: 2101

Anderson KC, Alix M, Charitonidou K, Thorsen A, Thorsheim G, Ganias K, dos Santos Schmidt T, Kjesbu OS (2020). Development of a new 'ultrametric'method for assessing spawning progression in female teleost serial spawners. Scientific Reports, 10: 9677

Karlou-Riga C, Petza D, Charitonidou K, Anastopoulos P, Koulmpaloglou DS, Ganias K (2020). Ovarian dynamics in picarel (*Spicara smaris*, L., Sparidae) and implications for batch fecundity and spawning interval estimation. Journal of Sea Research, 160: 101894

Tronbøl F, Johannesen E, Alix M, dos Santos Schmidt TC, Charitonidou K, Folkvord A, Kjesbu OS (2022). Tracking oocyte development and the timing of skipped spawning for north-east Arctic haddock (*Melanogrammus aeglefinus*). *Journal of Fish Biology*, 100: 1464-1474

Announcements in conferences from PhD thesis

Χαριτωνίδου Κ, Γκάνιας Κ (2019). Εφαρμογή του σαρωτή ιστολογικών τομών στη μικροσκοπική ανάλυση του αναπαραγωγικού ιστού των ψαριών. 41ο Επιστημονικό συνέδριο της Ελληνικής εταιρίας βιολογικών επιστημών, Κατερίνη 9- 11/05/2019.

Ganias K, Charitonidou K (2022). Estimating spawning interval as the ratio of oocyte growth period to the number of oocytes cohorts. International Symposium "Small Pelagic Fish: New Frontiers in Science and Sustainable Management", Lisbon, Portugal, 7 – 11/ 11 /2022.

Announcements in conferences during PhD

Charitonidou K, Kjesbu OS, Apostologamvrou C, Chatziioannou M, Domínguez-Petit R, Garabana D, Korta M, Santos M, Vafeidis D, van Damme CJG, Ganias K (2018). Validating the use of postovulatory follicles in spawning frequency estimations of the Atlantic Mackerel. 12th Panhellenic Symposium of Oceanography & Fisheries, Corfu, Greece, 30/05- 3/06/2018.

Charitonidou K, Malea P, Sperdouli I, Mylona Z, Fatouros D, Moustakas M (2018). Zinc uptake, photosystem II functioning and oxidative stress in the seagrass *Cymodocea nodosa* exposed to ZnO nanoparticles. 12th Panhellenic Symposium of Oceanography & Fisheries, Corfu, 30/05-3/06/2018.

Χαριτωνίδου Κ, Κάρλου-Ρήγα Κ, Πέτζα Δ, Αναστασόπουλος Π, Κουλμπαλόγλου ΔΣ, Γκάνιας Κ (2019). Δυναμική της ωοθήκης στη μαρίδα (*Spicara smaris*, L., Sparidae) και οι εφαρμογές της στις εκτιμήσεις γονιμότητας. 17ο Πανελλήνιο Συνέδριο Ιχθυολόγων, Κρήτη, Ελλάδα, 31/10/2019 - 3/11/2019.

Χαριτωνίδου Κ, Γκαραγκούνη Μ, Καρατζά Α, Λαχουβάρης Δ, Χρηστίδης Γ, Καρύδας Θ, Γκάνιας Κ (2023). Αναπαραγωγικό δυναμικό της κοινής σουπιάς *Sepia officinalis*, στο Θερμαϊκό κόλπο. 42ο Επιστημονικό συνέδριο της Ελληνικής εταιρίας βιολογικών επιστημών, Θεσσαλονίκη, Ελλάδα, 18-20/05/2023.

Καρατζά Α, Χαριτωνίδου Κ, Γκαραγκούνη Μ, Λαχουβάρης Δ, Χρηστίδης Γ, Καρύδας Θ, Γκάνιας Κ (2023). Δυναμική του πληθυσμού της κοινής σουπιάς, *Sepia officinalis*, σε ένα σημαντικό αλιευτικό πεδίο στο Θερμαϊκό κόλπο. 42ο Επιστημονικό συνέδριο της Ελληνικής εταιρίας βιολογικών επιστημών, Θεσσαλονίκη, Ελλάδα, 18-20/05/2023.